RATIONAL APPROACHES TOWARDS THE DESIGN OF (*E*)-8-(3-CHLOROSTYRYL)-CAFFEINE DERIVATIVES AS NOVEL REVERSIBLE INHIBITORS OF MONOAMINE OXIDASE B

Nevil Vlok
B. Pharm.

Dissertation submitted in partial fulfillment of the requirements for the degree *Magister Scientiae* in Pharmaceutical Chemistry at the North-West University, Potchefstroom Campus

Supervisor:	Prof. S.F. Malan
Co-supervisor:	Dr. J.P. Petzer
Assistant supervisor:	Prof. J.J. Bergh

2005
Potchefstroom

UITTREKSEL

Omkeerbare en selektiewe inhibeerders van monoamienoksidase B (MAO-B) word tans ondersoek as behandeling en voorkoming van Parkinson se siekte (PS) en Alzheimer se siekte. Die MAO-B inhibeer (*R*)-deprenyl word gereeld gebruik tesame met L-dopa tydens dopamienvervangingsterapie in PS. In teenstelling met omkeerbare inhibeerders sal die onomkeerbare inaktiveerders soos (*R*)-deprenyl die ensiem totaal inaktiveer en kan ensiemaktiwiteit slegs herstel word met *de novo* sintese van die MAO-B proteïen. As gevolg hiervan is talle studies tans onderweg wat die ontwikkeling van veiliger inhibeerders van MAO-B ten doel het. Met hierdie studie is dit onderneem om 'n farmakofoormodel te ontwikkel vir omkeerbare MAO-B-inhibisie deur die stereoelektroniese eienskappe van verskeie (*E*)-8-(gesubstitueerde-stiriel)kaffeïenanaloë te bestudeer. Hierdie groep verbindings is geselekteer as model omdat daar onlangs ontdek is dat (*E*)-8-(3-chlorostiriel)kaffeïen (CSC) 'n uitsonderlike goeie kompeterende inhibeerder van MAO-B is. (*E*)-8-(gesubstitueerde-stiriel)kaffeïen analoë is ook bekend as potente antagoniste van die adenosien A_{2A}-reseptor subtipe. Soortgelyke antagoniste word tans ondersoek as moontlike terapeutiese middels vir die simptomatiese verligting van motoriese afwykings soos wat byvoorbeeld by PS voorkom. Omdat MAO-B-inhibeerders tans ook ondersoek word as voorkomende terapie vir PS mag 'n dubbelwerkende middel wat as beide A_{2A}-antagonis en MAO-B-inhibeerder kan optree van groot waarde wees. In die behandeling van PS kan sulke dubbelwerkende middels die motoriese simptome verlig deur A_{2A}-reseptorantagonisme en terselfdertyd ook beskerm teen verdere neurodegenerasie deur MAO-B-inhibisie.

Tydens hierdie studie is nuwe (*E*)-8-(3-chlorostiriel)kaffeïenanaloë gesintetiseer en *in vitro* geëvalueer as kompeterende inhibeerders van MAO-B. Die analoë het slegs verskil ten opsigte van die substituent op die C-3 en C-4 posisie van die fenielring. Die verbindings is geëvalueer as kompeterende inhibeerders van bobbejaanlewer-MAO-B. Twee verskillende prosedures is gevolg om die inhiberingsaktiwiteit van die verbindings vas te stel. Die eerste metode was 'n spektrofotometriese prosedure waar MMTP, 'n struktuuranaloog van die neurotoksien MPTP, as substraat gedien het. Die tweede metode het gebruik gemaak van hoëdrukvloeistofchromatografie met bensielamien as substraat.

Die potensie waarmee die inhibeerder die MAO-B ensiem inhibeer is uitgedruk as die ensieminhibeerder dissosiasiekonstante (K_i-waarde). Die K_i-waardes wat deur die twee metodes bepaal is, vergelyk baie goed en strek oor 'n konsentrasie gebied van 0.1μM – 1.5μM. Die Lineweaver-Burke grafieke het vir al die verbindings aangedui dat die inhibisie kompeterend was.

Rekenaarmodelering is uitgevoer met die kaffeïenielanaloë om 'n drie-dimensionele hipotese daar te stel vir gebruik in toekomstige studies. Hierdie farmakofoormodel sou gebruik kon word om MAO-B-inhibisie deur soortgelyke kaffeïenielanaloë te voorspel. Die farmakofoor bevat 'n waterstofbindingontvanger, twee hidrofobiese groepe en 'n aromatiese ring. In 'n poging om spesifieke interaksies tussen die ensiem en die inhibeerders te bepaal, is sommige van die inhibeerders in die aktiewe setel van die gepubliseerde kristalstruktuur (PDB: 1S2Q) van MAO-B gepas. Met die 2 verbindings wat onderskeidelik die hoogste passingswaarde en die laagste passingswaarde getoon het, is dinamiese minimisering uitgevoer. Hierdie nuwe ligandkonformasies is vervolgens in die aktiewe setel gepas. Die molekulêre modelleringstudies het gunstige interaksies getoon tussen die inhibeerders en die ensiem en flavienadenien dinukleotied kofaktor (FAD). Die aminosure wat rondom die ligand geposisioneer is was: TYR60, TRP119, LEU167, PHE168, VAL169, ASN170, LEU171, CYS172, VAL173, THR174, PHE185, TYR188, PHE343, TYR398, TYR435 en FAD. Hierdie modelleringstudie het ook getoon dat waterstofbindings gevorm het tussen GLN206 en N-1 en N-7 van die xantiniel ring, asook tussen TYR435 en N-9. Verdere analise van die data ondersteun die hipotese dat die inhibeerders 'n lineêre konformasie moet besit, aangesien die hoeveelheid interaksies tussen die inhibeerder en die ensiem verminder as die inhibeerder nie lineêr is nie.

Met behulp van 'n Hansch-tipe struktuuraktiwiteitsverwantskapstudie (SAV) is daar vasgestel dat die potensie van MAO-B-inhibisie deur die (*E*)-8-stirielkaffeïenielanaloë afhanklik is van die Van der Waals volume (V_w), lipofilisiteit (π) en die Swain–Lupton elektroniese parameter (F) van C-3 substituente van die fenielring terwyl die potentsie van C-4 gesubstitueerde verbindings slegs afhanklik was van die Van der Waals volume (soos V_w) en lipofilisiteit van die substituente.

(*E*)-8-(gesubstitueerde-stiriel)kaffeïenanaloë is dus verteenwoordigend van 'n groep geneesmiddels wat as dubbelwerkende antiparkinsonisme middels kan optree. Deur inhibisie van MAO-B kan hierdie middels verder neurodegenerasie voorkom terwyl antagonisme van die A_{2A} reseptor verligting van die simptome van PS kan bewerkstellig.

ABSTRACT

Reversible and selective inhibitors of monoamine oxidase B (MAO-B) are under investigation for the treatment and prevention of Parkinson's disease (PD) and Alzheimer's disease. The mechanism-based inactivator of MAO-B, (*R*)-deprenyl is frequently used in combination with L-dopa as dopamine replacement therapy in PD. In contrast with reversible inhibitors, following treatment with inactivators such as (*R*)-deprenyl, enzyme activity can only be regained via *de novo* synthesis of the MAO-B protein. For these reasons, several studies are currently under way to develop safer inhibitors of MAO-B. The pupose of this study is to develop a pharmacophore model for reversible MAO-B inhibition by studying the stereoelectronic properties of several (*E*)-8-(substituted-styryl)caffeine analogues. This class of compounds was selected as model compounds since (*E*)-8-(3-chlorostyryl) caffeine (CSC) was recently found to be a high potency competitive inhibitor of MAO-B. (*E*)-8-(substituted-styryl)caffeine analogues are also known to be potent antagonists of the adenosine A_{2A}-receptor subtype. Such antagonists are currently being investigated as possible therapeutic agents for the symptomatic treatment of motor deficits such as those encountered in PD. Since MAO-B inhibitors are currently under investigation as preventative agents in PD, the possibility of designing dual acting antiparkinsonian drugs that can act both as A_{2A} antagonists and inhibitors of MAO-B may be of value. In PD such dual acting drugs could potentially enhance motility through antagonism of A_{2A} receptors and protect against further neurodegenerative processes, through inhibition of MAO-B.

In this study novel (*E*)-8-(3-chlorostyryl)caffeine analogues were synthesized and evaluated *in vitro* as competitive inhibitors of MAO-B. The analogues selected were mono substituted with various functional groups on C-3 and C-4 of the styryl phenyl ring.

The compounds were evaluated as competitive inhibitors of baboon liver MAO-B. Two different assays were followed to determine the inhibitory activity of the putative inhibitors. The first was a spectrophotometric assay that utilised MMTP, an analogue of the neurotoxin MPTP as substrate and the second was an HPLC method which utilised benzylamine as substrate. The potency of MAO-B inhibition by the synthesised inhibitors

were expressed as the enzyme-inhibitor dissociation constant (Ki value) and ranged from 0.1μM –1.5μM.

Molecular modelling studies were also carried out in order to establish a hypothesis for MAO-B inhibition by the CSC analogues. Such a pharmacophoric model may assist in future design and prediction of MAO-B inhibitors. The pharmacophore contains a hydrogen bond acceptor, two hydrophobic points as well as area for an aromatic ring. In order to determine specific interactions between the inhibitor and the enzyme the compounds were docked into the crystal structure of the MAO-B enzyme. The 2 compounds with respectively the highest and lowest conformational docking scores were then dynamically minimised and the new conformations were docked into the active site. These computational studies indicated favourable interactions of the inhibitors with the enzyme and the flavin-adenine dinucleotide cofactor (FAD). The amino acids that surrounded the ligand were found to be: TYR60, TRP119, LEU167, PHE168, VAL169, ASN170, LEU171, CYSH172, VAL173, THR174, PHE185, TYR188, PHE343, TYR398, TYR435 and FAD. Hydrogen bonds formed between GLN206 and N-1 and N-7 of the xanthinyl moiety, as well as between TYR435 and N-9. Further analysis of the data supported the idea that the inhibitors should have a linear conformation, since inhibitors that were not linear exhibited weaker interactions with the enzyme.

The results of a Hansch-type SAR study showed that the potency of MAO-B inhibition by (*E*)-8-styrylcaffeinyl analogues depends upon the van der Waals volume (V_w), lipophylicity (π) as well as the Swain–Lupton electronic parameter (F) of the substituents attached to C-3 of the styryl ring while the potency depends only upon descriptors of bulkiness (such as V_w) and lipophylicity of substituents attached to C-4.

In conclusion, the (*E*)-8-(substituted-styryl)caffeine analogues represent a class of dual acting antiparkinsonian drugs that may both provide relief of the symptoms through interaction with adenosine A_{2A} receptors and protect from further neurodegeneration through inhibition of MAO-B.

Table of content

CHAPTER 1

Introduction

Summary and abbreviations

Neurodegenerative disorders are a growing concern for the current world population. As a result, neuroprotection has risen as a growing field of interest. In studies done, MAO-B has been recognised to play an integral part in these disorders. (R)-Deprenyl, an irreversible MAO-B inactivator, for example, was found to block apoptotic cell death at low doses (Chalmers-Redman & Tatton, 1996). Another compound, (E)-8-(3-chlorostyryl)caffeine (CSC) was recently discribed to be a potent and reversible inhibitor of MAO-B in addition to antagonising adenosine A_{2A} receptors. Since adenosine A_{2A} receptor antagonists are reported to enhance motility in parkinsonian patients, such dual acting compounds may be of enhanced value in the treatment of PD. In this study additional analogues of CSC were synthesised and evaluated as MAO-B inhibitors in order to determine the structural requirements of this class of compounds to act as MAO-B inhibitors. Molecular modelling and docking studies were also carried out in order to establish a pharmacophoric model for predictive studies.

A_{2A}	–	Adenosine A_{2A} receptor
AADC	–	Aromatic amino acid decarboxylase
AD	–	Alzheimer's disease
COMT	–	Catechol *O*-methyltransferase
CSC	–	(*E*)-8-(3-chlorostyryl)caffeine
DA	–	Dopamine
GABA	–	γ-Amino-butyric acid
GP	–	Globus pallidus
MAO-B	–	Monoamine oxidase B
PD	–	Parkinson's disease
SAR	–	Structure activity relationship
SN	–	Substantia nigra
SNPC	–	Substantia nigra pars compacta

1.1. Background

Neuroprotection is an intensively studied subject due to its potential clinical application to the numerous neurodegenerative diseases, such as Parkinson's disease (PD) and Alzheimer's disease (AD). The therapies that are currently available to treat neurodegenerative diseases are inadequate and only a relatively minor improvement occurs when patients are treated.

PD is a late onset neurodegenerative disorder characterized by a progressive and relatively selective degeneration of dopaminergic neurons in the substantia nigra (SN) (Alexi *et al.*, 2000). The symptoms of PD are caused by a profound reduction in the stratial dopamine content caused by the death of dopaminergic neurons in the substantia nigra pars compacta (SNPC) and its projects to the striatum (Agid *et al.*, 1999). It is characterized clinically by bradykinesia, resting tremor and rigidity (Standaert & Young, 2000). Typical sporadic PD has a prevalence of 0.6% at 65 years of age, but the risk of developing PD increases with age to a prevalence of 4–5% at the age of 85 years (Alpevitch *et al.*, 1997). Monoamine oxidase B (MAO-B) plays a pivotal role in the metabolism of certain neurotransmitters and thus causes considerable pharmacological interest.

1.1.1. Monoamine oxidase B

In PD, dopamine (DA) replacement therapy with L-dopa is the first-line treatment. Unfortunately, the rapid metabolic transformation of L-dopa, at both peripheral and central levels, strongly hampers its high therapeutic potential. For this reason, L-dopa is typically combined with inhibitors of aromatic amino acid decarboxylase (AADC), such as benseramide and carbidopa, or with reversible and selective catechol-*O*-methyltransferase (COMT) inhibitors, such as entacapone and tolcapone and sometimes with selective and irreversible MAO-B inhibitors, such as (*R*)-deprenyl (Drucharch & Muiswinkel, 2000). These studies indicated that both L-dopa and (*R*)-deprenyl at high doses may induce neuronal apoptosis (Walkinshaw & Waters, 1995). In contrast, (*R*)-deprenyl at low doses exerts a significant neuroprotective effect by blocking apoptotic cell death (Walkinshaw & Waters, 1995). Various observations stress the need for new,

reversible and possibly safer MAO-B inhibitors in the therapy of PD. Recently, compounds have been discovered that reversibly inhibit MAO-B, as well as antagonizing adenosine A_{2A}-receptors (A_{2A}) (Chen *et al.*, 2001).

1.1.2. Adenosine A_{2A} receptor antagonists

Antagonists of the A_{2A} subtype of adenosine receptors have emerged as a leading candidate class of non-dopaminergic antiparkinsonian agents (Feigin, 2003), based primarily on their functional effects of improving motor deficits in rodent and primate models of PD (Jenner, 2003) as well as several preliminary clinical studies (Bara-Jimenez *et al.*, 2003). In addition, the A_{2A} receptor has also garnered enthusiasm as a promising therapeutic target in PD, because of the distinctive pattern of A_{2A} receptor expression, which is considerably enriched in the striatum and also within the striatum in a subset of γ-amino-butyric acid (GABA)ergic output neurons coexpressing high levels of the dopamine D_2 receptor and projecting to the globus pallidum (GP). This relatively restricted pattern of expression likely contributes to the low side-effect profile observed thus far in PD patients (Bara-Jimenez *et al.*, 2003).

1.2. Rationale and objectives of this investigation

1.2.1. Synthesis and biological evaluation

Recently, (*E*)-8-(3-chlorostyryl)caffeine (CSC; **1f**) has been reported to be a potent reversible inhibitor of MAO-B. Since CSC is also an antagonist of adenosine A_{2A} receptors, the possibility of designing dual acting drugs that are MAO-B inhibitors and A_{2A} antagonists appears to be of value. From the literature the following structural features of (*E*)-8-styrylcaffeine analogues appears to be important for MAO-B inhibition: (a) replacement of the 1,3-dimethyl groups of the xanthinyl moiety with ethyl groups decreased the potency of the compounds, (b) the 7-*N*-methylxanthinyl analogues were more potent than the corresponding 7*H*-xanthinyl analogues, (c) saturation of the styryl double bond lead to decreased activity, (d) the styryl moiety is essential for inhibition, (e) *trans* geometry is required, because the *cis* isomers are inactive and (f) an electron withdrawing substituent on the styryl moiety is important for potent inhibition (Petzer *et al.*, 2003).

Table 1: Compounds selected for this study.

	Position of the substituent on the phenyl moiety	
	3 position	**4 position**
-CF_3	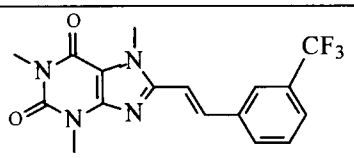 **1a**	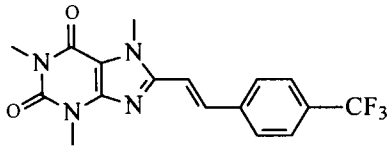 **1b**
-CH_3	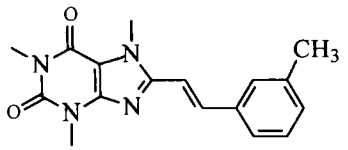 **1c**	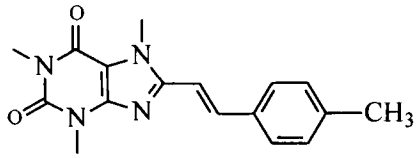 **1d**
-F		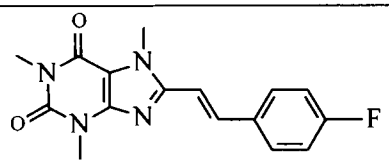 **1e**
-Cl	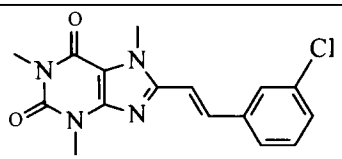 **1f**	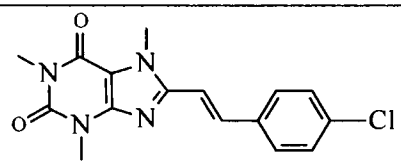 **1g**
-H	**1h**	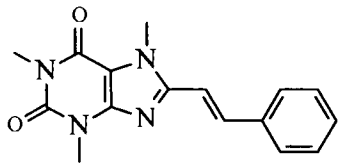

In the current study a series of (*E*)-8-(3-chlorostyryl)caffeine analogues were prepared and evaluated *in vitro* as competitive inhibitors of MAO-B. One of the objectives of this study was to determine the effect of different styryl substituents on MAO-B inhibition potency by (*E*)-8-styrylcaffeine analogues. For the purpose of this study the selected analogues were monosubstituted in either the 3- or 4-position of the phenyl ring. As

illustrated in table 1, substituents with both electron withdrawing (trifluoromethyl, fluoro and chloro) and electron donating effects (methyl) were chosen and compared with the unsubstituted (*E*)-8-styrylcaffeine (**1h**). Following preparation of the compounds (**1a – h**) illustrated in table 1, each analogue was evaluated as a reversible MAO-B inhibitor utilizing two different techniques. The potency by which each compound reversibly inhibits MAO-B was expressed as the enzyme-inhibitor dissociation constant, K_i.

1.2.2. Molecular modelling

The recent publication of the human MAO-B crystal structure (Binda *et al.*, 2003) permits modelling and docking of substrates and inhibitors into the enzyme active site. Using the compounds in table 1, molecular modelling was carried out in order to developed a hypothetic pharmacophore model for (*E*)-8-styrylcaffeine analogues as MAO-B inhibitors. The two compounds with the highest and lowest MAO-B inhibitory activity were docked into the active site of MAO-B to incorporate both sides of the activity spectrum. After the docking procedure, dynamic minimisation was applied to the enzyme and inhibitor complex at 500 K in order to determine an optimised configuration of the enzyme-inhibitor complex. From this analysis the hydrogen bonds to the surrounding amino acids were established. The models generated from these studies are aimed to assist future design of potent reversible inhibitors of MAO-B.

1.3. Summary

In this study several structure analogues of the adenosine A_{2A} receptor antagonist CSC will be prepared and evaluated as MAO-B inhibitors. The selected structures will differ from CSC by substitution of C-3 and C-4 of the phenyl ring. Computational and docking studies will also be undertaken in order to determine specific interactions between the CSC analogues and the active site of MAO-B. These studies are part of an effort to develop drugs that inhibit both MAO-B and antagonise the A_{2A} receptor.

CHAPTER 2

Literature Review

Summary and abbreviations

The purpose of this chapter is to give an overview of the literature related to MAO-B inhibition by CSC and analogues thereof. Also included in the discussion is the structure of the MAO-B enzyme and the role of the A_{2A} receptor as a drug target for the treatment of neurodegenerative disorders.

5-HT	–	Serotonin
Ach	–	Acetyl choline
CNS	–	Central nervous system
CSC	–	(*E*)-8-(3-chlorostyryl)caffeine
DA	–	Dopamine
FAD	–	Flavin-adenine dinucleotide
GPCR	–	G-protein coupled receptor
GPe	–	Globus pallidus pars externa
GPi	–	Globus pallidus pars interna
MAO-B	–	Monoamine oxidase B
$MMDP^+$	–	1-Methyl-4-(1-methylpyrrol-2-yl)-2,3-dihydropyridinium
MMP^+	–	1-Methyl-4-(1-methylpyrrol-2-yl)pyridinium
MMTP	–	1-Methyl-4-(1-methylpyrrol-2-yl)-1,2,3,6-tetrahydropyridine
MPTP	–	1-Methyl-4-phenyl-1,2,3,6-tetrahydropyridine
NA	–	Noradrenalin
NAc	–	Nucleus accumbens
PD	–	Parkinson's disease
PE	–	ß-Phenylethylamine
SNr	–	Substantia nigra pars reticulate

2.1. Background

Parkinson's disease (PD) is a devastating neurological disease that affects millions of people around the world. Idiopathic PD is a neurodegenerative disorder characterized pathologically by a marked loss of dopaminergic nigrostratial neurons and clinically by disabling movement disorders. The nature of the pathological process underlying clinical deterioration in PD remains elusive, although genetic mutations and environmental toxins have been implicated (Riederer *et al.*, 2001). It is a terminal late-onset neurodegenerative disease that results in muscle rigidity, bradykinesia, resting tremor and loss of postural reflex. Treatment of PD is divided into three categories: (1) protective or preventative, (2) symptomatic, and (3) restorative or regenerative.

In the symptomatic treatment of Parkinson's disease a useful approach consists in restoring an appropriate concentration of dopamine (DA) in the synaptic cleft of DA neurons of the central nervous system. Oral L-dopa substitution continues to be the most effective and well-tolerated symptomatic drug treatment for early PD, but leads to failure as a result of the development of drug induced dyskinesia, motor response oscillations, psychiatric complications and the progressive emergence of poorly responsive gait and balance problems (Chalmers-Redman & Tatton, 1996).

An alternative protective strategy involves the administration of an inhibitor of type B monoamine oxidase (MAO-B) in order to inhibit the metabolism of DA and consequently increase the DA concentration in the synaptic cleft of the remaining DA neurons of the nigrostratial pathway. Clinical use of (*R*)-deprenyl, an irreversible inhibitor of MAO-B, confirms this hypothesis and opens new prospectives in the treatment of PD (Chalmers-Redman & Tatton, 1996). Early studies established that (*R*)-deprenyl is neuroprotective in 1-methyl-4-phenyl-1,2,3,6-tetrahydropyridine (MPTP)-treated animals (Heikkila *et al.*, 1984). Other inactivators and competitive inhibitors of MAO-B exhibit similar effects (Castagnoli *et al.*, 1997). Although this neuroprotection was linked to blockade of the metabolic bioactivation of MPTP, the neuroprotective properties of (*R*)-deprenyl in MPTP animal models (Castagnoli *et al.*, 1997), also appears to involve unknown pathways that are independent of the inhibition of MPP^+ formation (Wu *et al.*, 1993).

In the pursuit of improved treatments for PD, the adenosine A_{2A} receptor has emerged as an attractive nondopaminergic target. Based on the compelling behavioural pharmacology and selective basal ganglia expression of this G-protein-coupled receptor (GPCR), its antagonists are now under clinical development as adjunctive symptomatic treatment for relatively advanced PD. The antiparkinsonian potential of A_{2A} antagonism has been boosted further by recent preclinical evidence that A_{2A} antagonists might favourably alter the course as well as the symptoms of the disease. In a recent study done with the MPTP mouse model of PD, the results indicated that the potent and selective A_{2A} antagonist (*E*)-8-(3-chlorostyryl)caffeine (CSC) **[1f]** may have neuroprotective properties (Chen *et al.*, 2001; Ikeda *et al.*, 2002). This protection may be dependent in part on the inhibition of the MAO-B catalysed bioactivation of MPTP, since CSC was also found to be a potent and selective competitive MAO-B inhibitor with a K_i value of 100 nM in mouse brain mitochondrial preparations (Chen *et al.*, 2002).

2.2. Morphology and function of enzymes

2.2.1. Monoamine oxidase B

Monoamine oxidase is a flavin-adenine dinucleotide (FAD)-containing enzyme, consisting of 520 amino acids and is located in the outer mitochondrial membranes of neuronal, glial and other cells. MAO catalyses the oxidative deamination of biogenic and xenobiotic amines to the corresponding aldehyde and ammonia in the periphery as well as in the central nervous system (Weyler *et al.*, 1990). Monoamine oxidase is covalently bound to the FAD cofactor via a thioether linkage between the 8-α-CH_3 group of the flavin molecule and a cysteine amino acid of the enzyme (Carriere *et* al., 1996). MAO isoenzymes are distinguished on the basis of their substrate preferences and sensitivity to inhibition by the MAO inhibitors clorgyline (selective MAO-A inhibitor) and (*R*)-deprenyl (selective MAO-B inhibitor) (Johnston, 1968).

MAO type A (MAO-A) is selectively and irreversibly inhibited by low concentrations (nM) of clorgyline. In the human central nervous system (CNS), MAO-A is mainly responsible for the deamination of serotonin (5-HT) and noradrenaline (NA). In the intestine, it oxidises tyramine.

MAO-B is relatively insensitive to clorgyline. MAO-B preferentially catalyses the deamination of ß-phenylethylamine (PE) and benzylamine and is irreversibly inhibited by low concentrations of (*R*)-deprenyl (0.8μM) **(2)**.

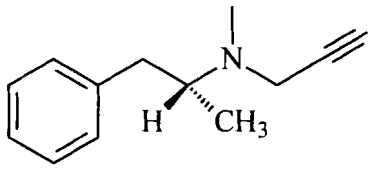

(*R*)-deprenyl **(2)**

Figure 1: Structure of (*R*)-deprenyl.

The active sites of the two isoforms of MAO share 93% homology. Cloning of the cDNA for MAO-A and MAO-B showed that approximately 70% of the total enzyme structure was identical and most probably originating from the same ancestor gene (Johnson *et al.*, 2004). For the MAO-B isoenzyme, two classes of inhibitors can be distinguished (Fowler & Tipton, 1984):

Reversible, competitive inhibitors which are structurally related to MAO substrates and can thus bind to the active site of the enzyme without any covalent bond formation.

Irreversible or "suicide" inhibitors (also known as mechanism based inactivators) which are initially bound to MAO-B in a reversible, competitive manner, but are then oxidised by the enzyme to the active inhibitor, which covalently binds to the enzyme's active site via the FAD cofactor, thus rendering it permanently ineffective for amine metabolism. This mode of inhibition is more persistent than that achieved by reversible inhibitors (weeks rather than hours), as its effects can only be overcome by *de novo* synthesis of the MAO-B enzyme (Abeles & Maycock, 1976).

Amine oxidations are important in a number of basic biological processes ranging from lysyl oxidation in the cross-linking of collagen to the degradative metabolism of polyamines and neurotransmitters. The oxidation of biogenic amines to the corresponding imines are catalysed by either the quinoprotein class of enzymes (usually primary amines) (Hartmann & McIntyre, 1997) or the flavin-containing amine oxidases (primary, secondary or tertiary amines) (Massey, 2000). In both cases, molecular oxygen is the usual electron acceptor with hydrogen peroxide formed as reaction product. Flavin amine

oxidases (Massey, 2000) catalyse the oxidation of amines via an oxidative cleavage of the α-CH bond of the substrate to form an imine intermediate with the concomitant reduction of the flavin cofactor (scheme 1). The imine product is subsequently hydrolysed to the corresponding aldehyde and ammonia (or amine for secondary or tertiary substrates). The reduced flavin coenzyme reacts with oxygen to form hydrogen peroxide and the oxidized form of the flavin to complete the catalytic cycle (Binda *et al.*, 2002a).

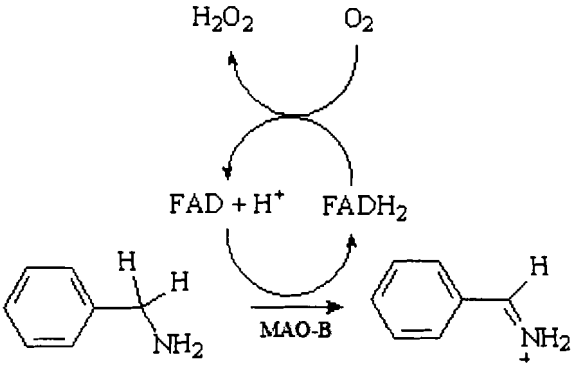

Scheme 1: Amine oxidation reaction catalysed by MAO-B, with benzylamine shown as example.

MAO-B is the major form of MAO in the human CNS (Squires, 1972) and has a half-life of at least 30 days in primates (Arnett *et al.*, 1987). The highest MAO-B concentrations are in the serotonergic and histaminergic neurons of the *raphae* and *posterior hypothalamus* with a very high concentration of MAO-A and MAO-B in the human basal ganglia (Arai *et al.*, 1983). Nigral MAO-B is located primarily in the glial cells (Denney *et al.*, 1988). The concentration of MAO-B in the *substantia nigra* is three-fold higher than that of MAO-A. The concentration of MAO-A is higher in the *pars compacta* than in the *reticula* and vice versa for MAO-B (Borroni *et al.*, 1998).

MAO-B is generally in excess in the tissues in which it occurs, so that it is necessary to inhibit at least 80% of the enzyme to achieve a pharmacological effect (Green *et al.*, 1977). It has been established that MAO-B concentration and activity increases with age while the MAO-A decreases (Fowler *et al.*, 1997). MAO-A activity is high at birth, rapidly decreases in the first year of the infant and then stabilizes, but MAO-B remains constant through early childhood and then increase with age (mostly at 50–60 years)

(Huttenlocher, 1979). The increase of MAO-B is the same in men and women, except in the hippocampus where only men appears to show an increase in MAO-B levels. Currently astrogliosis seems to be the most likely explanation for the increased MAO-B activity, although increases in neuronal MAO-B cannot be ruled out (Nicotera *et al.*, 2004). Another factor that influences MAO-B activity is tobacco smoke. MAO-B activity was found to be decreased by 40% in the brains of smokers (Alexoff *et al.*, 1996). Tobacco is positively associated with psychiatric diseases and also with a decreased risk of Parkinson's disease (Foyle *et al.*, 2000).

MAO-B activity has been found to be reduced in several psychiatric disorders and also in substance abuse. MAO-B inhibitors increase the levels of ß-phenylethylamine (PE) selectively which in turn potentiates DA and NA in the CNS. MAO-B inhibitors in combination with L-dopa is very effective in the treatment of PD and (*R*)-deprenyl in combination with an amine neurotransmitter precursor have anti-depressive effects (Yu, 1994).

MAO-B inhibitors may cause a decrease in oxidative stress in healthy dopaminergic neurons by decreasing H_2O_2 production and thus acting as neuroprotective agents. This theory results from experiments done in rats where (*R*)-deprenyl protected the *substantia nigra* from artificially induced depletion of gluthatione (Cano *et al.*, 1996). (*R*)-deprenyl causes direct upregulation of radical-metabolising systems (Gerlach *et al.*, 1996). It was also found that (*R*)-deprenyl attenuated O_2 consumption in mitochondrial preparations (Poirier *et al.*, 1997) and certain studies suggested that trapping of secondary peroxyl radicals, but not of $OH^{\bullet}$ itself, might be responsible for this protective effect of (*R*)-deprenyl (Huber *et al.*, 1997).

2.2.2. Adenosine A_{2A} receptors

Adenosine is not only an essential intracellular element of human biology, but also acts as a versatile extracellular transmitter under various physiological and pathological conditions. In the CNS, adenosine modulates sleep and arousal, locomotion, nociception, seizure susceptibility, neuroprotection, drug addiction, and other vitally important processes.

To date, four mammalian adenosine receptor subtypes (A_1, A_{2A}, A_{2B} and A_3) have been cloned and characterized in several species including human. Prior to their cloning, the receptors that inhibit adenylyl cyclase were classified as A_1 receptors and those that stimulate adenylyl cyclase were classified as A_2 receptors. A_1 and A_{2A} subtypes are expressed at restricted levels in the brain, where the A_{2A} receptor distinguishes itself

Table 2: Biological properties of the human adenosine A_{2A} receptor subtype (adapted from Xu *et al.*, 2005).

Structure in cell membrane	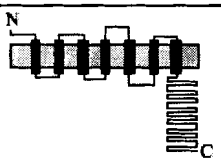
Human chromosome location	22q11.23
Amino acids	410
G-protein	G_s, G_{olf}, G15/16
Signalling pathway	↑ cAMP ↓IP_3
Distribution in brain	Restricted (Highly expressed in striatum, nucleus accumbens, olfactory tubercle; Low levels in other areas)
A_{2A} Receptor binding affinities (K_i-values, in nM)	
Agonists	
Adenosine	150
NECA	20
CGS21680	27
Antagonists	
Caffeine	2400
Theophylline	1700
CSC	54
MSX-2	5.0
SCH58261	0.6
KW-6002	2.2
ZM241385	0.8

further by its selective localization in the striatum and its related roles in basal ganglia function and disorders such as nociception (Fredholm *et al.*, 2001).

Similar to other adenosine receptors, the adenosine A_{2A} receptor has 7 transmembrane domains (table 2) and has the general structure that places it in the G-protein coupled receptor (GPCR) superfamily. Similar to the A_1 receptor, the A_{2A} receptor binds adenosine with high affinity (K_d of 0.1–1.0 μM), whereas A_{2B} and A_3 receptors have considerably lower affinity for adenosine (~10 μM) (Daly *et al.*, 1983). It has been suggested that basal extracellular levels of endogenous adenosine tonically activate the high-affinity receptors, whereas low-affinity receptor activation may require pathological elevations of extracellular adenosine concentrations (Von Lubitz *et al.*, 1994). The A_{2A} receptor is a glycoprotein containing a single carbohydrate chain and has a molecular mass of 45 kDA. The human A_{2A} receptor gene is located on chromosome 22 at position q11.23 (MacCollin *et al.*, 1994). Comparison of human, mouse and rat A_{2A} receptor-coding cDNA has demonstrated a high degree of homology (Fink *et al.*, 1992) reflecting a high degree of evolutionary conservation and the functional importance of the receptor.

Adenosine A_{2A} receptors as well as their corresponding mRNAs are expressed in the striatum. Autoradiographic studies have shown high levels of the A_{2A} receptor in the caudate nucleus, putamen, nucleus accumbens (NAc), olfactory tubercules and globus pallidus pars externa (GPe) of the human brain (Jarvis & Williams, 1989). Data from immunohistochemical studies, using a monoclonal antibody generated against purified recombinant human A_{2A} receptor (Rosin *et al.*, 1998) confirmed this selective localization of the A_{2A} receptor in the brain. *In situ* hybridisation studies have also shown that A_{2A} mRNA is enriched in caudate nucleus, putamen, NAc and olfactory tubercles in humans (Svenningsson *et al.*, 1997, 1998). Only low levels of the A_{2A} receptor gene transcript and protein are found in extrastratial structures (other than the olfactory tubercle). In the same immunohistochemical study mentioned earlier (Rosin *et al.*, 1998), low levels of immunoreactivity for the A_{2A} receptor were found in the cortex, hippocampus, thalamus and cerebellum. This anatomical evidence provides support for the many important modulary CNS functions of the A_{2A} receptor, for example in extrastratial areas such as cortex and hippocampus as suggested by the neuroprotective action of A_{2A} antagonists.

Recently, it was demonstrated that the A_{2A} receptor also exists in astrocytes in various areas of the brain (Hettinger *et al.*, 2001). Therefore, the action of adenosine as well as A_{2A} agonists and antagonists might be mediated by A_{2A} receptors in astrocytes and other glia as well as in neurons.

The adenosine A_{2A} receptor has been found to interact with several neurotransmitter receptors in the brain, including adenosine A_1, dopamine D_1 and D_2, glutaminergic (both ionotropic and metabotropic), opioid, calcitonin gene-related peptide and vasoactive intestinal peptide receptors. Activation of A_{2A} receptors attenuates the ability of an A_1 agonist to inhibit hippocampal excitablility (Cunha *et al.*, 1994). At the same time, A_1 receptor-mediated inhibition of A_{2A} actions has also been suggested (Abbracchio *et al.*, 1992). A_{2A} and D_1 receptors can also crosstalk (Morelli *et al.*, 1994), although this interaction might be indirect, at the network level, since they are differentially expressed in separate pathways in the basal ganglia (Gerfen *et al.*, 1990). The *N*-methyl-*D*-aspartame subtype of glutamate receptor has been reported to share a common adenosine 3′,5′-cyclic monophosphate signalling pathway with the A_{2A} receptor (Nash & Brotchie, 2000).

Adenosine A_2 receptors were initially defined by their stimulation of adenylyl cylase to increase cAMP levels through G_s-protein. Increased levels of cAMP lead to the activation of cAMP-dependent protein kinase A, which in turn phosphorolates and activates various receptors, ion channels, phosphodiesterases and phosphoproteins (Kull *et al.*, 1999). A_{2A} receptors generally couple to G_s-protein in peripheral tissues, but Kull *et al.* (2000) have shown that they are coexpressed with G_{olf}-protein rather than G_s-protein in GABAergic striatopallidal neurons and that stimulation of the A_{2A} receptor activates G_{olf}-protein in rat striatal membrane. Moreover, G_{olf}-protein is found to play a critical role in adenylyl cyclase responses to adenosine and dopamine in the striatum and A_{2A} agonist-induced cAMP production was decreased in $GTP\alpha_{(olf)}$ –protein of heterozygous knock-out mice (Corvol *et al.*, 2001). These data indicate that A_{2A} receptors may be coupled to different G proteins in different areas.

In the parkinsonian state, dopamine deficiency causes reduced activation of the dopamine receptors, which results in reduced inhibition of neurons of the indirect pathway and

decreased excitation of the direct pathway neurons. The net result is an excessive activation of neurons in the striatonigral direct pathway on basal ganglia output (Gpi-SNr) complex accompanied by an over-inhibition of thalamocortical motor centres (figure 2, middle panel). Accordingly the dopamine precursor L-dopa and other dopaminergic agonists are able to reinstate the equilibrium between these two neuronal pathways. Similarly, blocking adenosine A_{2A} receptors should partially reinstate the thalamocortical motor stimulatory activity as well (figure 2, right panel).

Insight into the mechanism by which caffeine (a non-selective A_1/A_2 receptor antagonist) protects dopaminergic neurons may also lead to novel PD therapeutics aimed at slowing the underlying neurodegenerative process. A first step in pursuing this intimation considered that caffeine's known molecular targets might mediate its protective effect. The CNS effects of caffeine appear to be mediated primarily by its antagonistic actions at the A_1 and A_{2A} subtypes of adenosine receptors (Fredholm *et al.*, 1999). A_{2A} receptors are particularly relevant to PD, because their expression in the brain is largely restricted to the striatum (Svenningsson *et al.*, 1999), the main target of the dopaminergic neurons that degenerate in PD. Furthermore, genetic or pharmacological inactivation of A_{2A} receptors is known to protect against excitotoxic and ischemic neuronal injury. Accordingly, relatively specific adenosine A_{2A} as well as A_1 receptor antagonists were tested for their ability to mimic caffeine's attenuation of MPTP toxicity. MPTP-induced nigrostratial lesions were reduced by pre-treatment with A_{2A} antagonists, including the xanthine-based compounds – CSC (Chen *et al.*, 2002), KW6002 (Appendix B, figure 1) (Chen *et al.*, 2001) – and those with nonxanthine structures, for example SCH 58261 (Chen *et al.*, 2001).

The specificity of CSC with respect to its neuroprotective effect in the MPTP model has been called into question with the serendipitous finding that it possesses dual independent actions of high-potency inhibition of MAO-B, as well as antagonism of the A_{2A} receptor (Petzer *et al.*, 2003). Although none of the other xanthine- or nonxanthine-based A_{2A} antagonists above possesses comparable (if any) MAO-B activity, the unexpected specificity of CSC even at low (nanomolar) concentrations raises an interesting therapeutic possibility.

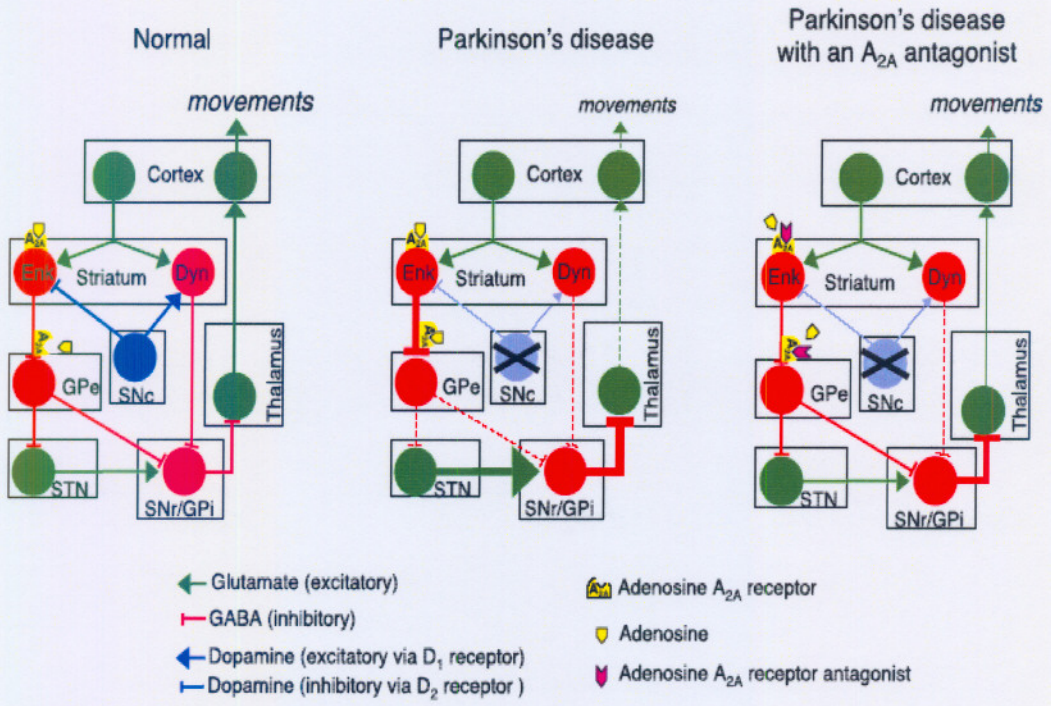

Figure 2: Schematic of the proposed mechanism of antiparkinsonian activity of A_{2A} receptor antagonists (Adapted from Xu *et al.*, 2005).

As depicted in a simplified basal ganglia diagram of the normal state (left panel of figure 2), the inhibitory influence of the striatonigral direct pathway on basal ganglia output (from the SNr/GPi complex) is counterbalanced by the disinhibitory influence of the striatopallidal indirect pathway to this complex. At the striatal level, dopamine, acting on D_1 receptors, facilitates transmission along the direct pathway and inhibits transmission along the indirect pathway throughout D_2 receptors. Adenosine excites neurons in the indirect pathway via adenosine A_{2A} receptors in the striatum and globus pallidus pars externa (GPe). The loss of striatal dopamine in PD (center panel of figure 2) disinhibits striatal spiny projection neurons of the indirect pathway, which leads to a marked suppressed activity of the GPe and therefore disinhibition of the subthalamic nucleus (STN). Depletion of dopamine leads also to a decreased activation of striatal spiny neurons in the direct pathway. The resulting imbalance between the activity in the direct and the indirect pathways leads to increased inhibitory output from the internal GP (GPi) and substantia nigra pars reticulate (SNr) with excess inhibition of thalamocortical

neurons, resulting in the characteristic reduced movement of PD. A_{2A} receptor blockade in PD (right panel of figure 2) should result in recovery of GPe activity. This in turn would alleviate excessive excitatory drive from the STN to the GPi-SNr complex, thereby restoring some balance between the direct and the indirect pathways. Note, however, that the reduced activity in the direct pathway can not be normalized by blocking adenosine A_{2A} receptors. Consequently, overactivity of GPi-SNr output neurons (and the resultant motor deficits) in PD may be only partially reversed by A_{2A} antagonists alone. (Xu *et al.*, 2005)

Apart from the motor disorders of PD, sleep is also disturbed in the majority of PD patients with severity and associated disability increasing as the disease progresses (Happe *et al.*, 2002). The causes of insomnia and poor quality sleep are numerous in PD and range widely from sleep fragmentation due to parkinsonism to side effects of antiparkinsonism drugs, to depression, to restless leg syndrome, to rapid eye movement behavioural disorder, as well as to medical problems that are just as common in the general population. Any of these causes of disrupted sleep can lead to daytime somnolence and further worsen parkinsonism and quality of life. Adenosine modulates sleep physiology and likely represents an endogenous "sleep factor". Its extracellular levels in the cholinergic basal forebrain rise during spontaneous wakefulness and during sleep deprivation, and elevating extracellular adenosine in this region induces sleep (Porkka-Heiskanen *et* al., 1997). Conversely, caffeine is widely known for its capacity to reduce sleep (and maintain wakefulness) across species. Studies done on WT mice proved that A_{2A} antagonists enhanced wakefulness (Urade *et al.*, 2003). Thus, the evidence that adenosine A_{2A} receptors modulate sleep should be factored into a full assessment of the antiparkinsonian potential of A_{2A} antagonists.

Pain, defined as an unpleasant or distressing sensory experience, has also been recognized as a feature of PD since the first descriptions of the disorder. Parkinson (1817) described abnormal pain sensations in patients afflicted with "the shaking palsy." These patients complained of "rheumatic pain" extending down the arm and fingers. Pain is estimated to occur in approximately 40% of patients with PD (Koller, 1984) and in a minority of individuals, it becomes severe enough to overshadow the motor symptoms of

the disorder. This pain is most often described as numbness, tingling, itching, coldness, burning, tightness and cramping with higher frequency during "off" periods. Evidence that adenosine A_{2A} receptors can also modulate nociception supports the analgesic potential of A_{2A} receptor antagonism (Bastia *et al.*, 2002). Accordingly, A_{2A} knock-out mice have been shown to have a higher nociceptive threshold for thermal stimuli than control animals (Ledent *et al.*, 1997). It has been found that the A_{2A} antagonist SCH 58261 produces antinociceptive effects at least in acute experimental models of pain (Bastia *et al.*, 2002). Although the nature of pain modulation by adenosine is clearly complex, the development of A_{2A} antagonists as antiparkinsonian drugs should also take into consideration the possibility that these drugs may modify the pain symptoms that PD patients frequently experience.

2.3. (E)-8-(3-chlorostyryl) caffeine and MAO-B inhibition

Recently, CSC and several of its analogues were shown to inhibit MAO-B with potencies ranging from moderate to high potency (tables 3–6). The majority of these CSC analogues were 1,3-disubstituted xanthinyl analogues bearing an (*E*)-8-styryl moiety modified on the phenyl ring. Among these were (*E*)-1,3-diethyl-8-(3,4-dimethoxystyryl)-7-methylxanthine [KW-6002 (**3a**)], a compound that successfully underwent clinical trials as a novel, non-dopaminergic agent for treatment of PD (Grondin *et al.*, 1999; Xu *et al.*, 2005).

Regarding the compounds listed in tables 3 to 6 the following relationships between the structures and MAO-B inhibition activity were reported: (a) replacement of the 1,3-dimethyl groups of the xanthinyl moiety with ethyl groups decreased the potency of the compounds, (b) the 7-*N*-methylxanthinyl analogues were more potent than the corresponding 7*H*-xanthinyl analogues, (c) saturation of the styryl double bond lead to decreased activity, (d) the styryl moiety is essential for inhibition, (e) *trans* geometry is required, because the *cis* isomers are inactive, (f) an electron withdrawing substituent on the styryl moiety is important for inhibition, (g) the xanthinyl moiety has better activity and thus presents a better concept structure for MAO-B inhibition than for example the benzimidazole moiety and (h) literature supports the idea of a planar aromatic tend to be MAO-B inhibitors (Petzer *et al.*, 2003).

Table 3: The K_i values for the inhibition of MAO-B and antagonism of A_{2A} by various (*E*)-8-styryl-7-methylxanthinyl derivatives (Table taken from Petzer *et al.*, 2003).

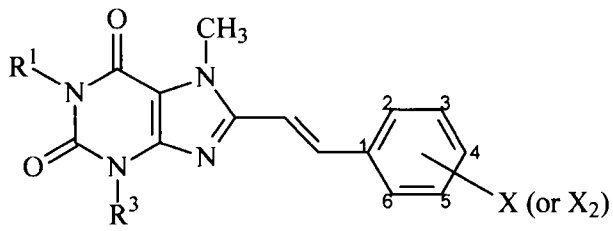

Compound	R^1/R^3	X or X_2	K_i value	
			MAO-B (μM)	A_{2A} (nM)
3a	Ethyl	3,4-Dimethoxy	28[a]; 21[b]; 17[b,c]	2.2[e]
3b	Methyl	3-Chloro	0.07[a]; 0.1[b,c];0.235[d]	54[f]; 36[g]
3c	Ethyl	3-Chloro	3[a]; 30[d]	Not reported
3d	Methyl	3,4-Dimethoxy	2.7[a]; 11	18[g]; 197[f]
3e	Methyl	H	3[a]; 3	94[f]
3f	Methyl	3-Fluoro	0.4[a]	83[f]
3g	Ethyl	3,4-Methylenedioxy	8[a]	6.1[h]
3h	Methyl	3-Nitro	0.16[a]	195[f]

[a]Baboon liver mitochondria. [d]Human liver mitochondria. [f]Jacobson *et al.*, 1993.

[b]C57BL/6 mouse brain mitochondria. [e]Shimada *et al.*, 1997. [g]Müller *et al.*, 1997.

[c]MPTP was used as substrate instead of MMTP. [h]Suzuki *et al.*, 1996.

Table 4: The K_i values for the inhibition of MAO-B by 8-(2-phenyl-ethyl)xanthines (Table taken from Petzer *et al.*, 2003).

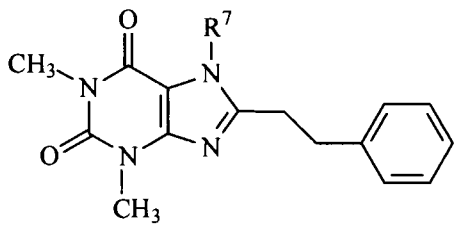

Compound	R^7	K_i value (μM)
4a	H	220[a]; 183[b]
4b	Methyl	30[a]; 36[b]

[a]Human liver mitochondria.

[b]Baboon liver mitochondria.

Table 5: The K_i values for the inhibition of MAO-B and antagonism of A_{2A} by various (*E*)-8-styryl-7H-methylxanthinyl derivatives (Table taken from Petzer *et al.*, 2003).

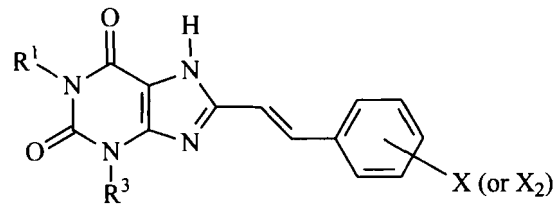

Compound	R^1/R^3	X or X_2	K_i value	
			MAO-B (μM)	A_{2A} (nM)
5a	Ethyl	3,4-Dimethoxy	63[a]	23[d]
5b	Methyl	3-Chloro	1.5[a]; 8.0[b]	Not reported
5c	Ethyl	3-Chloro	Not determined[c]	Not reported
5d	Methyl	3,4-Dimethoxy	6[a]	1100[e]
5e	Methyl	H	31[a]	291[e]
5f	Methyl	3-Fluoro	1.9[a]	516[e]
5g	Ethyl	3,4-Methylenedioxy	2.5[a]	15[e]
5h	Methyl	3-Nitro	1.7[a]; 9[b]	438[e]

[a]Baboon liver mitochondria.

[b]Human liver mitochondria.

[c]Due to limited solubility in the incubation mixture the K_i-value could not be obtained for this compound.

[d]Suzuki *et al.*, 1996.

[e]Jacobson *et al.*, 1993.

Table 6: The K_i values for the inhibition of MAO-B by (*E*)-2-styryl-benzimidazolyl derivatives (Table taken from Petzer *et al.*, 2003).

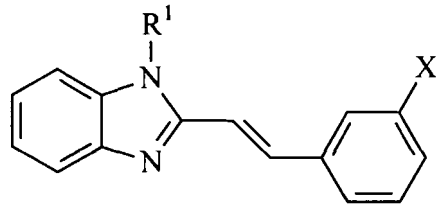

Compound	R^1	X	K_i values[a] (μM)
			MAO-B
6a	H	H	53
6b	H	Chloro	3.5
6c	H	Fluoro	5.3
7a	Methyl	H	17
7b	Methyl	Chloro	1.4
7c	Methyl	Fluoro	2.6

[a]The MAO-B source in all instances was baboon liver mitochondria and the enzyme substrate MMTP.

2.4. Enzymology and biological activity

For the purpose of this study, the potency of the reversible inhibitors for inhibition of MAO-B will be measured by two different techniques. The first technique relies on measuring the extent to which the inhibitor slows the rate of oxidation of MMTP to $MMDP^+$. Since $MMDP^+$ absorbs light maximally at 420 nm, this determination may be carried out spectrophotometrically. The second technique relies on measuring the effect of the inhibition of the rate of benzylamine oxidation by MAO-B. For this purpose the oxidation product, benzaldehyde, will be measured using HPLC analysis.

2.4.1. MMTP as substrate

The K_i value for competitive inhibition of MAO-B may be determined by measuring the extend to which various concentrations of the inhibitory compounds slows the rate of α-carbon oxidation of MMTP (**8**) to the corresponding dihydropyridinium metabolite, the 1-methyl-4-(1-methylpyrrol-2-yl)-2,3-dihydropyridinium, $MMDP^+$ (**9**; figure 3) (Nimkar *et al.*, 1996). $MMDP^+$ concentration is measured spectrophotometrically at 420 nm, a wavelength that is appart from the chromophores of both the substrate and the A_{2A} antagonists investigated (Petzer *et al.*, 2003). The chemical instability of **9** indicated the need to monitor for the formation of the 1-methyl-4-(1-methylpyrrol-2-yl)pyridinium species MMP^+ (**10**).

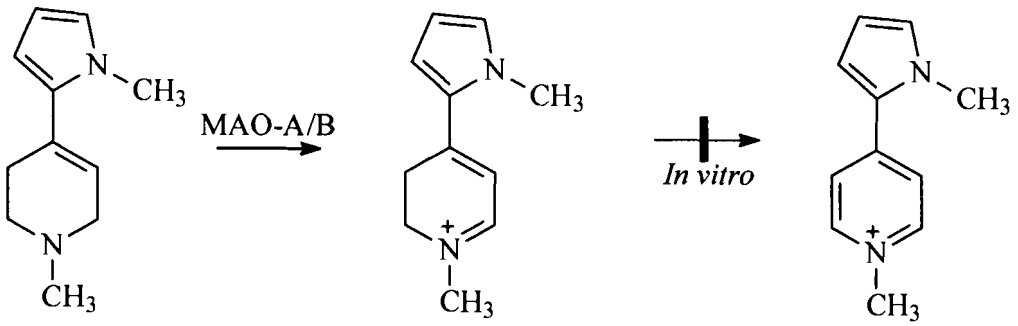

MMTP (**8**) $MMDP^+$ (**9**) MMP^+ (**10**)

Figure 3: The MAO catalysed oxidations of MMTP (**8**) to the corresponding dihydropyridinium species (**9**). The further oxidation of **9** to the pyridinium species **10** is not observed (Petzer *et al.*, 2003).

2.4.2. Benzylamine as substrate

The K_i value for competitive inhibition of MAO-B may be determined by measuring the extent to which various concentrations of the inhibitors slows the rate of benzaldehyde formation. This method is performed by HPLC, since background interference at the wavelength at which benzylaldehyde is detected (250 nm) is too high for accurate spectrophotometric analysis. As illustrated in figure 4, MAO oxidises the benzylamine (**11**) to an imine (**12**) which hydrolyses to form benzaldehyde (**13**) (figure 4).

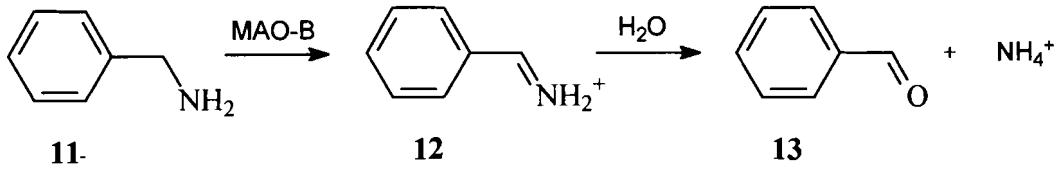

Figure 4: The oxidation of benzylamine (**11**) to benzaldehyde (**13**) (Petzer *et al.*, 2003).

2.5. Molecular models of MAO-B

MAO-B is implicated in a large number of neurological disorders, including PD and depression, and has been an important target for drug therapy over the past 40 years (Cesura & Pletscher, 1992). However, the enzyme is bound to the outer mitochondrial membrane through a C-terminal polypeptide segment and this feature has made structural investigation by X-ray crystallography more difficult. Despite these difficulties, the crystal structure of human MAO-B was recently solved.

Figure 5: Three dimensional structure of human MAO-B. The FAD-cofactor is in ball-and-stick rendering (yellow) and the membrane-binding region is formed by the protruding α-helix. The two cavities found in the substrate-binding domain is visible in blue.

The crystal structure (figure 5) reveals that MAO-B has a two-domain topology similar to that observed in other flavoenzymes. In both crystal forms, the enzyme crystallises as a dimer, which indicates that this oligomeric arrangement probably occurs also in the physiological environment. The 60-residue C-terminal tail (residues 460–520) forms an extended segment that traverses the protein surface and then folds into an α-helix. The helix protrudes from the basal face of the structure with its axis approximately parallel to the molecular two-fold axis, in an orientation suited to anchor the protein to the outer mitochondrial membrane. In addition to this transmembrane helix, two 290 Å apolar loops located at different positions in the sequence form two hydrophobic patches on the protein surface, which are also probably involved in membrane binding. Thus, MAO-B,

which is one of the very few known structures of a monotopically inserted membrane protein, appears to have a different method of membrane insertion than those of other monotopically inserted proteins such as prostaglandin synthase and squalene cyclase (Binda *et al.*, 2002b).

A second unique feature of the MAO-B structure is the presence of two adjacent cavities in the protein (figure 5). The largest cavity (420 Å and hydrophilic) is directly in front of the flavin ring and forms the substrate-binding site occupied by the inhibitor, pargyline (figure 6). For the substrate to be able to enter this cavity, it must first pass through an "entrance cavity" (290 Å) situated near the point where the protein surface intersects with the surface of the outer mitochondrial membrane. This observation raises the intriguing possibility that the anionic membrane surface may function in the electrostatic steering of the positively charged amine substrate to the entrance cavity binding site. In the substrate cavity, two tyrosyl side chains form an "aromatic sandwich" by facing each other in perpendicular orientations to the flavin, generating an "aromatic cage" that may form the recognition site for the substrate amino group (Binda *et al.*, 2002b). The peptide bond between flavin-substituted Cys-397 and Tyr-398 is in a *cis* conformation, which allows the proper orientation of the phenolic ring of Tyr-398 in the active site. The flavin ring exists in a twisted nonplanar conformation, which is observed in the oxidized form as well as in both the N(5) and the C(4a) adducts (Binda *et al.*, 2003).

The reported 1.7-Å resolution x-ray structure of the reversible isatin-MAO-B complex forms a basis for the interpretation of the enzyme's structure when bound to either reversible or irreversible inhibitors. Isatin competitively binds to purified, recombinant MAO-B with a Ki of $\approx$ 3 μM. The tight binding of the inhibitor leads to an improved crystal quality and diffraction data could be measured up to 1.7 Å resolution. A stereoview of this structure is shown in figure 7. The electron density of the dioxoindole ring shows its orientation in the substrate cavity to be perpendicular to the flavin ring with the oxo groups on the pyrrole ring pointing towards the flavin. The balance of the binding interactions involves many Van der Waals contacts between the isatin ring and amino acid residues in the solvent-inaccessible, hydrophobic substrate cavity (Binda *et al.*, 2003).

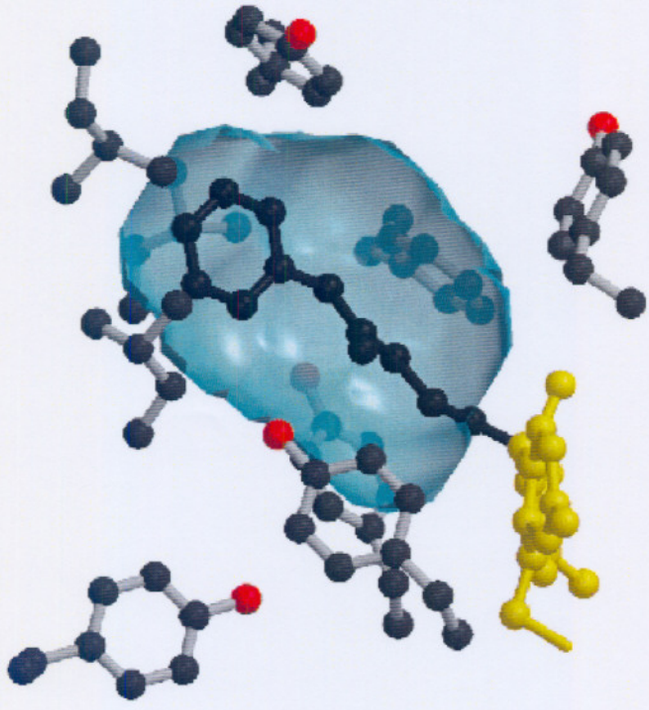

Figure 6: The active site of MAO-B. This figure shows the inactivator pargyline (black) bound in the substrate cavity (blue) (Adapted from Binda *et al.*, 2003).

1,4-Diphenyl-2-butene was found to be a reversible MAO-B inhibitor, which occupies both the entrance and substrate cavity space in the enzyme. Comparison of these two structures identifies Ile-199 as a "gate" between the two cavities. Rotation of the side chain of Ile-199 allows for either separation or fusion of the two cavities (Binda *et al.*, 2003).

The concept of cavity-spanning ligands is supported by analysis of the triclinic MAO-B crystals that were obtained by using the detergent lauryldimethylamine-*N*-oxide and used for the original structure determination. Refinement of this MAO-B crystal form (*P*1 symmetry with five dimmers per unit cell) shows the presence of a detergent molecule bound to each enzyme monomer. The *N*-oxide end of the molecule is positioned near the flavin and the aliphatic side chain traverses the space formerly defined by the substrate and entrance cavities (Binda *et al.*, 2003).

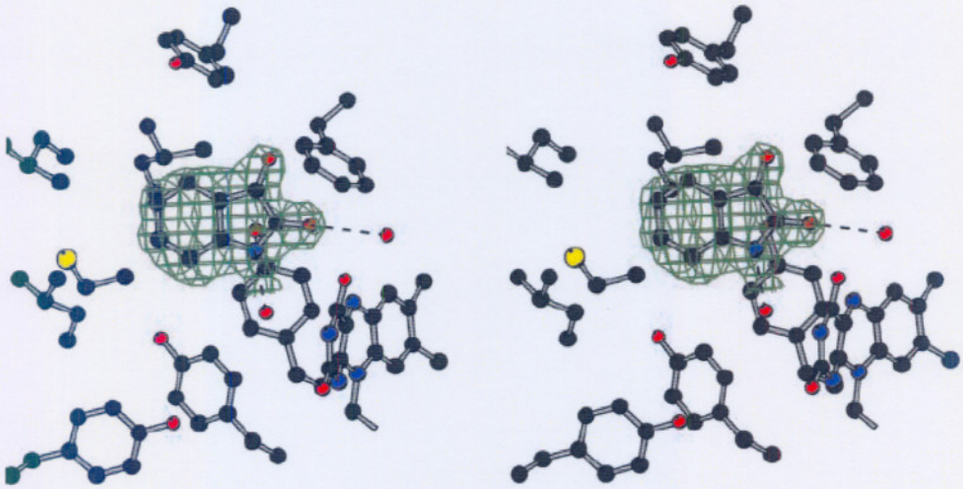

Figure 7: Stereoview of the isatin binding site of MAO-B. Carbons are in black, nitrogens in blue, oxygens in red, and sulphurs in yellow. H-bonds involving inhibitor atoms are outlined by dashed lines (Binda *et al.*, 2003).

MAO-B is attached to the mitochondrial outer membrane via the 39 amino acids at the C-terminus; however, there may be additional interactions of the protein with the membrane. FAD binds to MAO via a single covalent bond at Cys-397. Noncovalent interactions include Glu-34 (interacts with the ribose), Tyr-44, Thr-45, Lys-296 and Trp-388 (interact with the isoalloxazine ring of FAD). The disruption of any of these interactions results in the inactivation of the enzyme. The substrate binding site consists of an aromatic sandwich between the aromatic portions of Tyr-398 and Tyr-435, a catalytic Cys-365 residue, and a specificity-determining Tyr-326 residue (figure 8).

According to Binda *et al.* (2003) the major part of the cavity is hydrophobic, which allows for the tight binding of apolar substrates and inhibitors. The only hydrophilic region is near the flavin and is required for recognition and directionality of the substrate amine functionality. This hydrophilic region is located between Tyr-398 and Tyr-435, which together with the flavin form an aromatic cage for amine recognition. Mutagenesis studies targeting the tyrosine side chains in MAO-B support the key role of these residues in substrate binding (Geha *et al.*, 2002).

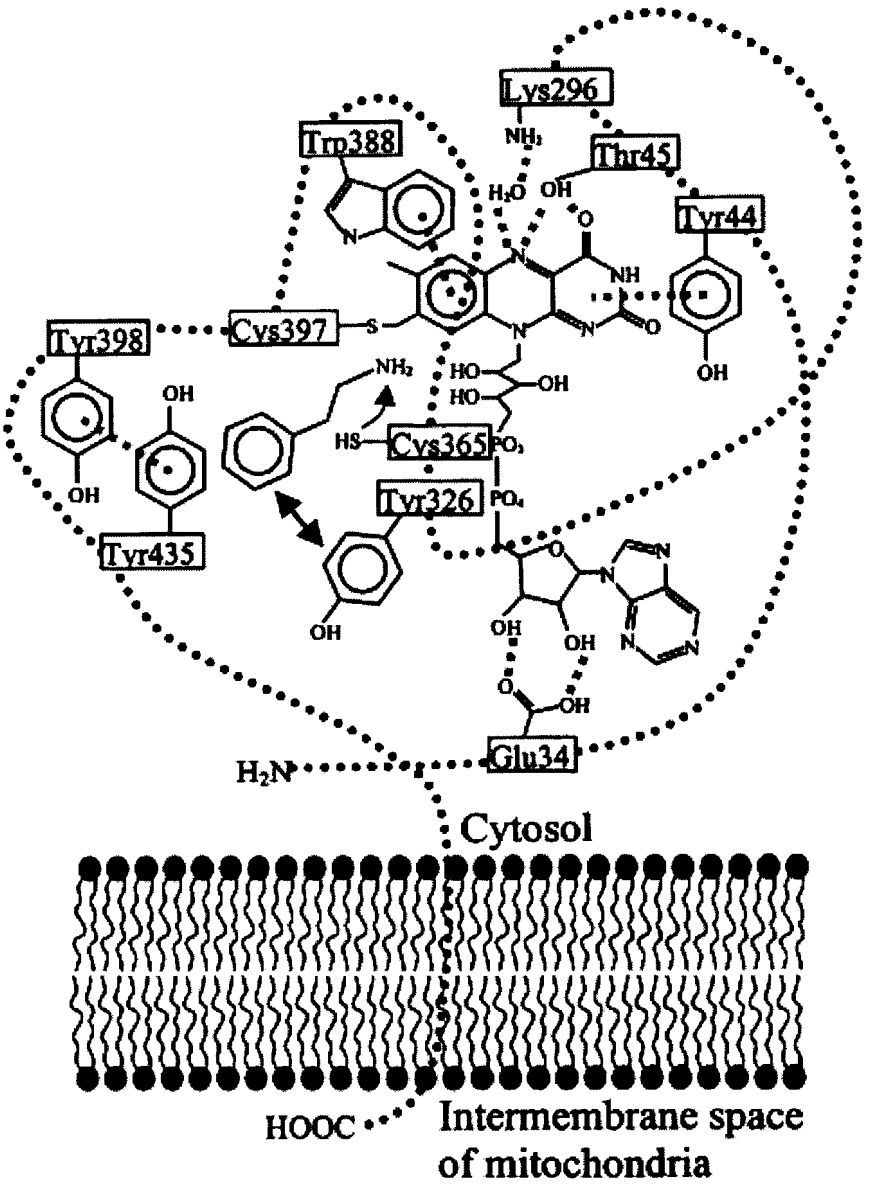

Figure 8: A schematic model of the MAO active site (Adapted from Ooms *et al.*, 2003).

In a study by Ooms *et al.* (2003), the analysis of the optimal model for 3-methyl-8-(4,4,4-trifluoro-butoxy)indeno[1,2-*c*]pyridazin-5-one (a very potent and selective MAO-B inhibitor), identified from their docking study, revealed that this compound positions in the vicinity of the FAD cofactor and that the carbonyl and pyridazine functional groups of the indeno[1,2-*c*]pyridazine-5-one nucleus form H-bonds with Tyr-188, Tyr-398, and Tyr-435.

Hubalek *et al.* (2005) identified in their studies that different species do not exhibit the same inhibitor properties for MAO-B. Therefore, discretion must be used when extrapolating the conclusions of studies done on MAO-B from differing species to the human enzyme.

2.6. Summary

This chapter described the potentially very important role of the adenosine A_{2A} receptor in the treatment of PD. CSC, an A_{2A} antagonist frequently used to investigate the pharmacology of the A_{2A} receptor, was also found to be an excellent MAO-B inhibitor. In this study additional CSC analogues will be prepared and evaluated as MAO-B inhibitors. With the availability of several x-ray crystal structures of MAO-B specific interactions between CSC and the MAO-B active site will be described. This study forms part of an effort to develop potent and reversible MAO-B inhibitors.

CHAPTER 3

The synthesis of CSC analogues

Summary and abbreviations

The purpose of this chapter is to describe the preparation of the CSC analogues selected for this study. In the introductory section of this chapter the rationale for the selection of the analogues will be discussed.

CSC	–	(*E*)-8-(3-chlorostyryl)caffeine
DSC	–	Differential scanning calorimetry
EDAC	–	1-Ethyl-2-[3-(dimethylamino)-propyl]carbodiimide
EI-MS	–	Electron ionization mass spectrometry
MAO-B–		Monoamine oxidase B
MMTP	–	1-Methyl-4-(1-methylpyrrol-2-yl)-1,2,3,6-tetrahydropyridine
NMR	–	Nuclear magnetic resonance
PD	–	Parkinson's disease

3.1. Selection of compounds

Due to their role in the metabolism of monoamine transmitters, monoamine oxidase A and B (MAO-A and –B) are of considerable pharmacological interest. Inhibitors of MAO represent a useful tool for the treatment of neurological and psychiatric diseases. In particular reversible MAO-A inhibitors are used as antidepressant and antianxiety drugs (Volz & Gleiter, 1998), while selective inhibitors of MAO-B are under investigation for the treatment and prevention of Parkinson's disease (PD) (Youdim & Riederer, 2004) and Alzheimers disease (Saura, 1994). The mechanism-based inactivator of MAO-B, (*R*)-deprenyl (**2**), is frequently used in combination with L-DOPA as dopamine replacement therapy in PD (Rabey *et al.*, 2000). The beneficial effects of (*R*)-deprenyl may be dependent on the inhibition of the MAO-B catalyzed oxidation of dopamine in the CNS, consequently conserving the depleted supply of dopamine and delaying the need for

levodopa in patients diagnosed with early PD (Rabey *et al.*, 2000). Inhibition of dopamine oxidation also results in the stoichiometric reduction of the production of hydrogen peroxide, which is thought to play a role in the etiology of neurodegenerative diseases such as PD (Youdim *et al.*, 1995). (*R*)-deprenyl is also reported to exert a neuroprotective effect by blocking apoptotic cell death (Tatton & Greenwood, 1991; Tatton, 1993), and accordingly is clinically used to postpone the emergence of symptoms that require the initiation of levodopa therapy in PD patients (LeWitt, 2004). In contrast with reversible inhibitors, following treatment with inactivators such as (*R*)-deprenyl, enzyme activity can only be regained via *de novo* synthesis of the MAO-B protein. Aside from the safety considerations associated with irreversible inhibitors, (*R*)-deprenyl is also metabolized to (*R*)-methamphetamine, a compound with vasopressor properties (Riederer *et al.*, 2004). For these reasons, several studies are currently underway to develop safer inhibitors of MAO-B as an alternative to (*R*)-deprenyl (Gnerre *et al.*, 2000). In contrast to (*R*)-deprenyl, these inhibitors are required to be reversible while retaining selectivity.

A promising lead compound, (*E*)-8-(3-chlorostyryl)caffeine (CSC) (**1f**) was recently found to inhibit MAO-B with an K_i value of 70nM (Chen *et al.*, 2001; Chen et al., 2002). Several analogues of CSC were also prepared as part of an effort to define the structural requirements of this class of compounds to act as inhibitors of MAO-B (Petzer *et al.*, 2003). (*E*)-8-Styrylcaffeinyl analogues are also of special interest since these compounds are known to be potent antagonists of the adenosine A_{2A} receptor subtype (Suzuki *et al.*, 1993; Müller *et al.*, 1997). Adenosine A_{2A} receptor antagonists (A_{2A} antagonists) are currently being investigated as possible therapeutic agents for the symptomatic treatment of motor deficits such as those encountered in PD (Xu *et al.*, 2005). One such compound, KW-6002 (**14**) (figure 9), is currently undergoing clinical trials for this purpose (Bara-Jiminez *et al.*, 2003; Shimada *et al.*, 1997). Results from recent studies in animal models of PD suggest that antagonism of the A_{2A} receptor may not only relieve the symptoms of the disease but may also protect against the underlying neuronal degeneration (Ikeda *et al.*, 2002; Chen *et al.*, 2001). Since MAO-B inhibitors are frequently used as antiparkinsonian agents, the possibility of designing drugs that act both as A_{2A} antagonists and inhibitors of MAO-B may be of value. We have therefore chosen to expand on the known (*E*)-8-styrylcaffeinyl analogues that are MAO-B inhibitors by

studying additional analogues (**1a–h**) of CSC in an attempt to elucidate specific structural features of CSC that may be responsible for its potency as an MAO-B inhibitor. Earlier studies suggested that structural features important for MAO-B inhibition are the *trans* configuration of the styryl alkene and 1,3,7-trimethyl substitution of the xanthinyl ring system (Petzer *et al.*, 2003). The principal aim is to determine whether substitution of C-3 of the styryl ring with an electron withdrawing group is essential for potent MAO-B inhibition as suggested by the structure of CSC and an earlier study (Petzer *et al.*, 2003).

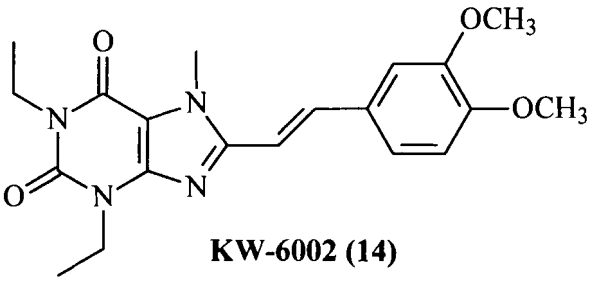

KW-6002 (14)

Figure 9: The structure of the A_{2A} antagonist, KW-6002 **(14)**.

3.2. Materials and instrumentation

All starting materials not described elsewhere were obtained from Sigma-Aldrich and were used without purification. The oxalate salt of MMTP (**8**) was a generous gift from Prof. Neal Castagnoli, Jr. Melting points (mp) were determined on a Gallenkamp melting point apparatus or by differential scanning calorimetry (DSC) on a Shimadzu DSC-50 instrument. All melting points are uncorrected. Proton and carbon NMR spectra were recorded on a Varian Gemini 300 spectrometer. Proton (^{1}H) spectra were recorded at a frequency of 300 MHz and carbon (^{13}C) spectra at 75 MHz. Chemical shifts are reported in parts per million (δ) downfield from the signal of tetramethylsilane dissolved in deuterated chloroform ($CDCl_3$). Spin multiplicities are given as s (singlet), d (doublet), t (triplet), q (quartet) or m (multiplet) and the coupling constants (*J*) are given in hertz (Hz). Direct insertion electron ionization mass spectra (EI-MS) were obtained on a VG 7070E mass spectrometer.

3.3. General procedures

3.2.1 1,3-Dimethyl-6-aminouracil (D)

The preparation of **D** was accomplished using the method described by Blicke & Godt (1954). N, N'-Dimethylurea (**A**; 40 mmol), cyanoacetic acid (**B**; 40 mmol) and 5 ml of acetic anhydride were heated, with the exclusion of moisture at 60 °C for 3 hours. The excess anhydride and the acetic acid formed during the reaction were removed under reduced pressure. A 5% sodium hydroxide solution (84 ml) was added slowly to the cooled, stirred residue (**C**) whereupon the 1,3-dimethyl-6-amino-uracil (**D**) precipitated.

3.2.2 1,3-Dimethyl-5-nitro-6-aminouracil (E)

A solution of 1.488 g of sodium nitrite in 9 ml water was added to the cooled, stirred mixture of D obtained from above and it was acidified by the dropwise addition of 3 ml of acetic acid (37%) over a period of 20 minutes. The stirring was continued for an additional 3 hours at room temperature. The mixture was thoroughly cooled, the violet precipitate (**E**) was filtered and washed with 5 ml water and 5 ml diethylether.

3.2.3 5,6-Diaminouracil (F)

To compound **E** (2 g) was added 10.9 ml of 35% ammonia. The resulting yellow-orange ammonium salt was warmed on a oil bath, stirred and a solution of 28.5 g of sodium hydrosulfide in 250 ml water was added during a 20 minute period. The salt dissolved and the solution was stirred and heated for 15 minutes. After cooling to 0 °C the white precipitate (**F**) that formed was collected by filtration.

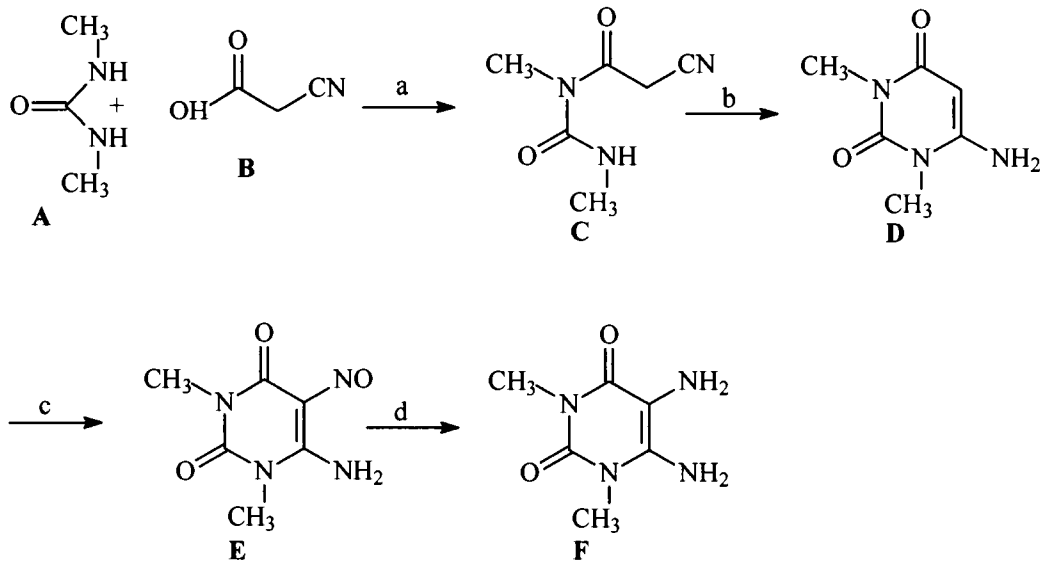

Figure 10: Sythetic pathway to substituted 5,6-diaminouracil derivatives **(F)**. (a) acetic anhydride. (b) NaOH (aq). (c) $NaNO_2$, CH_3CO_2H. (d) $Na_2S_2O_4$.

3.2.4 (*E*)-8-(substituted styryl)caffeine analogues (1a-h)

The preparations of **1a–h** were accomplished using the procedure described by Suzuki *et al.* (1993). To a solution of 1,3-dimethyl-5,6-diaminouracil (**F**, 2.7 mmol) and 1-ethyl-2-[3-(dimethylamino)propyl]-carbodiimide hydrochloride (EDAC; 3.9 mmol) in 20 ml dioxane/H_2O (1:1) was added the appropriately substituted *trans*-cinnamic acid (**G**, 2.9 mmol). The pH of the suspension was adjusted to 5 with 2N aqueous hydrochloric acid and stirring was continued for an additional 2 hours. Following neutralization with 1N aqueous sodium hydroxide the reaction was cooled to 0 °C and the precipitate was collected by filtration. The crude product was dissolved in 30 ml aqueous sodium hydroxide (1N)/dioxane (1:1) and refluxed for 45 minutes. After cooling to 0 °C the solution was acidified to a pH of 4 with 4N aqueous hydrochloric acid and the resulting precipitate was collected by filtration. The resulting 1,3-methyl-(*E*)-8-styryl-7*H*-xanthinyl analogues (**H**) may be used in the subsequent reaction without further purification. To a stirred suspension of **H** (0.16 mmol) and potassium carbonate (0.25 mmol) in a 5 ml DMF was added iodomethane (0.32 mmol). After the mixture was stirred at 50 °C for 60 minutes, the insoluble materials were removed by filtration and

sufficient water was added to the filtrate to precipitate the product (**1**) which was collected by filtration.

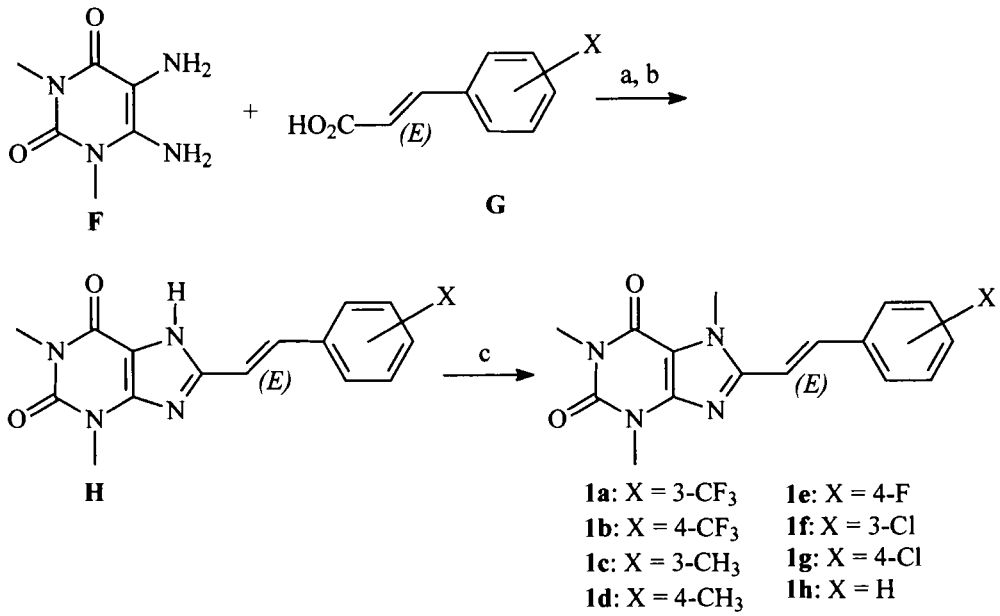

Figure 11: Synthetic pathway to (*E*)-8-styrylcafeinyl analogues **1**. (a) EDAC, dioxane/H_2O. (b) NaOH (aq), reflux. (c) CH_3I, K_2CO_3, DMF.

Following recrystallization from a mixture of methanol/ethyl acetate (9:1) analytically pure samples of **1** were obtained. For previously reported **1f** and **1h** we found the melting points to be 210 °C and 222 °C [from methanol/ethyl acetate (9:1)] while the reported melting points are 205 °C and 220-222 °C, respectively (Jacobson *et al.*, 1993). The characterisations of the prepared compounds (**1a–e** and **1g–h**) are summarised in 3.4.

3.4. Synthesis of compounds

3.4.1. (*E*)-8-(3-trifluoromethylstyryl)caffeine

(1a) was prepared from 1,3-dimethyl-5,6-diaminouracil (**F**) and *trans*-3-trifluoromethylcinnamic acid in a yield of 35%: mp 243.7 °C; ^{1}H-NMR ($CDCl_3$) δ 3.40 (s, 3H), 3.61 (s, 3H), 4.08 (s, 3H), 6.96 (d, 1H, J = 15.8 Hz), 7.51 (m, 1H), 7.59 (d, 1H, J = 7.8 Hz), 7.72 (d, 1H, J = 6.32 Hz), 7.80 (s, 1H), 7.81 (d, 1H, J = 15.8 Hz); ^{13}C-NMR ($CDCl_3$) δ 27.94 (CH_3), 29.73 (CH_3), 31.61 (CH_3), 108.22 (C), 113.02 (CH), 122.07 (C),

123.72 (CH), 125.81 (CH), 129.48 (CH), 130.51 (CH) , 131.32 (C), 131.76 (C), 136.45 (CH), 148.53 (C), 149.19 (C), 151.67 (C), 155.28 (C); EI-MS *m/z* 364 ($M^{\cdot+}$).

3.4.2. (*E*)-8-(4-trifluoromethylstyryl)caffeine

(1b) was prepared from 1,3-dimethyl-5,6-diaminouracil (**F**) and *trans*-4-trifluoromethylcinnamic acid in a yield of 64%: mp 230.2 °C; ^{1}H-NMR ($CDCl_3$) δ 3.35 (s, 3H), 3.57 (s, 3H), 4.04 (s, 3H), 6.95 (d, 1H, *J* = 15.8 Hz), 7.62 (m, 4H), 7.77 (d, 1H, *J* = 15.7 Hz); ^{13}C-NMR ($CDCl_3$) δ 27.87 (CH_3), 29.67 (CH_3), 31.50 (CH_3), 108.14 (C), 113.52 (CH), 125.76 (CH), 127.38 (CH), 130.68 (C), 131.12 (C), 136.28 (CH), 138.83 (C), 148.42 (C), 149.07 (C), 151.55 (C), 155.16 (C); EI-MS *m/z* 364 ($M^{\cdot+}$).

3.4.3. (*E*)-8-(3-methylstyryl)caffeine

(1c) was prepared from 1,3-dimethyl-5,6-diaminouracil (**F**) and *trans*-3-methylcinnamic acid in a yield of 24%: mp 216.1 °C; ^{1}H-NMR ($CDCl_3$) δ 2.36 (s, 3H), 3.37 (s, 3H), 3.59 (s, 3H), 4.02 (s, 3H) 6.86 (d, 1H, *J* = 15.8 Hz), 7.15 (d, 1H, *J* = 7.0 Hz), 7.26 (m, 1H), 7.34 (d, 2H, *J* = 7.9 Hz), 7.74 (d, 1H, *J* = 15.8 Hz); ^{13}C-NMR ($CDCl_3$) δ 21.33 (CH_3), 27.86 (CH_3), 29.69 (CH_3), 31.45 (CH_3), 107.82 (C), 110.96 (CH), 124.58 (CH), 127.89 (CH), 128.78 (CH), 130.32 (CH), 135.41 (C), 138.43 (CH), 138.55 (C), 148.52 (C), 149.99 (C), 151.65 (C), 155.17 (C); EI-MS *m/z* 310 ($M^{\cdot+}$).

3.4.4. (*E*)-8-(4-methylstyryl)caffeine

(1d) was prepared from 1,3-dimethyl-5,6-diaminouracil (**F**) and *trans*-4-methylcinnamic acid in a yield of 80%: mp 205.5 °C; ^{1}H-NMR ($CDCl_3$) δ 2.35 (s, 3H), 3.37 (s, 3H), 3.58 (s, 3H), 4.00 (s, 3H) 6.81 (d, 1H, *J* = 15.7 Hz), 7.17 (d, 2H, *J* = 8.0 Hz), 7.43 (d, 2H, *J* = 8.1 Hz), 7.73 (d, 1H, *J* = 15.8 Hz); ^{13}C-NMR ($CDCl_3$) δ 21.37 (CH_3), 27.83 (CH_3), 29.67 (CH_3), 31.40 (CH_3), 107.74 (C), 110.14 (CH), 127.27 (CH), 129.61 (CH), 132.71 (C), 138.25 (CH), 139.79 (C), 148.52 (C), 150.13 (C), 151.64 (C), 155.13 (C); EI-MS *m/z* 310 ($M^{\cdot+}$).

3.4.5. (*E*)-8-(4-fluorostyryl)caffeine

(1e) was prepared from 1,3-dimethyl-5,6-diaminouracil (**F**) and *trans*-4-fluorocinnamic acid in a yield of 55%: mp 242.26 °C; ^{1}H-NMR ($CDCl_3$) δ 3.36 (s, 3H), 3.58 (s, 3H), 4.02 (s, 3H), 6.78 (d, 1H, J = 15.8 Hz), 7.13 (m, 2H), 7.52 (m, 2H), 7.72 (d, 1H, J = 15.8 Hz); ^{13}C-NMR ($CDCl_3$) δ 27.85 (CH_3), 29.67 (CH_3), 31.44 (CH_3), 107.87 (C), 110.95 (CH), 128.99 (CH), 129.10 (CH), 131.75 (C), 136.93 (CH), 148.48 (C), 149.71 (C), 151.61 (C), 155.15 (C), 161.71 (C); EI-MS *m/z* 314 ($M^{\cdot+}$).

3.4.6. (*E*)-8-(3-chlorostyryl)caffeine

(1f) was prepared from 1,3-dimethyl-5,6-diaminouracil (**F**) and *trans*-3-chlorocinnamic acid in a yield of 71.8%: mp 210 °C (lit. 205 °C).

3.4.7. (*E*)-8-(4-chlorostyryl)caffeine

(1g) was prepared from 1,3-dimethyl-5,6-diaminouracil (**F**) and *trans*-4-chlorocinnamic acid in a yield of 17%: mp 226.9 °C; ^{1}H-NMR ($CDCl_3$) δ 3.37 (s, 3H), 3.58 (s, 3H), 4.02 (s, 3H), 6.84 (d, 1H, J = 15.7 Hz), 7.34 (d, 2H, J = 8.5 Hz), 7.47 (d, 2H, J = 8.5 Hz), 7.71 (d, 1H, J = 15.8 Hz); ^{13}C-NMR ($CDCl_3$) δ 27.89 (CH_3), 29.70 (CH_3), 31.49 (CH_3), 107.99 (C), 111.71 (CH), 128.45 (CH), 129.17 (CH), 133.97 (C), 135.28 (C), 136.79 (CH), 148.50 (C), 149.55 (C), 151.63 (C), 155.19 (C); EI-MS *m/z* 330 ($M^{\cdot+}$).

3.4.8. *E*)-8-styrylcaffeine

(1h) was prepared from 1,3-dimethyl-5,6-diaminouracil (**F**) and *trans* cinnamic acid in a yield of 82%: mp 220–222 °C (lit. 220–222 °C).

3.5. Summary

Following recrystalisation from a suitable solvent the structures and purity of the compounds were verified by mass spectrometry, ^{1}H-NMR and ^{13}C-NMR. For compound **1f** and **1h** the physical data were also compared to the corresponding literature values as cited in the experimental Section. The *trans* geometry of the styryl alkene was confirmed by proton-proton coupling constants in the range of 15.7–15.8 Hz of the olefinic proton signals. The preparation of the compounds gave relatively good yields.

CHAPTER 4

Enzymology, methods and SAR study

Summary and abbreviations

In this chapter the evaluation of CSC and its structural analogues (prepared as described in the previous chapter) as reversible inhibitors of monoamine oxidase B (MAO-B) is described. The results of these assays are presented and the relationships between the structures of the inhibitors and the MAO-B inhibition activity are discussed.

CSC	–	(*E*)-8-(3-Chlorostyryl)caffeine
FAD	–	Flavin-adenine dinucleotide
HAT	–	Hydrogen atom transfer
HPLC	–	High performance liquid chromatography
MAO-B	–	Monoamine oxidase B
$MMDP^+$	–	1-Methyl-4-(1-methylpyrrol-2-yl)-2,3-dihydropyridinium
MMTP	–	1-Methyl-4-(1-methylpyrrol-2-yl)-1,2,3,6-tetrahydropyridine
SET	–	Single electron transfer

4.1. Introduction

Monoamine oxidase (MAO) is a flavin-adenine dinucleotide (FAD)-containing enzyme, consisting of 520 amino acids and is located in the outer mitochondrial membranes of neuronal, glial and other cells. MAO catalyses the oxidative deamination of biogenic and xenobiotic amines to the corresponding aldehyde and ammonia in the periphery as well as in the central nervous system (Weyler *et al.*, 1990). Monoamine oxidase is covalently bound to the FAD cofactor in the C-terminal region through a thioether linkage from the 8-α-CH_3 group of the flavin molecule to a cysteine amino acid on the enzyme (Carriere *et*

al., 1996). MAO isoenzymes are distinguished on the basis of their substrate preferences and sensitivity to inhibition by the MAO inhibitors clorgyline (selective MAO-A inhibitor) and (*R*)-deprenyl (selective MAO-B inhibitor) (Johnston, 1968).

4.2. The mechanism of action of monoamine oxidase B

Monoamine oxidase catalyses the α-carbon oxidation of amines to imines and iminiums with simultaneous reduction of the covalently bound FAD cofactor. The enzyme is regenerated by reoxidation of the reduced FAD with simultaneous reduction of molecular oxygen to hydrogen peroxide. One mole of hydrogen peroxide is produced for each mole of substrate oxidized.

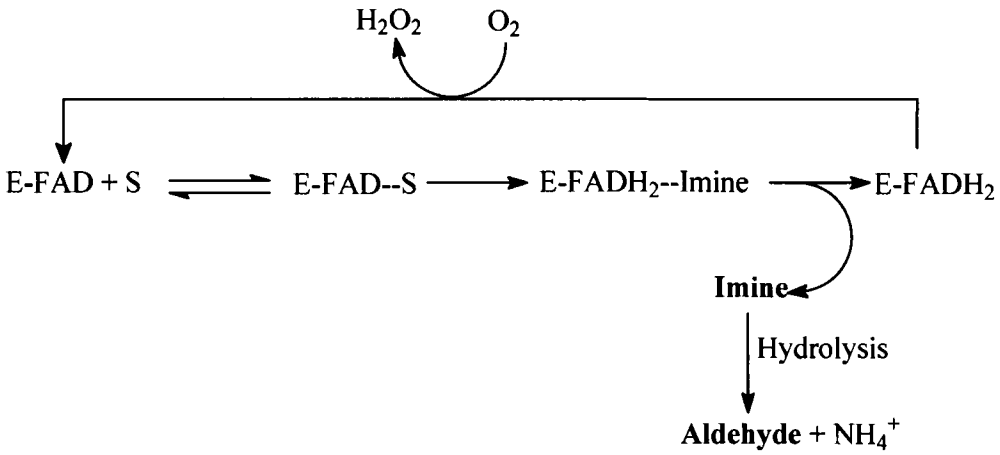

Figure 12: The kinetic mechanism of MAO-B. (E-FAD: monoamine oxidase, S: amine, $E\text{-}FADH_2$: reduced enzyme)

The literature gives three possible mechanisms explaining the catalytic action of monoamine oxidase. The first mechanism by which MAO catalyses an α-carbon oxidation of amines may proceed via a *single electron transfer* (SET) pathway (Silverman, 1995). According to this mechanism one electron is transferred from the nitrogen lone pair to the oxidised flavin of MAO to generate an aminyl radical species. Following deprotonation of the α-carbon a second electron is transferred to the flavin to give an iminium species. Primary iminiums are hydrolysed to yield the matching aldehyde, hence the terminology oxidative deamination.

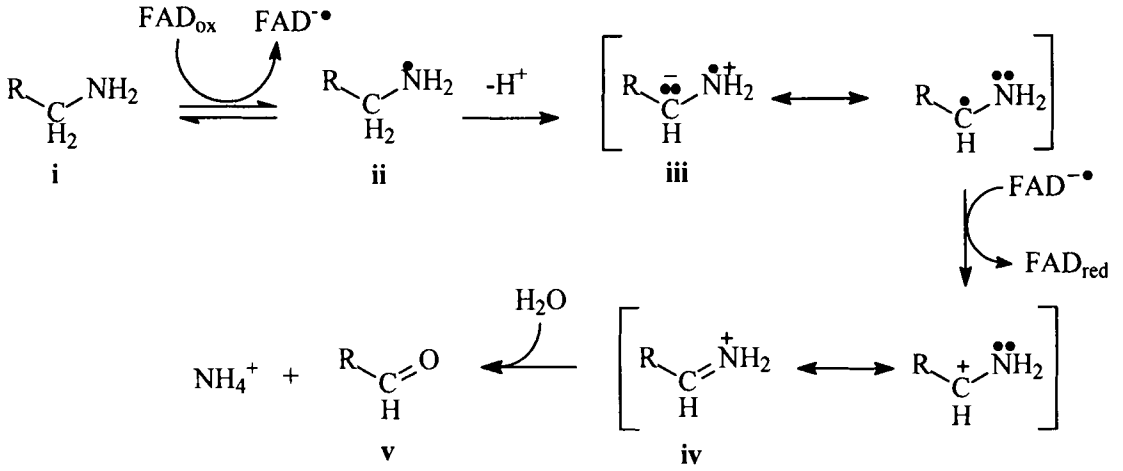

Figure 13: The proposed SET pathway for MAO-catalysed α-carbon oxidation of amines. ((**i**) amine; (**ii**) aminyl radical species; (**iii**) Product after the loss of a proton; (**iv**) iminium species; (**v**) matching aldehyde.)

The second mechanism bypasses the initial electron transfer in favour of *direct atom abstraction* (also referred to as the hydrogen atom transfer pathway (HAT)) from the α-carbon (**i**) to give an aminyl radical intermediate. An ensuing single electron transfer to the flavin radical yields the iminium species (Ottoboni *et al.*, 1989) that hydrolyses readily to form an aldehyde. The inability to detect the initial aminyl radical species intermediate in the SET pathway supports this mechanism (Wang & Silverman, 2000).

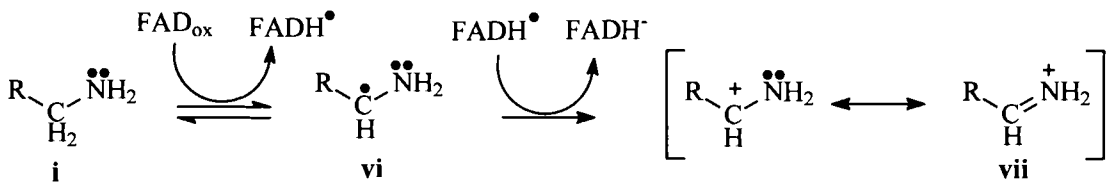

Figure 14: The proposed HAT pathway for MAO catalysed α-carbon oxidation of amines.((**i**) amine; (**vi**) aminyl radical intermediate; (**vii**) iminium species.)

The third mechanism is the *polar nucleophilic* or *group transfer* mechanism in which MAO catalysis is proposed to occur via nucleophilic attack at the oxidised flavin 4a position by the amine. It is proposed that an amino acid base in the active site facilitates the proton abstraction from the α-carbon of the amine-flavin adduct. The elimination of

the reduced flavin results in the formation of the iminium product (Miller & Edmondson, 1999).

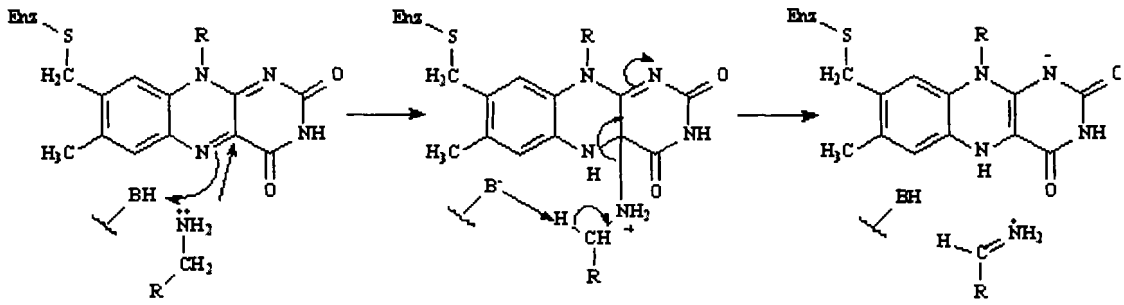

Figure 15: The proposed polar nucleophilic pathway for MAO catalysed α-carbon oxidation of amines.

4.3. Enzyme kinetics

4.3.1. K_m determination

If all conditions in a reaction are kept constant except for increasing the concentration of the enzyme substrate [S], the initial velocity (V_i, the velocity when very little substrate has been consumed) of an enzymatic reaction increases to a maximum value, V_{max}. The enzyme is saturated with substrate at this point and V_i is unaffected by further increases in substrate concentration. The substrate concentration [S] that produces half-maximal velocity ($V_{max}/2$), termed the K_m value or Michaelis constant, is determined experimentally by graphing V_i vs. [S]. The K_m value may approximate, with certain assumptions, a binding constant (K_d) for the enzyme-substrate complex. A numerically small K_m indicates a high affinity of the substrate for the enzyme, since the affinity of an enzyme for the substrate is equal to the inverse of K_d (Rodwell, 1993). The Michaelis-Menten equation describes the behaviour of many enzymes under the influence of varied substrate concentrations (equation 1).

$$V_i = \frac{V_{max} \times [S]}{K_m + [S]} \qquad \textbf{Equation 1}$$

Many enzymes give saturation curves that do not readily permit accurate measurement of V_{max} (and also K_m) when V_i is plotted vs [S]. A straight line is obtained by inversion of

the Michaelis-Menten equation (equation 2) and graphing the inverse of the initial velocity ($1/V_i$) as a function of the inverse of substrate concentration (1/[S]). This plot is known as a double reciprocal plot or Linewaever-Burke plot (figure 16). The K_m and V_{max} values can be easily obtained from this plot since the y-axis intercept is equal to $1/V_{max}$ and the slope is K_m/V_{max}. The x-axis intercept is equal to $-1/K_m$ (Segel, 1993).

$$\frac{1}{V} = \left(\frac{K_m}{V_{max}}\right) x \left(\frac{1}{[S]}\right) + \frac{1}{V_{max}} \qquad \textbf{Equation 2}$$

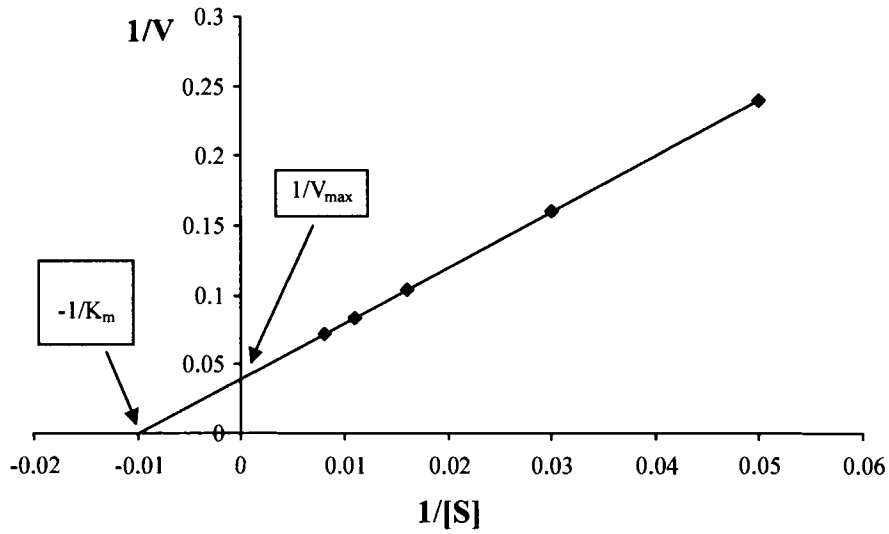

Figure 16: An example of the Lineweaver-Burke plot ($1/V_i$ versus 1/[S]).

When [S] is approximately equal to K_m, V_i is very responsive to changes in substrate concentrations and the presence of inhibitors. Therefore substrate concentrations that bracket the reported apparent K_m values are used when examining the effects A_{2A} antagonists have on the MAO-B catalytic rate.

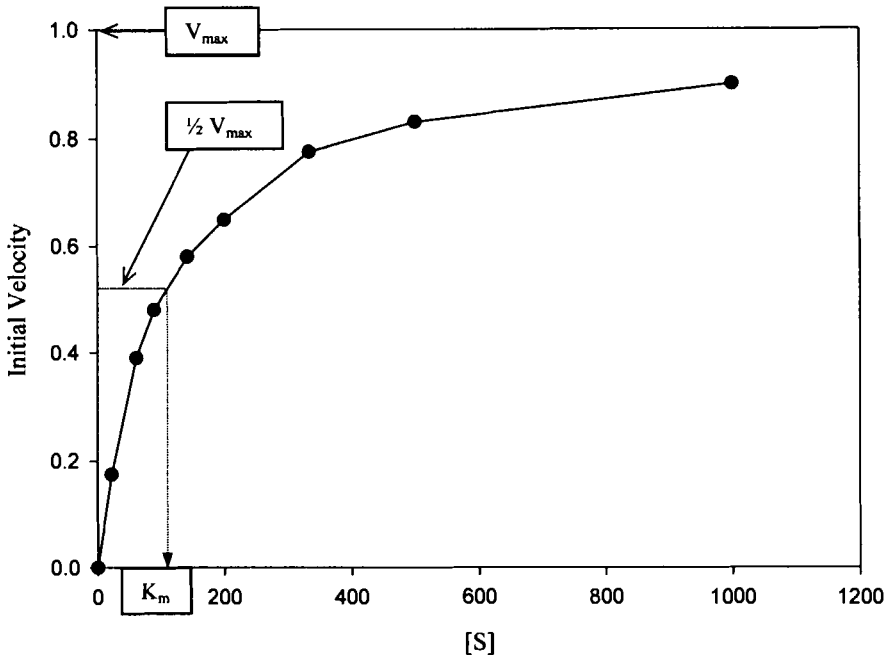

Figure 17: Graphical representation of the Michaelis-Menton equation (V_i vs. [S]).

4.3.2. K_i determination

Classic competitive inhibition occurs at the substrate-binding (catalytic) site of an enzyme in a manner that prevents the substrate from binding. The inhibitor and substrate compete for the binding at the same site and the combination of an inhibitor and enzyme is reversible. The Lineweaver-Burke plot in figure 18 is a graphical representation of competitive inhibition. With the addition of a competitive inhibitor to an enzyme-substrate reaction, the slope of the straight line is increased while the y-axis intercept remains unchanged. This results in an increase of the x-axis intercept value (it becomes less negative). Competitive inhibitors therefore raise the apparent K_m value for a substrate while V_{max} remains unaffected. The form of the Michaelis-Menten equation that includes the inhibitor effects on the initial velocity is given in equation 3.

$$V_i = \frac{V_{max} \times [S]}{K_m\left(1 + \frac{[I]}{K_i}\right) + [S]} \qquad \textbf{Equation 3}$$

The inverse of this equation describes the double reciprocal plot in the presence of a competitive inhibitor (equation 4)

$$\frac{1}{V_i} = \frac{K_m}{V_{max}}\left\{1 + \frac{[I]}{K_i}\right\} x \frac{1}{[S]} + \frac{1}{V_{max}} \qquad \textbf{Equation 4}$$

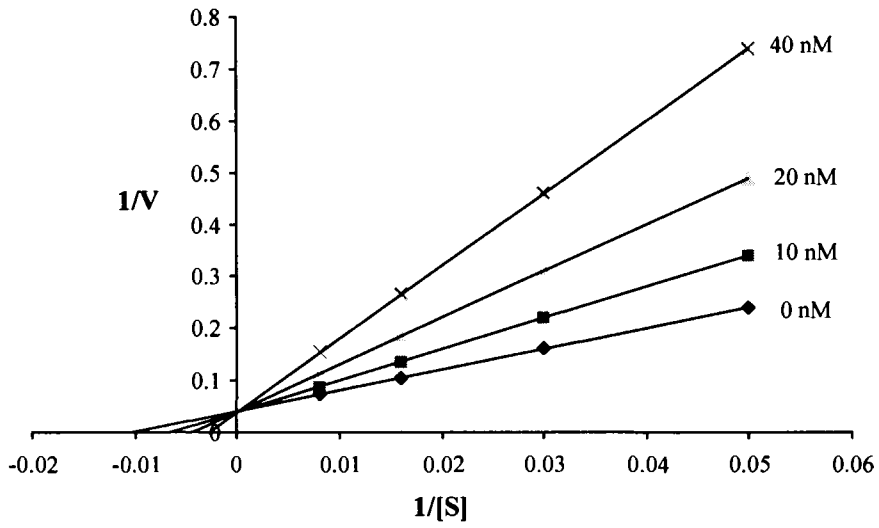

Figure 18: The double reciprocal plot in the presence of different fixed concentrations of a competitive inhibitor.

The affinity of a inhibitor for the active site of an enzyme is described by the K_i value of a competitive inhibitor. For a series of competitive inhibitors, those with the lowest K_i values will cause the greatest degree of inhibition at a fixed concentration of inhibitor [I]. The K_i value for an inhibitor can be determined from the secondary plot in which the slope of each reciprocal plot is graphed vs. the corresponding inhibitor concentration (figure 19). The x-axis intercept is equal to $-K_i$. In the presence of a concentration of inhibitor [I] that is approximately equal to K_i the substrate concentration has to double to maintain the same velocity as in the absence of the inhibitor. It is generally assumed that if plasma or tissue concentrations of a competitive inhibitor exceed the K_i, a measurable inhibition of the enzyme is likely to occur. Conversely, if the plasma or tissue concentrations are less than K_i, inhibition of the enzyme may be negligible (Kakkar *et al.*, 1999).

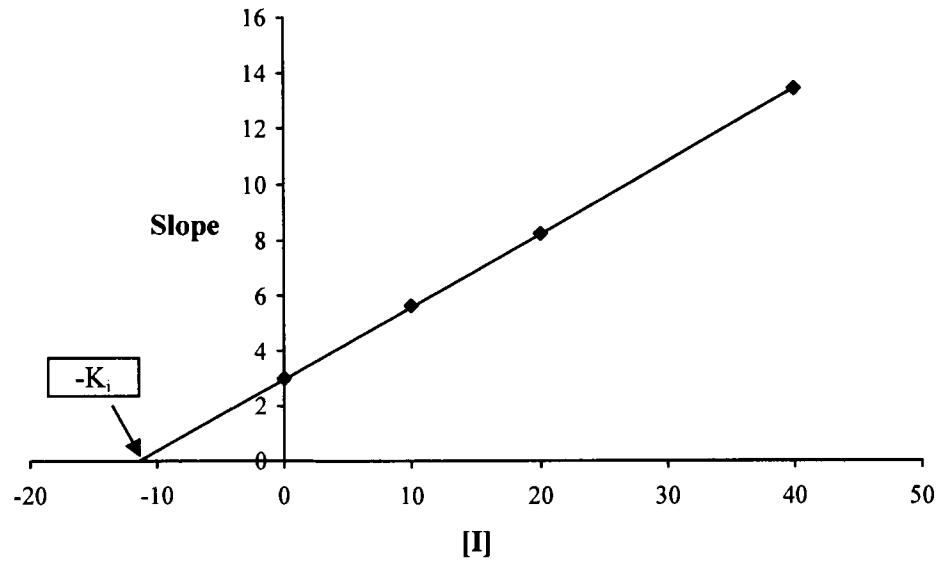

Figure 19: Secondary plot of the slope from the double reciprocal plot versus inhibitor concentration.

4.4. Determination of MOA-B catalytic activity

The literature reports several assays for the determination of MAO-B catalytic activity. For the purpose of this study we chose two different substrates to measure the activity of MAO-B. In the first instance the extent by which various concentrations of the test inhibitors slowed the rate of the oxidation of MMTP **(8)** to the corresponding dihydropiyridinium metabolite $MMDP^+$ **(9)** was measured spectrophotometrically (Inoue *et al.*, 1999). In a second approach benzylamine **(11)**, a selective MAO-B substrate, was utilized to measure the K_i values. Benzylamine is arguably the most thoroughly characterized substrate of MAO-B and is frequently used in inhibition studies involving this enzyme (Krueger *et al.*, 1995). In this assay, when using purified MAO-B as enzyme source which is relatively free from background interference, the concentration of the α - carbon oxidation product, benzaldehyde (λ_{max} = 250 nm), may be measured spectrophotometrically (Walker & Edmondson, 1994). In contrast, background absorption in the near UV wavelength range when using mitochondrial fraction as enzyme source is too high to accurately measure benzaldehyde concentrations by spectrophotometry. Even protein precipitation and subsequent centrifugation of the

incubations does not solve this challenge. For this reason it was decided to measure the extent of benzylamine oxidation by HPLC-UV analysis following a discontinuous assay.

4.4.1. Linearity of benzylamine oxidation with time

In order to select a suitable incubation time for benzylamine with baboon liver MAO-B, we determined the time interval for which the MAO-B catalyzed benzaldehyde formation remains linear under our assay conditions.

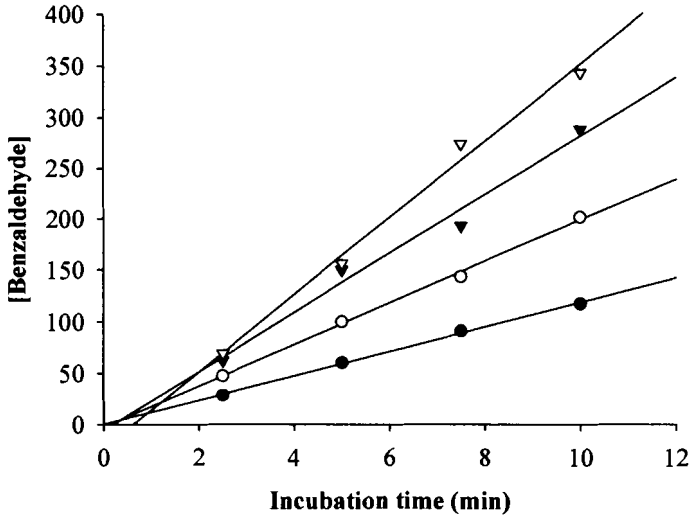

Figure 20: Linearity in the oxidation of benzylamine by baboon liver MAO-B (0.15 mg/mL of the mitochondrial preparation). The concentration of benzaldehyde produced was measured by HPLC analysis following termination of the enzyme catalyzed reaction at time points of 2.5, 5, 7.5 or 10 minutes. The concentration of benzaldehyde produced is expressed as n moles/mg mitochondrial protein. The concentrations of benzylamine used in this study were 125 μM (filled circles), 250 μM (open circles), 500 μM (filled triangles) and 750 μM (open triangles).

Various concentrations of benzylamine (125–750 μM) were incubated with the mitochondrial isolate (0.15 mg protein/ml) at 37 °C for various periods of time (2.5–10 min). For the purpose of this study no inhibitor was included in the reaction incubations. Following termination of the reactions by the addition of 10 μL perchloric acid, the concentrations of the MAO-B generated benzaldehyde were measured by HPLC analysis.

Graphs of benzaldehyde concentration as a function of time were constructed. As illustrated in figure 20 benzylamine oxidation by MAO-B is linear for at least 10 minutes following inhibition of the enzyme reaction.

4.4.2. K_m determination of benzylamine for baboon liver MAO-B

The steady state rate of benzylamine oxidation by baboon liver MAO-B was measured by HPLC analysis as outlined above.

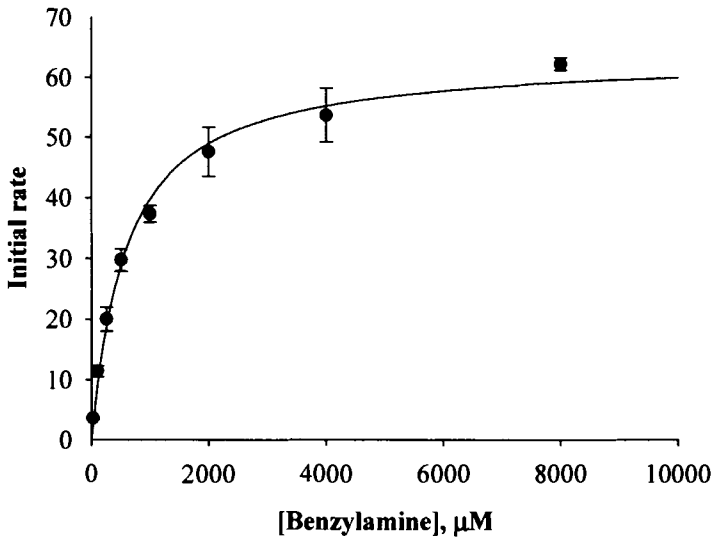

Figure 21: Determination of the K_m value of benzylamine oxidation by baboon liver MAO-B. The concentration of benzaldehyde produced was measured by HPLC analysis following an 8 minute incubation with 0.15 mg/ml baboon liver mitochondria at 37 °C. A K_m value of 616 ± 23µM was estimated by fitting the data to the Michaelis–Menten equation using a nonlinear least-squares fitting routine. All measurements were conducted in triplicate and the benzylamine concentration in the incubations ranged from 25 to 8000µM. The initial rates are expressed as nmoles.mg protein^{-1}.min^{-1} of benzaldehyde formed.

In order to determine a K_m value for the oxidation of benzylamine, rates were measured with eight different substrate concentrations spanning at least two orders of a magnitude (25–8000 µM). The enzyme concentration utilized was 0.15 mg/mL of the baboon liver

homogenate and all incubations were carried out at 37 °C for a time period of 8 min. Benzaldehyde concentrations were measured with the aid of a linear calibration curve prepared over a range of 1.5 to 50μM. The kinetic data (initial rates as a function of substrate concentration) were fitted to the Michaelis-Menten equation (Segel, 1993) using a nonlinear least-squares fitting routine incorporated into the SigmaPlot software package. This determination was carried out in triplicate and the K_m value was found to be 616 ± 23μM (mean ± standard deviation).

4.4.3. Studies with clorgyline and (*R*)-deprenyl

Mitochondrial fractions obtained from baboon liver tissue are reported to be devoid of MAO-A activity (Petzer *et al.*, 2003). In order to verify this, MAO-A was inactivated by preincubating the mitochondrial preparations (0.3 mg of protein/ml) with clorgyline (3×10^{-8}M) for a period of 15 minutes at 37 °C.

The MAO-B form of the enzyme was inactivated by preincubating the mitochondrial preparations (0.3 mg of protein/ml) with (*R*)-deprenyl (3×10^{-7}M) (Inoue *et al.*, 1999). The solvent for these incubations was 100mM sodium phosphate buffer (pH 7.4). Following these preincubations, the mitochondrial homogenates were added to various concentrations of MMTP (30–120μM) to a final concentration of 0.15 mg/ml. After another 15 min incubation, the reaction was terminated by the addition of 10 μL perchloric acid and the concentration of the reaction product, $MMDP^+$, was measured as described above. As shown in figure 22 clorgyline addition to the mitochondrial factor had no effect on the oxidation rate of MMTP, while (*R*)-deprenyl completely suppressed $MMDP^+$ formation. These results verify the absence of MAO-A in the mitochondrial fraction of baboon liver mitochondria.

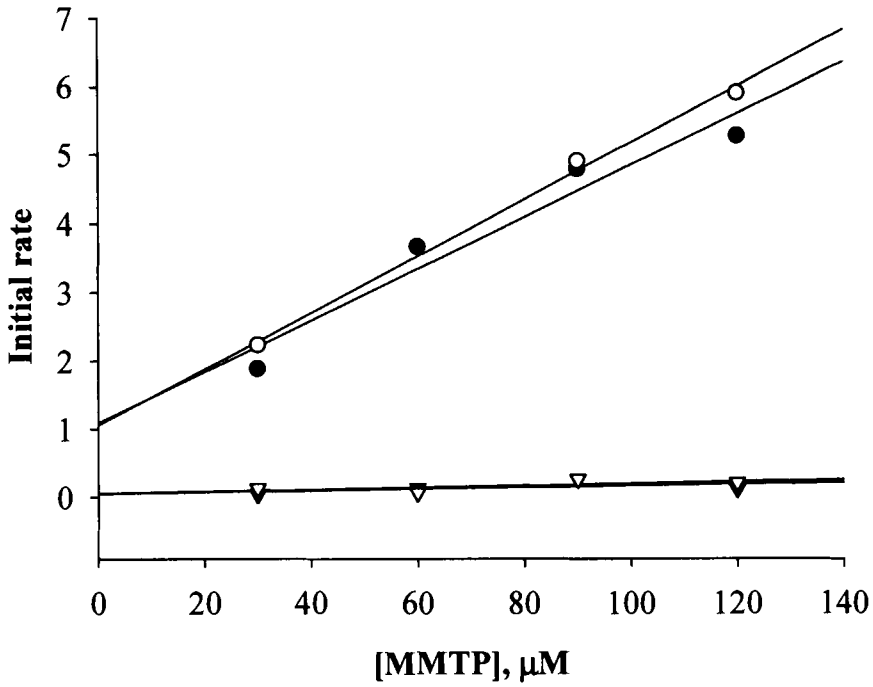

Figure 22: The rate of baboon liver MAO-B catalyzed oxidation of various concentrations of MMTP in the absence (filled circles) and presence of 3×10^{-8}M clorgyline (open circles), 3×10^{-7}M (*R*)-deprenyl (filled triangles) and in the presence both clorgyline and (*R*)-deprenyl (open triangles).

4.5. Inhibition studies

4.5.1. Materials and instrumentation

The oxalate salt of MMTP (**8**) was supplied by Prof. Neal Castagnoli, Jr. HPLC analyses were performed with an Agilent 1100 HPLC system equipped with a variable wavelength detector and a Macherey-Nagel CC 125/4 Nucleosil C18 column (4.6 × 100 mm, 5 μm). UV-Vis spectra were recorded on a Milton-Roy Spectronic 1201 spectrophotometer.

4.5.2. MAO-B activity measurements and inhibition studies.

Mitochondria were isolated from baboon liver tissue as described by Salach and Weyler (1987) and stored at –70 °C. The mitochondrial isolate was suspended in sodium phosphate buffer (100mM, pH 7.4 containing 50% glycerol, w/v) and the protein concentration was determined by the method of Bradford (1976). For the inhibition

studies on MAO-B we utilized the MAO-A and –B mixed substrate MMTP (K_m = 60.9μM for baboon liver MAO-B; Inoue *et al.*, 1999) and the MAO-B selective substrate benzylamine (K_m = 616 ± 23μM for baboon liver MAO-B). Since baboon liver mitochondria are devoid of MAO-A activity, inactivation of this enzyme was unnecessary in the studies where MMTP was utilized as substrate (Inoue *et al.*, 1999). A typical incubation (500 μL final volume in 100mM sodium phosphate buffer, pH 7.4) contained MMTP (30–120μM) or benzylamine (125–750μM), the mitochondrial isolate (0.15 mg protein/ml) and various concentrations of the test inhibitors. Stock solutions of the inhibitors were prepared in DMSO and were added to the incubation mixtures to yield a final DMSO concentration of 4% (v/v). The samples were incubated at 37 °C and the incubation times were 15 min for MMTP and 8 min for benzylamine. For these time periods the MAO-B catalyzed production of $MMDP^+$ (Inoue *et al.*, 1999) and benzaldehyde were linear with time. The reactions were terminated by the addition of 10 μL 70% perchloric acid and the samples were centrifuged at 16,000*g* for 10 minutes. The supernatant fractions were removed and the concentrations of the MAO-B generated products, $MMDP^+$ (where MMTP served as substrate) and benzaldehyde (where benzylamine served as substrate), were measured. $MMDP^+$ formation was measured spectrophotometrically at a wavelength of 420 nm (ε = 25,000 M^{-1}) (Inoue *et al.*, 1999) while benzaldehyde concentrations were measured using HPLC analysis. In the latter case, a reversed phase C18 column was used and the mobile phase consisted of 60% distilled water [containing 0.6% (v/v) glacial acetic acid and 1% (v/v) triethylamine], 30% methanol and 10% acetonitrile at a flow rate of 1 ml/min. A volume of 50 μL of the supernatant was injected into the HPLC system and the elution of benzaldehyde (3.97 min) was monitored at a wavelength of 250 nm. Quantitative estimations of benzaldehyde were made by means of a linear calibration curve ranging from 6.25 to 50μM. Initial rates were expressed as n moles of product ($MMDP^+$ or benzaldehyde) formed per mg mitochondrial protein per min. Competitive K_i values were determined by calculating the initial rates of substrate oxidation in the absence and presence of varying concentrations of the inhibitors and constructing Lineweaver-Burke plots with increasing concentrations of the inhibitor. The slopes of the Lineweaver-Burke plots were plotted as a function of the inhibitor concentration and the K_i value were determined from the

abscissa intercept (intercept = $-K_i$) (Segel, 1993). Linear regression analysis was performed using the SigmaPlot software package (Systat Software Inc.).

4.5.3. Calculations

The initial velocity (V_i) of MAO-B catalytic oxidation was calculated using one of the equations below. For the spectrophotometric determination of MAO-B activity (with MMTP **(8)** as substrate) the measured absorbance (Abs) of the dihydropyridinium metabolite $MMDP^+$ **(9)**, the reported extinction coefficient (ε) for $MMDP^+$ (24,000 M^{-1}) together with the enzyme concentration [E] (0.15 mg protein/mL) and incubation time (15 minutes) were substituted in equation 5. The dimension of V_i in this equation is mol.mg $protein^{-1}.min.^{-1}$ of the dihydropyridinium formed.

$$V_i = \frac{Abs}{\varepsilon} \times \frac{1}{[E]} \times \frac{1}{Time} \qquad \textbf{Equation 5}$$

In the case of benzaldehyde quantitative determinations were carried out by HPLC analysis. The initial velocity (V_i) of the enzyme reaction with benzaldehyde as substrate was expressed as concentration (n moles) of benzaldehyde per mg protein per minute. Equation 6 was used to calculate V_i.

$$V_i = (nmoles\ of\ benzaldehyde\ produced)\ \text{x}\ \frac{1}{[E]}\ \text{x}\ \frac{1}{Time} \qquad \textbf{Equation 6}$$

4.6. SAR study

Values for the substituent parameters σ_m, σ_p, F, π and E_s were obtained from the publication of Hansch & Leo (1995) and those for the Van der Waals volume (V_w) from Hansch & Leo (1979). Stepwise multiple linear regression analysis of the $\log K_i$ values as a function of the substituent parameters was carried out with the Statistica software package (StatSoft Inc.). In order to estimate the significance of the regression equations the F statistic was employed. An F value higher than the critical F value was judged to be significant and critical F values were calculated as described recently (Livingstone & Salt, 1995). The critical F value (F_{max}) for 5% significance for models constructed from

ten logK_i values (table 2) and which contains one parameter (out of a possible five: V_w, E_s, π, σ_m, F) was calculated to be 15.27 while a model containing two parameters has an F_{max} value of 12.95. The F_{max} value for models constructed from nine logK_i values (table 7) and which contains one parameter (out of a possible five: V_w, E_s, π, σ_p, F) was calculated to be 17.29 while the F_{max} for two parameter models was calculated to be 15.75.

4.7. Results and discussion

All of the (*E*)-8-styrylcaffeinyl analogues (**1a–h**) tested were found to be inhibitors of MAO-B. As demonstrated by example with (*E*)-8-(4-methylstyryl)caffeine (**1d**) (figure 23), the lines of the Lineweaver–Burke plots intersected indicating that the mode of inhibition was competitive (Segel, 1993). The K_i values for the inhibition of MAO-B are presented in table 7. The lead compound for this study, CSC (**1f**), was shown (Chen *et al.*, 2002) to be a very potent inhibitor with a K_i value of 148nM for the inhibition of benzylamine oxidation by MAO-B. The similarity in range of this value with that obtained with MMTP as substrate (128nM) is an indication of the reliability of the K_i estimations and also suggests that specific alterations in experimental conditions (such as change of substrate or analytical technique) do not affect the estimated values to a large extent. In accordance with this view, for the other analogues (**1a–e** and **1g–h**) tested, the differences between the K_i values estimated by the two different techniques are within the range expected for experimental error (table 7).

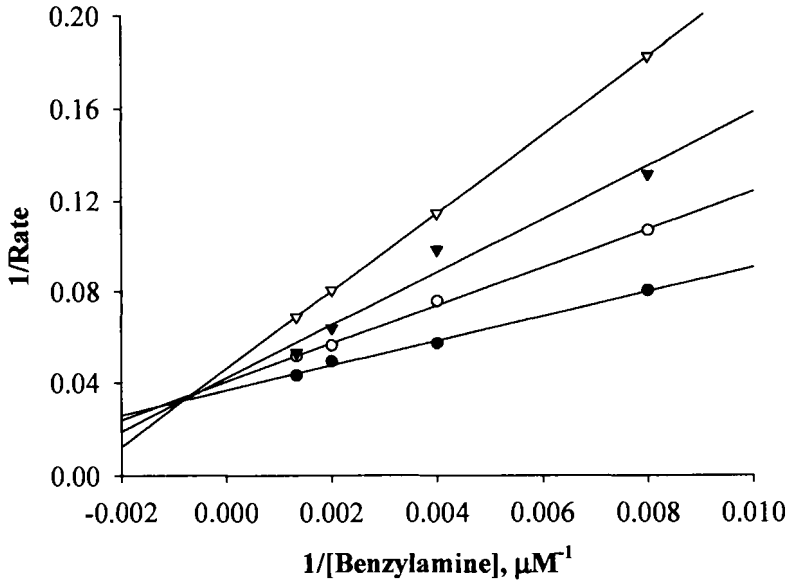

Figure 23: Lineweaver–Burke plots of the oxidation of benzylamine by baboon liver MAO-B in the absence (filled circles) and presence of various concentrations of **1a** (open circles, 0.1μM; filled triangles, 0.2μM; open triangles, 0.4μM). The concentration of the baboon liver mitochondrial preparation was 0.15 mg/ml and the rates are expressed as nmoles.mg protein^{-1}.min^{-1} of benzaldehyde formed.

Qualitative inspection of the results in table 7 suggests that the potency of MAO-B inhibition by (*E*)-8-styrylcaffeinyl analogues bearing substituents on C-3 of the styryl ring (**1a, 1c, 1f, 1i**) depends upon the electronic characteristics of the substituent since those analogues with electron withdrawing groups (**1a** and **1d–e**) are significantly more potent as inhibitors than the unsubstituted analogue (**1h**) and the analogue bearing an electron donating methyl group (**1c**). In contrast, potency of inhibition by analogues bearing substituents on C-4 of the styryl ring (**1b, 1d, 1e, 1g**) appears to be dependent upon the size the substituent since inhibition by those analogues with relatively bulky substituents (**1b** and **1d-e**) are more potent than the unsubstituted analogue (**1h**) and the analogue bearing a C-4 fluorine substituent (**1e**). In order to quantify these apparent relationships between MAO-B inhibitory activity and the physiochemical properties of the substituents, a Hansch-type SAR (Hansch & Leo, 1995; Kutter & Hansch, 1969; Fuller *et al.*, 1968) study was carried out by stepwise multiple linear regression. Five

parameters were used to describe each substituent. The Van der Waals volume (V_w) (Bondi, 1964) and Taft steric parameter (E_s) (Hansch *et al.*, 1995) were used as descriptors of bulkiness while the lipophylicity of the substituents were described by the Hansch constant (π) (Fujita *et al.*, 1964). The classical Hammett (σ_m or σ_p) and Swain–Lupton (F) constants (Swain & Lupton, 1968) served as electronic parameters. All physiochemical values of the substituents were obtained from standard compilations (Hansch & Leo, 1995; Hansch *et al.*, 1995; Hansch & Leo, 1979).

Table 7: The K_i values for the inhibition of MAO-B by (*E*)-8-styrylcaffeinyl analogues. The values of the selected physiochemical parameters used in the SAR study are also listed (Hansch & Leo, 1995; Hansch & Leo, 1979).

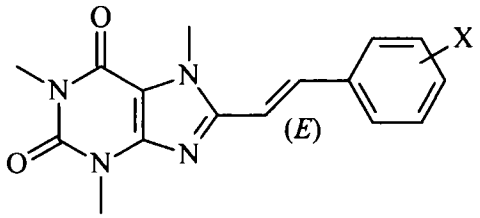

Compd	X	K_i value (nM) [a]		V_w [d]	π [e]	F [e]
		7 as substrate [b]	**10** as substrate [c]			
1f	3-Cl	70 [f], 128	148	1.07	0.71	0.42
1a	3-CF_3	133	188	1.11	0.88	0.38
1c	3-CH_3	1431	1526	1.01	0.56	0.01
1i	3-F	400 [g]	–	0.36	0.14	0.45
1h	H	2704 [g] 2864	2316	0.08	0.00	0.00
1g	4-Cl	260	187	1.07	0.71	0.42
1b	4-CF_3	245	238	1.11	0.56	0.38
1d	4-CH_3	367	373	1.01	0.88	0.01
1e	4-F	1559	1374	0.36	0.14	0.45

[a] The enzyme source used was MAO-B from baboon liver mitochondria. [b] MMTP served as enzyme substrate. [c] Benzylamine served as enzyme substrate. [d] Values obtained from Hansch & Leo (1979). [e] Values obtained from Hansch & Leo (1995). [f] K_i value obtained from Chen *et al.* (2002). [g] K_i value obtained from Petzer *et al.* (2003).

The analogues were divided into two groups – those bearing substituents on C-3 of the styryl ring (**1a, 1c, 1f, 1i**) and those with substituents on C-4 of the styryl ring (**1b, 1d–e,**

1g). The unsubstituted (*E*)-8-styrylcaffeinyl analogue (**1h**) was considered a member of each group. Results of the statistical analysis for the two groups are shown in table 8 and 9, respectively. For analogues substituted at C-3 of the styryl ring (table 8) the only single substituent parameters that show a meaningful correlation with the logarithm of the K_i values (expressed in μM) are the Hammett electronic parameter (σ_m) and the Swain–Lupton F constant. Regression analysis of logK_i with σ_m and F exhibits good correlations with R^2 values of 0.89 and 0.88, respectively. The statistical F test values were found to be 54.9 and 50.7 for the two correlations (a higher F value indicates a better fit) (Livingstone & Salt, 2005) with confidence levels of >99.9%. All other single-parameter correlations with the logK_i values exhibited poorer statistical correlations. Correlation was improved by including an additional substituent parameter to the regression analysis. Two-parameter fits with V_w and F or with π and F yielded correlation coefficients of 0.97 and 0.98, respectively. For these correlations, the probabilities that V_w and π are zero are only 0.82% and 0.16%, respectively. Therefore, the best mathematical description of binding affinity (logK_i) of C-3 substituted (*E*)-8-styrylcaffeinyl analogues to MAO-B are:

$$\text{Log}K_i = -1.98(\pm 0.18)F - 0.60(\pm 0.11)\pi + 0.47(\pm 0.06) \qquad \textbf{Equation 7}$$

$$(F = 143.5 \text{ and } R^2 = 0.98)$$

The negative value of both the F (–1.98 ● 0.18) and the π (–0.60 ● 0.11) parameter coefficients indicate that the potency (logK_i) of MAO-B inhibition by (*E*)-8-styrylcaffeinyl analogues may be enhanced by substitution with lipophylic C-3 functional groups with electron withdrawing characteristics. Since the Van der Waals volume (V_w) is also negatively correlated (–0.41 ● 0.11; Table 8) with logK_i, larger C-3 substituents also appears to enhance MAO-B inhibition potency.

For analogues substituted at C-4 of the styryl ring (table 9) the single-parameter fits that shows the best correlations with the logK_i values are the Van der Waals volume V_w and the Hansch constant (π) of the substituents. The regression analysis exhibits F values of 163.9 and 140.2 with a confidence level of >99.9% for the two correlations. The mathematical description of the binding affinity (logK_i) of C-4 substituted (*E*)-8-styrylcaffeinyl analogues to MAO-B may therefore be presented as:

$$\text{Log}K_i = -1.02(\pm 0.08)V_w + 0.54(\pm 0.07) \qquad \textbf{Equation 8}$$

$$(F = 163.9 \text{ and } R^2 = 0.95)$$

or

$$\text{Log}K_i = -1.28(\pm 0.11)\pi + 0.38(\pm 0.06) \qquad \textbf{Equation 9}$$

$$(F = 140.2 \text{ and } R^2 = 0.95)$$

Table 8: Correlations of the MAO-B inhibition constants (logK_i) of (*E*)-8-styrylcaffeinyl analogues bearing substituents on C-3 of the styryl ring (**1a, 1c, 1f, 1h–i**) with steric, electronic and hydrophobic substituent parameters.[a]

Parameter	Correlation (slope)	*y*-intercept	Coefficient of determination	F[b]	Significance[c]
σ_m	-2.38 ± 0.32	0.19 ± 0.09	0.89	54.9	0.00015
F	-2.50 ± 0.35	0.29 ± 0.11	0.88	50.7	0.00019
V_w	-0.85 ± 0.35	0.36 ± 0.31	0.45	5.8	0.048
E_s	0.40 ± 0.19	0.15 ± 0.26	0.39	4.5	0.073
π	-1.22 ± 0.40	0.32 ± 0.24	0.58	9.5	0.018
$V_w + F$	-0.41 ± 0.11	0.52 ± 0.09	0.97	83.6	0.0082
	-2.11 ± 0.22				0.000081
$\pi + F$	-0.60 ± 0.11	0.47 ± 0.06	0.98	143.5	0.0016
	-1.98 ± 0.18				0.000036

[a] The logK_i values (expresses in μM) obtained with both substrates (**8** and **11**) were used in the linear regression analysis; [b] The F test statistic relates the mean squares due to regression to the error variance. Higher F values indicate a better fit and a regression equation with an F value higher than the critical F value may be deemed significant. Critical F values may be calculated as described recently (Livingstone & Salt, 2005). [c] The significance is the fractional probability that the coefficient of the added variable is zero.

As observed with the analogues substituted at the C-3 position, the negative value of the V_w parameter coefficient (–0.92 ± 0.11) suggest that the potency (logK_i) of MAO-B inhibition may be enhanced by substitution with bulky C-4 functional groups. On the

other hand, the electronic contribution of the C-4 substituents to logK_i appears to be negligible since in a two-parameter fit with V_w and F, the probability of the term containing F being zero is 45%. The same argument applies to the other electronic parameter (σ_p) considered in this study (data not shown). There is also a meaningful correlation (R^2 = 0.95; F = 140.2) between the Hansch constants (π) of the C-4 substituents and the logK_i values. Hydrophobic C-4 functional groups appears to favour inhibition potency since the sign of the π parameter coefficient (–1.28 ± 0.11) is negative. Again there does not seem to be an electronic contribution of the C-4 substituents to logK_i since in a two parameter fit of logK_i with π and F or of logK_i with π and σ_p the probability of the terms containing σ_p and F are 17.8% and 97.5%, respectively (data not shown).

Table 9: Correlations of the MAO-B inhibition constants (logK_i) of (*E*)-8-styrylcaffeinyl analogues bearing substituents on C-4 of the styryl ring (**1b, 1d–e, 1g–h**) with steric, electronic and hydrophobic substituent parameters.[a]

Parameter	Correlation (slope)	*y*-intercept	Coefficient of determination	F[b]	Significance[c]
σ_p	-0.94 ± 0.56	-0.08 ± 0.15	0.26	2.8	0.13
F	-0.77 ± 0.72	-0.01 ± 0.23	0.12	1.3	0.32
V_w	-1.02 ± 0.08	0.54 ± 0.07	0.95	163.9	0.000001
E_s	0.44 ± 0.11	0.24 ± 0.15	0.65	14.7	0.005
π	-1.28 ± 0.11	0.38 ± 0.06	0.95	140.2	0.000002
$V_w + F$	-1.00 ± 0.09	0.56 ± 0.07	0.96	78.7	0.000008
	-0.14 ± 0.18				0.45

[a] The logK_i values (expresses in μM) obtained with both substrates (**8** and **11**) were used in the linear regression analysis; [b] The F test statistic relates the mean squares due to regression to the error variance. Higher F values indicate a better fit and a regression equation with an F value higher than the critical F value may be judged as significant. Critical F values may be calculated as described recently (Livingstone & Salt, 2005)[c]. The significance is the fractional probability that the coefficient of the added variable is zero.

4.8. Summary

The K_i values for the inhibition of MAO-B by (*E*)-8-styryl caffeine analogues were determined using two techniques. In order to determine whether there are relationships between the structures of the compounds and their inhibition potency, a Hansch-type SAR study was carried out. The results indicated that the MAO-B inhibition potency of (*E*)-8-styrylcaffeine analogues bearing C-3 substituents are dependant upon electronic properties as well as descriptors of bulkiness and lipophylicity. Substituents that are electron withdrawing and relatively large and lipophylic appear to enhance MAO-B inhibition potency. For (*E*)-8-styrylcaffeine analogues bearing substituents on the C-4 position, the potency of MAO-B inhibition appears to depend only upon descriptors of size and lipophylicity. For these analogues larger lipophylic substituents appear to enhance inhibition potency.

CHAPTER 5

Molecular modelling

Summary and abbreviations

In this chapter the molecular modelling is reported in order to gain insight into the mode of binding between the CSC analogues and the MAO-B active site. The results of the hypothesis generation as well as the docking of the CSC analogues in the MAO-B substrate cavity are discussed.

CoMFA	–	Comparative molecular field analyses
CSC	–	(*E*)-8-(3-Chlorostyryl)caffeine
FAD	–	Flavin-adenine dinucleotide
MAO-B	–	Monoamine oxidase B
PD	–	Parkinson's disease
SAR	–	Structure-activity relationships
UNCERT	–	Uncertainty factor

5.1. Introduction

Molecular modelling is a general term that covers a wide range of molecular graphics and computational chemistry techniques used to build, display, manipulate, simulate, analyse molecular structures and to calculate properties of these structures. Molecular modelling is used in a number of different research areas, and therefore the term does not have a rigid definition. To a chemical physicist, molecular modeling might imply performing a high quality quantum mechanical calculation using a supercomputer on a structure with 4 or 5 atoms; to an organic chemist, molecular modelling may mean displaying and modifying a candidate drug molecule on a desktop computer.

Monoamine oxidase B (MAO-B), an FAD containing enzyme located in the outer mitochondrial membranes of neuronal, glial and other cells, catalyses the oxidative deamination of biogenic and xenobiotic amines to the corresponding aldehyde and ammonia in the periphery as well as in the central nervous system. MAO-B preferentially catalyses the deamination of β-phenylethylamine and benzylamine

and is irreversibly inhibited by nanomolar concentrations of (*R*)-deprenyl, a mechanism based inactivator (Grimsby *et al.*, 1990).

Table 10: The training set used in the generation of the hypothesis for MAO-B inhibition.

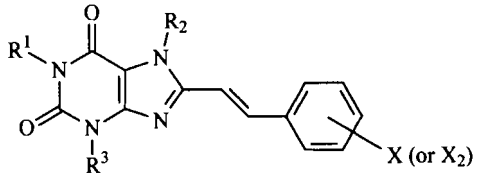

Compound	R^1/R^3	R^2	X/X_2
1a	Methyl	Methyl	3-CF_3
1b	Methyl	Methyl	4-CF_3
1c	Methyl	Methyl	3-CH_3
1d	Methyl	Methyl	4-CH_3
1e	Methyl	Methyl	4-F
1f	Methyl	Methyl	3-Cl
1g	Methyl	Methyl	4-Cl
1h	Methyl	Methyl	H
1i	Methyl	Methyl	3-F
3a	Ethyl	Methyl	3,4-Dimethoxy
3b	Methyl	Methyl	3-Chloro
3c	Ethyl	Methyl	3-Chloro
3d	Methyl	Methyl	3,4-Dimethoxy
3e	Methyl	Methyl	H
3f	Methyl	Methyl	3-Fluoro
3g	Ethyl	Methyl	3,4-Methylenedioxy
3h	Methyl	3-Nitro	Methyl
4a	Ethyl	H	3,4-Dimethoxy
4b	Methyl	H	3-Chloro
4c	Ethyl	H	3-Chloro
4d	Methyl	H	3,4-Dimethoxy
4e	Methyl	H	3-Fluoro
4f	Methyl	H	H
4g	Ethyl	H	3,4-Methylenedioxy
4h	Methyl	H	3-Nitro

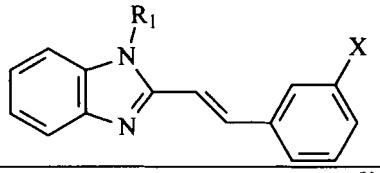

Compound	R^1	X
6a	H	H
6b	H	Chloro
6c	H	Fluoro
7a	Methyl	H
7b	Methyl	Chloro
7c	Methyl	Fluoro

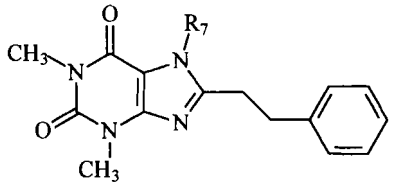

Compound	R^7
5a	H
5b	Methyl

Due to the key role played by MAO-B in the metabolism of neurotransmitters, inhibititors of MAO-B represent a useful approach for the potential treatment of several psychiatric and neurological diseases. In particular, reversible and selective MAO-B inhibitors are under investigation for the treatment of Parkinson's disease (PD) and Alzheimer's disease (Wouters, 1998).

In this study a computational study was conducted using several classes of moderate to potent reversible MAO-B inhibitors (**1a–i, 3a–h, 4a–h, 5a-b, 6a–c and 7a–c**; table 10), some of which are also reported to be A_{2A} antagonists. Hypothesis generation was used to establish a general MAO-B inhibitor pharmacophore. Finally, the availability of the X-ray crystal structure of human MAO-B (Binda *et al.*, 2003) enabled the docking of these compounds within the active site of MAO-B.

5.2. Establishing a hypothesis for MAO-B inhibition

In the drug discovery process, one of the critical tasks is building a model with the characteristics of the drug under development, also known as a hypothesis. A hypothesis in this case is a set of characteristics that distinguishes a set of molecules for activity at a desired target. A hypothesis can contain an arbitrary set of 3D data, 2D (topological) data, 1D (scalar) parameters, and constraint descriptions. The hypothesis is constructed by assembling substructures and chemical functions from which general properties are determined in a specific special position to predict the activity of theoretical molecules to their specific area of action.

5.2.1. Selection of compounds

The compounds necessary for hypothesis generation (training set) must contain certain structural relationships and comparable activities in order to generate a more specific and accurate model. The compounds selected as the training set for the hypothesis were from several classes of moderate to potent reversible MAO-B inhibitors (**1a–f, 1h–i, 3a–h, 4a–b, 5a-h, 6a–c and 7a**; Petzer *et al.*, 2003). These compounds contain structural similarities and accounts for a relatively potent range of activity. Studies have been performed with certain of these structures and certain

structure-activity relationships (SAR) have been established for inhibitory action on the MAO-B enzyme, thus rendering it suitable for hypothesis generation.

5.2.2. Method

The compounds were drawn on the interface provided by Catalyst 4.9®. The structures were then optimized to a minimum energy conformation. From these conformations several conformational models were generated representing the flexibility of these molecules. The conformational model emphasizes coverage and consists of a representative set of conformers taken from the range of energetically reasonable conformations of the molecules. Catalyst 4.9® provides two types of conformational analysis: *fast* and *best quality*. The *best quality* method was selected, because it provides the best conformational coverage possible within Catalyst. This is the method of choice if the conformational models are to be used for hypothesis generation, since the arrangement in space of chemical features are considered instead of the arrangement of atoms and it provides the most comprehensive evaluation of flexible ring systems. After conformation generation, the compounds (with their individual conformers) were listed on a spreadsheet together with their activities. Hypogen® was used to calculate the hypotheses. For hypothesis generation Hypogen® gave better results, because HipHop® doesn't use quantitative properties for its calculations, but only displays properties involved in the hypothesis without activity prediction The program parameters were set to search for at least 1 hydrogen bond acceptor, at least 2 hydrophobic groups and at least 1 aromatic ring. The total number of features that the hypotheses should have were set to a minimum of three to convey the three points in space needed for a three dimensional structure. The uncertainty factor (UNCERT) was set to 1.8. After a run of hypothesis calculations, the log file gave the calculated values for each hypothesis generated. The values of interest are the *total cost* of each generated hypothesis, the *weight cost* of each generated hypothesis, the *total fixed cost* of the calculation run (at which the regression value is set to 1) and the *total cost of the null hypothesis* (at which the regression value is set to 0). The hypothesis's total cost should be as close as possible to the total fixed cost and should differ with 40–

60 bits from the total cost of the null hypothesis. The weight cost should be relatively close to 2.

5.2.3. Results and discussion

A hypothesis indicating the features necessary for MAO-B inhibition was obtained.

A	Hypothesis total cost	92.0215
B	Hypothesis weight	2.56
C	Total fixed cost	60.4481
D	Total cost (null hypothesis)	139.827

The hypothesis total cost (**A**) differed from the total cost of the null hypothesis (**D**) with 47.8055 which is well in the 40–60 range, assuring a 75–90% accuracy (Catalyst® tutorial guide).

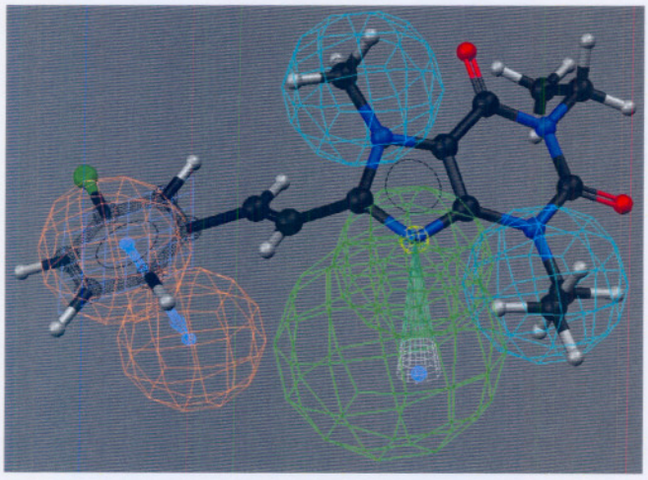

Figure 24: The final hypothesis with compound **3c** embedded in the hypothesis. (Colour key: green = hydrogen bond acceptor; blue = hydrophobic group; amber = aromatic ring)

The final hypothesis contained four features: one hydrogen bond acceptor, two hydrophobic groups and one aromatic ring (figure 24).

The regression model of this hypothesis with the set of training compounds gave a regression value of 0.818275 (figure 25).

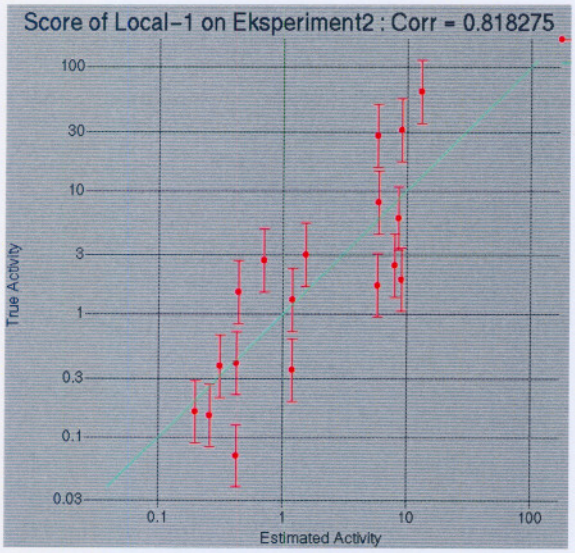

Figure 25: Regression model for the hypothesis obtained with the training set.

Three compounds (**1g, 6b–c**) were fitted into the hypothesis in order to establish the validity of the model. For these analogues the predicted inhibition activity correlated with the measured activity with a correlation coefficient of 0.98 (figure 26).

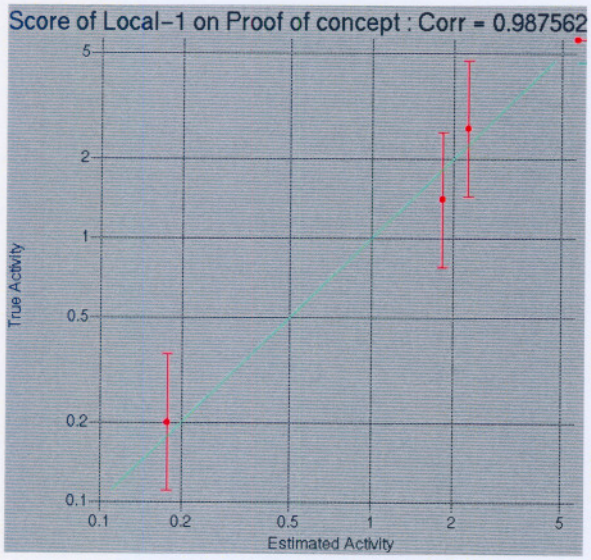

Figure 26: Correlation between predicted inhibition activity and measured activity for compound **1g**, and **6b–c**. The inhibition activities were predicted with the hypothesis generated in figure 24.

5.3. The substrate binding site of MAO-B

Docking is the procedure of fitting one molecule onto another molecule. It may involve the coupling of two types of molecule or the fitting of a ligand into the active cavity of another molecule or protein. Docking is a very useful tool to determine the possibility of a theoretical model to bind to a receptor, before actually synthesising the molecule. It is extensively utilised to determine the properties necessary for high potency. Since the crystal structure of MAO-B was recently published (Binda *et al.*, 2003) docking studies are possible with this enzyme.

There are many types of interactions that may occur between a ligand and a macromolecule as well as between atoms or subunits within the molecules. A few of these interactions are dispersion interactions, hydrogen bonding, hydrophobic interactions, electrostatic interactions, ionic binding, ion-dipole interactions, dipole-dipole interactions, ion induced dipole interactions, charge transfer and covalent bonding.

FAD is an integral part of MAO-B and functions as a co-factor in ligand binding. FAD is covalently bound to MAO-B through a 8α-S-cysteinyl bond to the Cys397 of the MAO-B enzyme (Kearney *et al.*, 1971). FAD is situated in a hydrophobic surrounding within MAO-B with specific interactions dominated by hydrogen bonding to either side chains or the peptide backbone of the protein. The only electrostatic interaction is between the anionic pyrophosphate of the FAD and the positively charged guanidine group of Arg42 (Edmondson *et al.*, 2004). The pyrophosphate bond also has extensive hydrogen bonds to water molecules and to the peptide bonds of Thr426 and Ser15. A specific interaction of Thr45 with the FAD is also proposed (Kirksey *et al.*, 1998). The ribose ring of the FAD adenosine moiety is specifically hydrogen bonded to the carboxylate of Glu34, to a guanidine group of Arg36 and to a water molecule (Edmondson *et al.*, 2004). Mutation studies carried out with Glu34 indicated a 90% loss of activity of human MAO-B (Zhou *et al.*, 1998). Therefore, the hydrogen bonds between the carboxylate of Glu34 and the ribose ring may be important for FAD binding prior to covalent incorporation as well as for maintaining structural integrity of the covalently bound FAD to MAO-B.

The specific adenine ring interactions with the protein include only hydrogen bonds to the peptide bond of Val235 and an additional hydrogen bond to a water molecule (figure 27).

In addition to the covalent thioether linkage to Cys397, hydrogen bonds between the 2-carbonyl oxygen of the pyrimidine ring and the N–H of the Met436 peptide bond and a water molecule are observed. Another hydrogen bond system is found in the pyrimidine ring between the N(3)–H and the carbonyl oxygen of Tyr60 while the N–H of Tyr60 forms a hydrogen bond with the 4-carbonyl oxygen. Hydrogen bonds are also observed between the carbonyl oxygen in position 4 and the N–H of Ser59 and there is also a water molecule that is hydrogen bonded to the N-5 position of the flavin and the 1-amino group of Lys296 (figure 27; Edmondson *et al.*, 2004).

MAO-B contains two cavities in the enzyme. The smaller entrance cavity is situated with a opening to the exterior of the enzyme and is connected to the substrate cavity. Ile199 serves as a "gate" between these two cavities. Rotation of the side chain allows for either fusion or separation of the two cavities (Binda *et al.*, 2003). Tyr435, FAD and Tyr398 form an aromatic cage wherein the ligand binds. The substrate cavity is further surrounded by Tyr326, Phe343, Leu171, Ile199, Cys172 and Ile198 (Binda *et al.*, 2003).

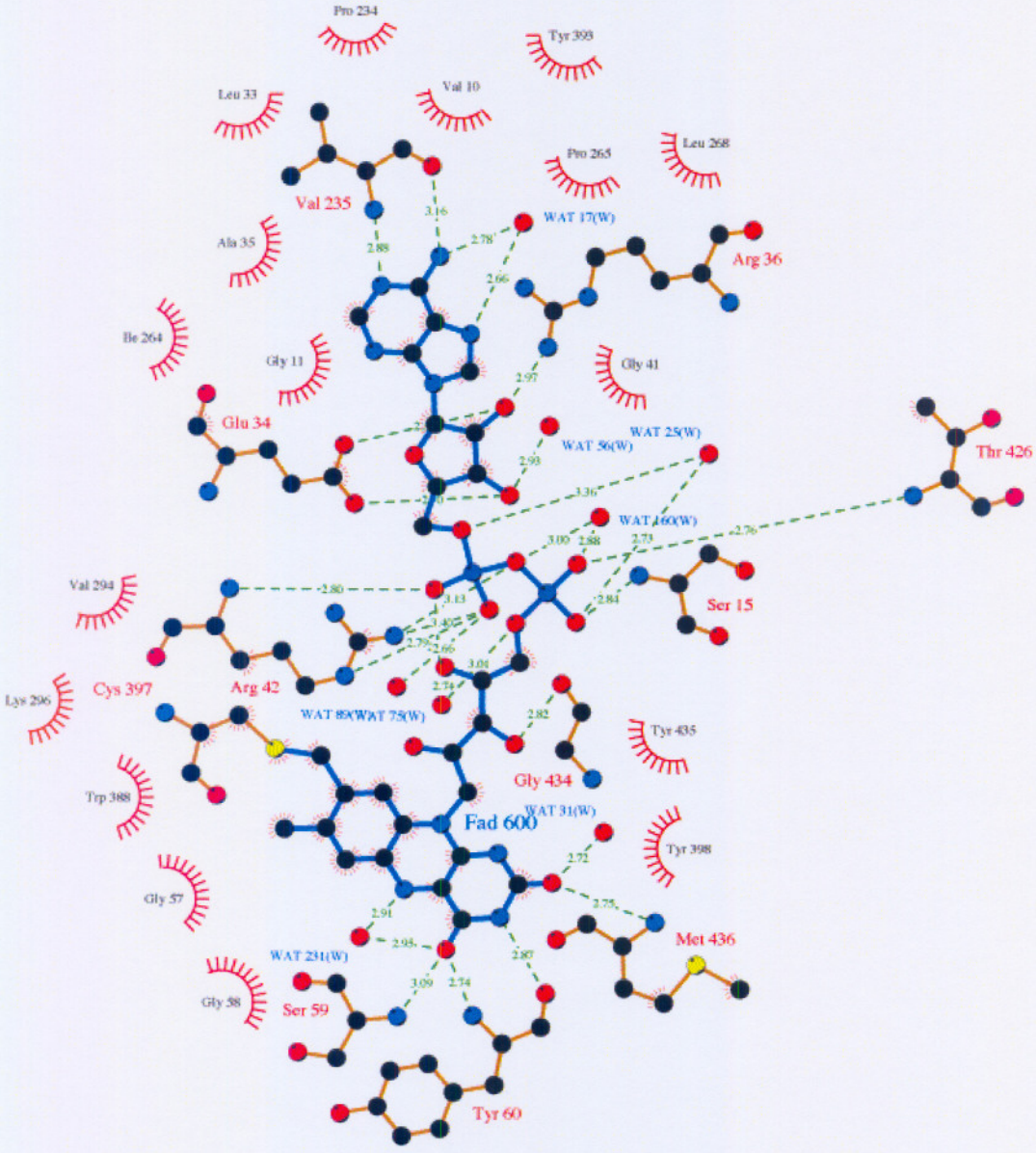

Figure 27: Illustration of FAD binding site in MAO B. Dashed lines indicate H-bonds. Carbons are in black, nitrogens in blue, oxygens in red, and sulfurs are shown as cyan spheres (Adapted from Edmondson *et al.*, 2004).

5.4. Docking studies using Cerius²

Cerius² is a molecular modelling program capable of determining possible sites for ligand binding. For these studies we used the MAO-B crystal structure (PDB: 1S2Q; Binda *et al.*, 2004). 1S2Q, a PDB file containing the coordinates for the

MAO-B enzyme co-crystallized with the inactivator rasagiline. Rasagiline is covalently bound to FAD. The docked inhibitor was used by Cerius$^{2®}$ to determine the area of the active site of the MAO-B enzyme. The different conformations of the synthesised compounds (**1a-h**) generated by Catalyst 4.9® were exported to Cerius$^{2®}$ as an SD file in order to facilitate docking of these conformations into the determined active site of the enzyme.

5.4.1. Method

The PDB file 1S2Q (Binda *et al.*, 2004)) was downloaded and opened in Cerius$^{2®}$. The solvent was removed and saved for further use in InsightII®. After searching for the active site by means of a docked ligand search, a site model was created wherein the different drug conformations were fitted into (figure 28).

The LigantFit® module of Cerius$^{2®}$ (2002) was used to fit the conformations of the compounds into the active site. The DREIDING 2.21 force field and Gasteiger charges was used throughout the experiment and other values were set to default unless otherwise specified. The compounds exported from Catalyst 4.9® were saved in a structural data (SD) file and fitted into the protein using the defined site model. The results of the fit were included into a study table and the compounds were sorted in order of the docking score. The conformations with the highest and lowest docking scores respectively were exported to InsightII® for further manipulation within MAO-B.

With the comparison of the activities of the conformers and their individual docking scores, there wasn't a good correlation, although the highest scoring compound had good activity and the lower scoring compounds has lower activities. The more linear conformers presented with better docking scores.

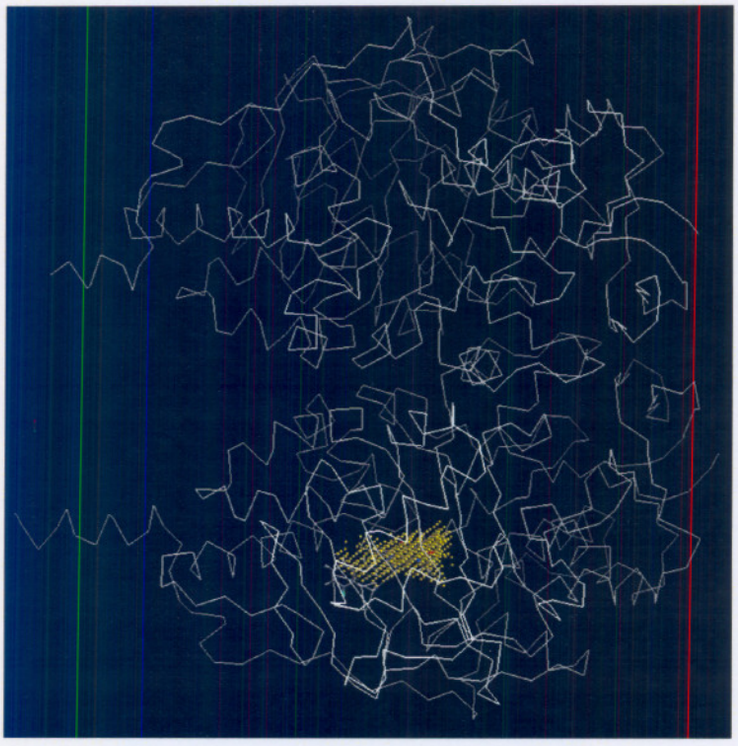

Figure 28: The active site of MAO-B (yellow) as determined by site search in trace rendering.

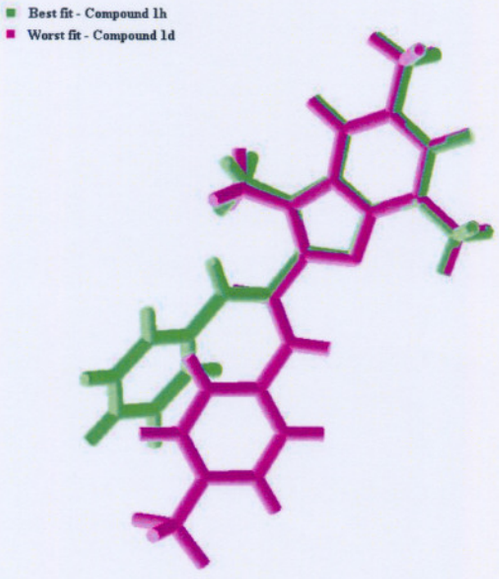

Figure 29: The comparison of the conformations of the best (green) and worst (magenta) fit of the compounds in the site model generated by Cerius$^{2®}$.

5.5. *Docking studies using InsightII®*

InsightII® is a comprehensive graphic molecular modeling program. In conjunction with the molecular mechanics/dynamics program such as Discover or CHARMm the InsightII® program can be used to build and manipulate virtually any class of molecule or molecular system. It is more focused on macromolecular modelling than Cerius$^{2®}$ and was then used for further manipulation of the MAO-B enzyme and the selected compounds in the enzyme.

5.5.1. Method

The crystallographic data of MAO-B (PDB: 1S2Q; Binda *et al.*, 2004) was used for all calculations. The ligand (rasagiline) was firstly replaced by **1i** and then by **1d** consecutively. Water molecules were deleted form the crystal structure. The protein and the compounds were assigned partial charges using the CVFF force field. Docking was performed to correctly place the compounds in the active cavity. The InsightII® Build® subroutine was used to add the hydrogen atoms of the protein applicable at a pH of 7.4 and then dynamic minimisation was carried out using Discover_3 and the CVFF force field. The temperature of the dynamics was set to 500 K with 2000 steps and a time step of 10 fs. Energy minimisation was set to 5000 iterations and the Polak-Rebieré method was used. After the minimisation of MAO-B with either of the compounds embedded in it, a RMS fit was performed to confirm that the protein was still in its original fixed conformation as depicted by the PDB file.

5.5.2. Results and discussion

Useful information can be gained from the study of minimum energy structures. However, these structures are static models, whereas in reality, molecules are flexible structures subject to thermal motion. The technique of molecular dynamics was used to simulate the thermal motion of the MAO-B structure as a function of time, using the forces acting on the atoms to drive the motion. Starting with the molecular mechanics energy description of the structure as described above, the forces acting on the atoms can be evaluated. As the masses of the atoms are known,

Newton's second law of motion (force = mass x acceleration) may be used to compute the accelerations, and thus the velocities, of the atoms. The accelerations and velocities may then be used to calculate new positions for the atoms over a short time step (around 1 femto second, where a femto second is equal to 10^{-15} seconds), thus moving each atom to a new position in space. This process iterates many thousands of times, generating a series of conformations of the structure known as a trajectory. A simulation is frequently run for tens of picoseconds (1 picosecond is equal to 10^{-12} seconds). The velocities of the atoms are related directly to the temperature at which the simulation is run. A simulation run at 300 K provides information on structural fluctuations that occur around the starting conformation, perhaps to illustrate which parts of a molecule are more flexible, and can also provide information on the pathways of conformational transitions. If the temperature of the simulation is increased, more energy is available to climb and cross energetic barriers. Thus high-temperature (e.g., 500 K) simulations were used to search conformational space.

A low molecular weight inhibitor molecule like isatin only occupies the substrate cavity, whereas longer molecules like 1,4-diphenyl-2-butene occupy both the entrance and substrate cavities (Binda *et al.*, 2003). Comparison of **1d** and **1i** with the larger 1,4-diphenyl-2-butene it could be expected that the inhibitors of the current study would probably also span the two cavities of MAO-B. This binding mode may enhance the affinity of these compounds for the enzyme via hydrophobic interactions with entrance cavity residues such as Leu167, Leu164, Ile316 and Pro104 and these interactions may explain the low micro to nano molar K_i-values of the (*E*)-8-(3-chlorostyryl)caffeine (CSC) analogues.

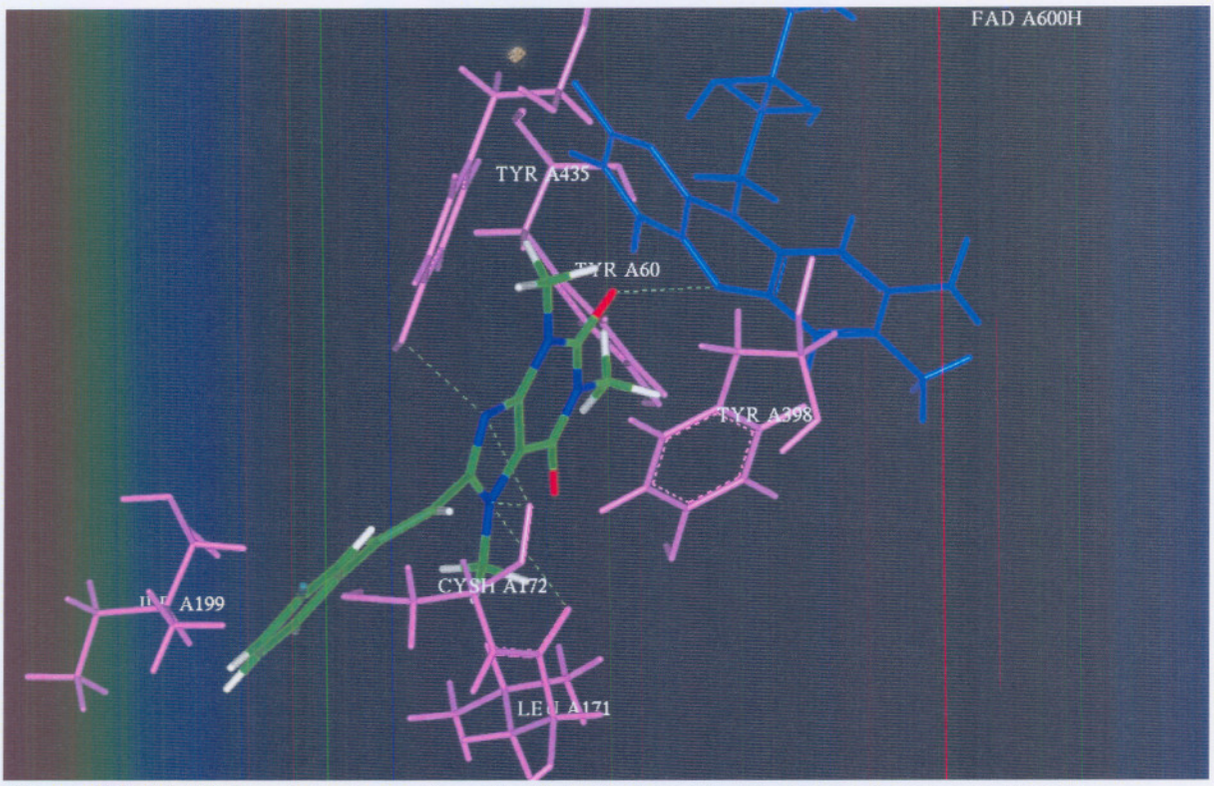

Figure 30: MAO-B substrate cavity with **1i** docked inside. Hydrogen bonds are shown as green dotted lines.

Also of importance are hydrogen bonds between **1i** and the MAO-B enzyme (Cys172, Leu171, Tyr435 and FAD; figure 30). From the studies it is clear that the two carbonyl oxygens of the xanthine moeity act as good hydrogen-bond acceptors when in close range of a hydrogen bond donor group (Tyr188 and FAD). The nitrogens at positions 7 and 9 of the xanthine act as hydrogen bond acceptors, forming hydrogen bonds with Cys172, Leu171 and Tyr435.

The compounds that exhibited the best inhibition activity towards MAO-B appeared to exist in a linear extended conformation in which the phenyl ring and the xanthinyl aromatic ring are almost co-planar (figure 30). In contrast, inhibitors with conformations where there are relatively large deviations from co-planarity between the phenyl and the xanthine exhibited weaker inhibition activity towards MAO-B. These compounds (**1h**) exist in a bent conformation and binds to only the substrate cavity of the enzyme. Those compounds with extended conformations showed

extended binding into the entrance cavity, a property that may be responsible for its enhanced inhibition.

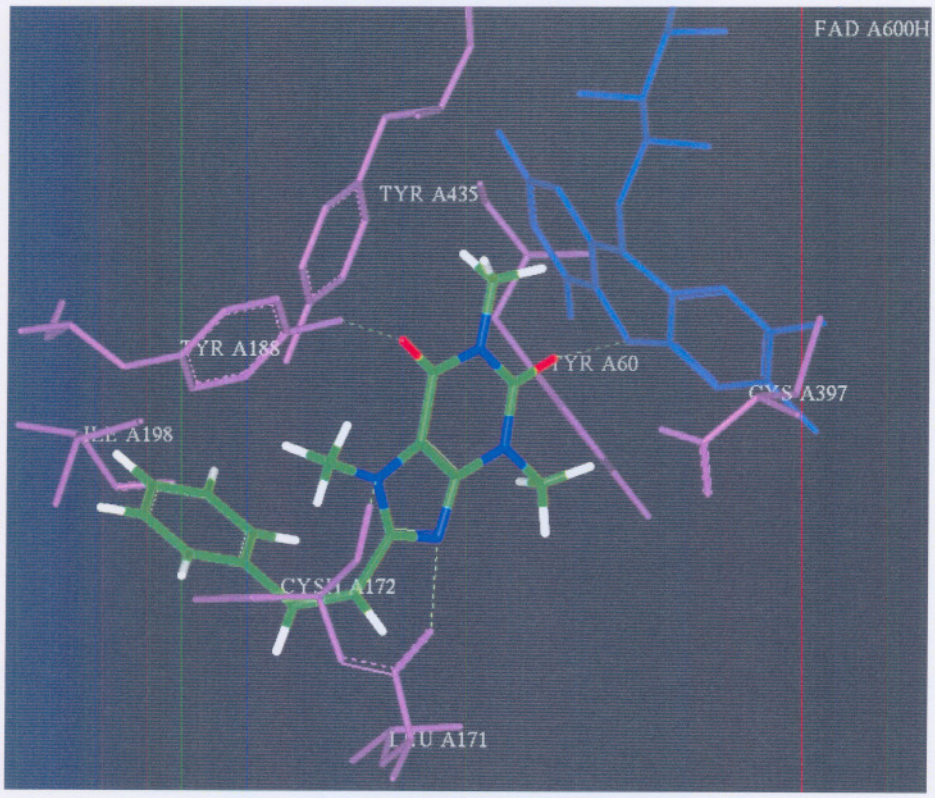

Figure 31: The unsubstituted CSC analogue (**1h**) docked in the MAO-B substrate cavity. Hydrogen bonds are indicated with the dotted green lines.

The RMS values obtained were well within experimental limits with a value of 0.008598.

In conclusion, the two carbonyl oxygens of the xanthinyl as well as the N-7 and N-9 atoms seems to be important for the MAO-B inhibition activity since these functionalities are involved in hydrogen bonding with the surrounding amino acids and FAD. The conformation of the styryl double bond also appears to be a determining feature in their activity since compounds with potent activity appear to be stretched-out in order to bind to both the entrance and substrate cavities of the enzyme.

5.6. Summary

A three dimensional hypothesis for the inhibition of MAO-B was generated using several CSC analogues that are known to inhibit MAO-B. For this purpose the molecular modelling program Catalyst® was used. The best hypothesis for this series of compounds contained two hydrophobic groups, one aromatic ring and one hydrogen bond acceptor. The active site of the reported crystal structure of MAO-B was identified by using Cerius^{2}®. This was followed by fitting the dynamically minimised conformers of the inhibitors into the active site with the LigandFit® subroutine. The fitted conformers were scored and the highest scoring conformer and lowest scoring conformer were selected and used in InsightII® for further manipulation. In InsightII® the conformers were separately docked into the substrate cavity and the interactions between the inhibitors and the enzyme were determined. Hydrogen bonding to the xanthinyl moiety and the conformation of the styryl side chain were found to be the determining factors for interaction to the MAO-B enzyme.

CHAPTER 6

Discussion and conclusion

Summary and abbreviations

In this chapter an overview of structural requirements of the (E)-8-(3-chlorostyryl)caffeine (CSC) analogues to act as reversible inhibitors of monoamine oxidase B (MAO-B) is given. The results of this study are presented and the relationships between the structures of the inhibitors and the MAO-B inhibition activity are discussed.

CSC – (*E*)-8-(3-Chlorostyryl)caffeine

MAO-B – Monoamine oxidase B

MPTP – 1-Methyl-4-phenyl-1,2,3,6-tetrahydropyridine

PD – Parkinson's disease

Parkinson's disease (PD) is a terminal late-onset neurodegenerative disease that results in muscle rigidity, bradykinesia, resting tremor and loss of postural reflex. Idiopathic PD is characterised pathologically by a marked loss of dopaminergic nigrostratial neurons. The nature of the pathological process underlying clinical deterioration in PD remains elusive, although genetic mutations and environmental toxins have been implicated (Riederer *et al.*, 2001). The current treatment for PD is inadequate. L-dopa is used for dopamine replacement therapy, but leads to failure as a result of the development of drug induced dyskinesia, motor response oscillations, psychiatric complications and the progressive emergence of poorly responsive gait and balance problems.

In the pursuit of improved treatments for PD, the adenosine A_{2A} receptor has emerged as an attractive nondopaminergic target. The antiparkinsonian potential of A_{2A} antagonism has been boosted by recent preclinical evidence that A_{2A} antagonists might favourably alter the course as well as the symptoms of the disease. CSC (**1f**) was recently shown to have neuroprotective properties and this protection may be dependent in part on the

inhibition of the MAO-B catalysed bioactivation of MPTP, since CSC was also found to be a potent and selective competitive MAO-B inhibitor (Chen *et al.*, 2002).

In this study a series of (*E*)-8-(3-chlorostyryl)caffeine analogues were synthesised and evaluated *in vitro* as competitive inhibitors of MAO-B. One of the objectives of this study was to determine the effect of different C-3 and C-4 phenyl substituents on MAO-B inhibition potency by (*E*)-8-styrylcaffeine analogues. For the purpose of this study the selected analogues were monosubstituted in either the 3- or 4-position of the styryl ring. Substituents with both electronwithdrawing (trifluoromethyl, fluoro and chloro) and electron donating effects (methyl) were chosen and compared to the unsubstituted (*E*)-8-styrylcaffeine (**1h**). Following synthesis of these compounds, each analogue was evaluated as a reversible MAO-B inhibitor utilizing two different techniques. The potency by which each compound reversibly inhibits MAO-B was expressed as the enzyme-inhibitor dissociation constant, K_i. Using the compounds in table 1 (chapter 1), molecular modelling has been carried out in order to establish a hypothetic pharmacophore model for the (*E*)-8-styrylcaffeine analogues as MAO-B inhibitors. The two compounds with the best and lowest MAO-B inhibitory activity were docked into the active site of MAO-B. After the docking procedure, dynamic minimisation was applied to the enzyme and inhibitor complex at 500 K in order to determine an optimised configuration of the enzyme-inhibitor complex. From this analysis the hydrogen bonds to the surrounding amino acids were established. The models generated from these studies are aimed to assist future design of potent reversible inhibitors of MAO-B.

6.1. Summary of study

6.1.1. Synthesis

A promising lead compound, (*E*)-8-(3-chlorostyryl)caffeine (CSC) (**1f**) was recently found to inhibit MAO-B with a K_i value of 70nM (Chen *et al.*, 2001; Chen et al., 2002). Several analogues of CSC were also prepared as part of an effort to define the structural requirements of this class of compounds to act as inhibitors of MAO-B (Petzer *et al.*, 2003). Since MAO-B inhibitors are frequently used as antiparkinsonian agents, the possibility of designing drugs that act as both A_{2A} antagonists and inhibitors of MAO-B

may be of value. We have therefore chosen to expand on the known (*E*)-8-styrylcaffeinyl analogues that are MAO-B inhibitors by evaluating additional analogues (**1a–h**) of CSC in an attempt to elucidate specific structural features of CSC that may be responsible for its potency as an MAO-B inhibitor. Earlier studies suggested that structural features that are important for MAO-B inhibition are the *trans* configuration of the styryl alkene and 1,3,7-trimethyl substitution of the xanthinyl ring system (Petzer *et al.*, 2003). The principal aim was to determine whether substitution of C-3 of the styryl ring with an electron withdrawing group is essential for potent MAO-B inhibition as suggested by the structure of CSC and an earlier study (Petzer *et al.*, 2003).

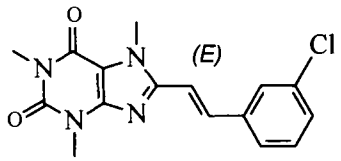

Figure 32: The structure of CSC that served as lead compound for this study.

The structures selected for this study were all (*E*)-styrylcaffeine analogues mono substituted at C-3 or C-4 of the styryl ring. Among the substituents selected were electron withdrawing (Cl, F, and CF_3) and electron donating (CH_3) functional groups. For comparison, the unsubstituted (*E*)-8-styrylcaffeine was also synthesised. 5,6-Diaminouracil served as key starting material for the preparation of the analogues. Condensation of 5,6-diaminouracil with the appropriately substituted cinnamic acid in the presence of a carbodiimide coupling reagent followed by basic ring closure offered the 1,3-diamethyl-8-styryl-7H-xanthine analogues. Following 7-methylation with methyliodide the target compounds were obtained in fair yield.

6.1.2. Enzymology, methods and SAR study

The literature reports several assays for the determination of MAO-B catalytic activity. For the purpose of this study, we chose two different substrates to measure the activity of MAO-B. In the first instance the extent by which various concentrations of the test inhibitors slowed the rate of the oxidation of MMTP **(8)** to the corresponding dihydropyridinium metabolite $MMDP^+$ **(9)** was measured spectrophotometrically (Inoue

et al., 1999). In a second approach benzylamine **(11)**, a selective MAO-B substrate, was utilized to measure the K_i values.

All of the (*E*)-8-styrylcaffeinyl analogues (**1a–h**) tested were found to be inhibitors of MAO-B. The lines of the Lineweaver–Burke plots in all cases intersected indicating that the mode of inhibition was competitive (Segel, 1993). The K_i values for the inhibition of MAO-B are presented in table 7. The lead compound for this study, CSC (**1f**), was confirmed (Chen *et al.*, 2002) to be a very potent inhibitor with a K_i value of 148nM for the inhibition of benzylamine oxidation by MAO-B. The similarity in range of this value with that obtained with MMTP as substrate (128nM) is an indication of the reliability of the K_i estimations and also suggests that specific alterations in experimental conditions (such as change of substrate or analytical technique) do not affect the estimated values to a large extent. In accordance with this view, for the other analogues tested (**1a–e** and **1g–h**), the differences between the K_i values estimated by the two different techniques are within the range expected for experimental error (table 7).

It was found that the MAO-B inhibition potency of (*E*)-8-styrylcaffeine analogues substituted at C-3 of the phenyl ring depended on the electronic properties of the substituent as well as the size and lipophylicity. A Hansch type SAR study indicated that larger lipophylic substituents that are electron withdrawing favours inhibition. For (*E*)-8-styrylcaffeine analogues bearing C-4 substituents inhibition potency appeared to be dependent only upon the size and lipophylicity of the substituent. Larger and more lipophylic substituents enhanced inhibitory potency.

6.1.3. Molecular modelling

A three dimensional hypothesis for the inhibition of MAO-B by CSC analogues was constructed with the molecular modelling software package Catalyst®. The best hypothesis generated contained 2 hydrophobic groups, 1 aromatic ring and 1 hydrogen bond acceptor. Three inhibitors were fitted into the hypothesis as proof of concept. The inhibitors selected were of low, moderate and good activity. A very good correlation was found between the K_i values predicted by the hypothesis and those experimentally determined.

Following the hypothesis generation, docking studies were undertaken. The energy minimised conformers generated by Catalyst® were docked into the reported active site of MAO-B by using the LigandFit® Cerius^{2}® software package. The fitted conformers were scored and both the highest scoring conformer (**1i**) and lowest scoring conformer (**1d**) were used in InsightII® for further manipulation. In InsightII® the conformers were separately docked into the substrate cavity, dynamically minimised and the different interactions were determined between the compounds and the enzyme and FAD.

The results of these studies indicated that most of the CSC analogues probably bind to the substrate cavities of MAO-B with the styryl side chain protruding into the entrance cavity. This binding may explain the high potency of these compounds as MAO-B inhibitors, since conformers such as **1h** which appear to bind only to the substrate cavity exhibits lower inhibition activity. Hydrophobic interaction between the inhibitor and entrance cavity residues (Leu167, Leu164, Ile316 and Pro104) appear to account for the difference in activities. Hydrogen bonds were indicated between **1i** and Cys172, Leu171, Tyr435 and FAD (figure 31). The two carbonyl oxygens on the xanthine ring of the inhibitors seem to act as good hydrogen-bond acceptors. The N-7 and N-9 nitrogens act as hydrogen bond acceptors, forming hydrogen bonds with Cys 172, Leu 171 and Tyr 435.

6.2. Discussion

Results from this study and the literature suggests that the structural features of CSC analogues that are important for reversible MAO-B inhibition are the following: (a) replacement of the 1,3-dimethyl groups of the xanthinyl moiety with ethyl groups decreases the potency of the compounds, (b) the 7-*N*-methylxanthinyl analogues are more potent than the corresponding 7*H*-xanthinyl analogues, (c) saturation of the styryl double bond leads to decreased activity, (d) the styryl moiety is essential for inhibition, (e) *trans* geometry is required, because the *cis* isomers are inactive, (f) an electron withdrawing substituent on the styryl moiety is important for inhibition, (g) the xanthinyl moiety is a superior system for MAO-B inhibition in contrast to the benzimidasole moiety and (h) a planar compound may be better competitive inhibitors of MAO-B (Petzer *et al.*, 2003).

In order to gain further insight into the interactions between the inhibitors and MAO-B we carried out a Hansch-type SAR study. As illustrated by equation 7, the negative signs of both the F and the π parameter terms indicate that the potency ($\log K_i$) by which selected (*E*)-8-styrylcaffeinyl analogues inhibit MAO-B are enhanced by substitution with lipophylic electron withdrawing C-3 functional groups. Since the Van der Waals volume (V_w) is also negatively correlated (table 8) with $\log K_i$, larger C-3 substituents also appears to enhance MAO-B inhibition potency.

$$\text{Log}K_i = -1.98(\pm 0.18)F - 0.60(\pm 0.11)\pi + 0.47(\pm 0.06) \qquad \textbf{Equation 7}$$

$$(F = 143.5 \text{ and } R^2 = 0.98)$$

For analogues substituted at C-4 of the styryl ring (table 9) the single-parameter fits that shows the best correlations with the $\log K_i$ values are the Van der Waals volume V_w and the Hansch constant (π) of the substituents. The mathematical description of the binding affinity ($\log K_i$) of C-4 substituted (*E*)-8-styrylcaffeinyl analogues to MAO-B may therefore be presented as:

$$\text{Log}K_i = -1.02(\pm 0.08)V_w + 0.54(\pm 0.07) \qquad \textbf{Equation 8}$$

$$(F = 163.9 \text{ and } R^2 = 0.95)$$

or

$$\text{Log}K_i = -1.28(\pm 0.11)\pi + 0.38(\pm 0.06) \qquad \textbf{Equation 9}$$

$$(F = 140.2 \text{ and } R^2 = 0.95)$$

There is also a meaningful correlation ($R^2 = 0.95$) between the Hansch constants (π) of the C-4 substituents and the $\log K_i$ values. As observed with the analogues substituted at the C-3 position, the negative sign of the V_w parameter coefficient suggest that the potency ($\log K_i$) of MAO-B inhibition may be enhanced by substitution with bulky C-4 functional groups. On the other hand, the electronic contribution of the C-4 substituents

to $\log K_i$ appears to be negligible since in a two-parameter fit with V_w and F, the probability of the term containing F being zero is 45%. The same argument applies to the other electronic parameter (σ_p) considered in this study. Hydrophobic C-4 functional groups appear to favour inhibition potency since the sign of the π parameter coefficient is negative. Again there does not seem to be an electronic contribution of the C-4 substituents to $\log K_i$ since in a two parameter fit of $\log K_i$ with π and F or of $\log K_i$ with π and σ_p the probability of the terms containing σ_p and F as being zero are 17.8% and 97.5%, respectively.

The docking of the CSC analogues into the substrate cavity suggested that the compounds with a extended conformation may bind to both the entrance and substrate cavities, resulting in enhanced affinity and inhibition. Substitution on the phenyl ring of the styryl moiety seemed to facilitate this binding mode, since only the unsubstituted analogue (**1h**) existed in a bent conformation which resulted in binding to only the substrate cavity. These observations are supported by the Hansch-type SAR study which indicated that larger hydrophobic substituents on the styryl ring enhanced binding activity. This may presumably be due to the interactions between the substituents and the amino acid residues of the entrance cavity.

6.3. Conclusion

(*E*)-8-(3-chlorostyryl)caffeine was used as lead compound for the preparation of several analogues that may be potent MAO-B inhibitors. The SAR studies provided insight into the structural properties needed for potent inhibition of MAO-B by the CSC analogues. The inhibitors should contain bulky groups on either C-3 or C-4. The substituents on C-3 should also be lipophylic electron withdrawing groups in order to enhance the potency of inhibition. Substitution on the phenyl ring of the CSC analogues is pivotal for potent inhibition, because the compounds will convert to a curled up conformation and so lessen the amount of possible interaction points. For potent MAO-B inhibition, the inhibitor should further possess two hydrophobic groups, one hydrogen bond acceptor and one aromatic ring. This class of compounds are also reported to be A_{2A} antagonists and thus may have enhanced therapeutic potential for PD treatment since both MAO-B inhibition and A_{2A} antagonists are currently used in the treatment of PD..

REFERENCES

ABBRACCHIO, M.P., FOGLIAATO, G., PAOLETTI, A.M., ROVATI, G.E. & CATTABENI, F. 1992. Prolonged *in vitro* exposure of rat brain slices to adenosine analogues: selective desensitisation of adenosine A_1 but not A_2 receptors. European journal of pharmacology, 227:317–324.

ABELES, R.H. & MAYCOCK, A.L. 1976. Suicide enzyme inactivators. Accounts of chemical research, 9:313–319.

AGID, Y., DAMIER, P., GRAYBIEL, A.M. & HIRSCH, E.C. 1999. The substantia nigra of the human brain. II. Patterns of loss of dopaminergic-containing neurons in Parkinson's disease. Brain, 122:1437–1448.

ALEXI, T., BORLOGAN, C.V., FAULL, R.L.M., WILLIAMS, C.E., CLARK, R.G., GLUCKMAN, P.D. & HUGHES, P.E. 2000 Neuroprotective strategies for basal ganglia degeneration: Parkinson's and Huntington's diseases. Progress in neurobiology, 60:409–470.

ALEXOFF, D., CILENTO, R., FOWLER, J.S., LOGAN, J., MACGREGOR, R., PAPPAS, N., SCHYLER, D., SHEA, C., VOLKOW, N.D., WANG, G.J., WARNER, D., WOLF, A.P. & ZEZULKOVA, I. 1996. Inhibition of monoamine oxidase B in the brains of smokers. Nature, 379:733–736.

ALPEROVITCH, A., AMADUCCI, L., BRETELER, M.M., DARTIGUES, J.F., DE RIYK, M.C., LOPEZ-POUZA, S., MANUBENS-BERTRAN, J.M., ROCCA, W.A. & TZOURIO, C. 1997. Prevalence of parkinsonism and Parkinson's disease in Europe: the EUROPARKINSON Collaborative Study European Community Concerted Action on the Epidemiology of Parkinson's disease. Trends in neurosurgery and psychiatry, 62:10–15.

ARAI, Y., FOWLER, C.J., ORELAND, L. & STRENSTROM, A. 1983. Monoamine oxidase activity and localization in the brain and the activity in relation to psychiatric disorders. (In: Beckmann, H. & Riedere, P., ed., Modern problems in

pharmacopsychiatry. Monoamine oxidase and its selective inhibitors. Basel: Karger. p.246–254)

ARNETT, C.D., FOWLER, J.S., HALLDIN, C., LANGSTROM, B., MACGREGOR, R.R., SCHLYER, D.J. & WOLF, A.P. 1987. Turnover of brain monoamine oxidase measured *in vivo* by positron emission tomography using L-[^{11}C]deprenyl. Journal of neurochemistry, 49:522–527.

BARA-JIMENEZ, W., SHERZAI, A., DIMITROVA, T., FAVIT, A., BIBBIANI, F., GILLESPIE, M.,MORRIS, M.J., MOURADIANM M.M. & CHASE, T.N. 2003. Adenosine A_{2A} receptor antagonist treatment of Parkinson's disease. Neurology, 61:293–296.

BASTIA, E., VARANI, K., MONOPOLI, A. & BERTORELLI, R. 2002. Effects of a(1) and A_{2A} adenosine receptor ligands in mouse acute models of pain. Neuroscience letters, 328:241–244.

BINDA, C., MATTEVI, A. & EDMONDSON, D.E. 2002a. Structure-function relationships in flavoenzyme-dependant amine oxidations. A comparison of polyamine oxidase and monoamine oxidase. Journal of biological chemistry, 277:23973–23976.

BINDA, C., EDMONDSON, D.E., HUBALEK, F., MATTEVI, A. & NEWTON-VINSON, P. 2002b. Structure of the outer-membrane mitochondrial monoamine oxidase B. Nature structural & molecular biology, 9:22–26.

BINDA, C., LI, M., HUBALEK, F., RESTELLI, N., EDMONDSON, D.E. & MATTEVI, A. 2003. Insights into the model of inhibition of human mitochondrial monoamine oxidase B from high-resolution strystal structures. Proceedings of the national academy of sciences of the United States of America, 100:9750–9755.

BINDA, C., HUBALEK, F., LI, M., HERZIG, Y., STERLING, J., EDMONDSON, D.E., MATTEVI, A. 2004. Crystal structure of MAO-B in complex with N-propargyl-1(R)-2-aminoindan (rasagiline). [Web:] http://www.rcsb.org/pdb [Date of access: 17 August 2005].

BONDI, A. 1964. Van der Waals Volumes and Radii. Journal of physical chemistry, 68:441–451.

BLICKE, F.F. & GODT, H.C., Jr. 1954. Reactions of 1,3-dimethyl-5,6-diaminouracil. Journal of the American chemical society, 76:2798–2800.

BORRONI, E., CESURA, A.M., GOTTOWIK, J., GRAY, J., LUQUE, J.M. MALHERBE, P., RICHARDS, J.G. & SAURA, J. 1998. Monoamine oxidases: from brain maps to physiology and transgenetics to pathophysiology. Journal of neural transmission, 52:173–187.

BRADFORD, M.M. 1976. A rapid and sensitive method for the quantitation of microgram quantities of protein utilizing the principle of protein-dye binding. Analytical biochemistry, 72:247–254.

CANO, J., DE LA CRUZ, C.P. MACHADO, A., REVILLA, E., RODRIGUEZ-GOMEZ, J.A. & STEFFEN, V. 1996. Protection of the aged substantia nigra of the rat against oxidative damage by (-)-deprenyl. British journal of pharmacology, 117:1756–1760.

CASTAGNOLI, K., PALMER, S., ANDERSON, A., BUETERS, T. & CASTAGNOLI, N. JR. 1997. The neuronal nitric oxide synthase inhibitor 7-nitroindazole also inhibits the monoamine oxidase-b-catalyzed oxidation of 1-methyl-4-phenyl-1,2,3,6-tetrahydropyridine Chemical research in toxicology, 10:364-368.

CESURA, A.M. & PLETCHER, A. 1992. The new generation of monoamine oxidase inhibitors. Progression in drug research, 38:171–297.

CHALMERS-REDMAN, R.M. & TATTON, W.G. 1996. Modulation of gene expression rather than monoamine oxidase inhibition: (-)-deprenyl-related compounds in controlling neurodegeneration. Neurology, 47:S171–S183.

CHEN, J.F., XU, K., PETZER, J.P., STAAL, R., XY, Y.H. & BEILSTEIN, M. 2001. Neuroprotection by caffeine and A_{2A} adenosine receptor inactivation in a model of Parkinson's disease. Journal of neuroscience, 21:RC143:1–6.

CHEN, J.-F., STEYN, S., STAAL, R., PETZER, J.P. XU, K., VAN DER SCHYF, C.J., CASTAGNOLI, K., SONSALLA, P.K., CASTAGNOLI, N. JR. & SCHWARZSCHILD, M.A. 2002. 8-(3-Chlorostyryl)caffeine may attenuate MPTP neurotoxicity through dual actions of monoamine oxidase inhibition and A_{2A} receptor antagonism Journal of biological chemistry, 277:36040–36044.

CORVOL, J.C., STUDLER, J.M., SCHONN, J.S., GIRAULT, J.A. & HERVE, D. 2001. Gaplha(olf) is necessary for coupling D_1 and A_{2A} receptors to adenylyl cyclase in the striatum. Journal of neurochemistry, 76:1585–1588.

CUNHA, R.A., JOHANSSON, B., VAN DER PLOEG, I., SEBASTIAO, A.M., RIBIERO, J.A. & FREDHOLM, B.B. 1994. Evidence for functionally important adenosine A_{2A} receptors in the rat hippocampus. Brain research, 649:208–216.

DALY, J.W., BUTTS-LAMB, P. PADGETT, W. 1983. Subclasses of adenosine receptors in the central nervous system: interaction with caffeine and related methylxanthines. Cellular & molecular biology, 3:69–80.

DENNEY, R., JELLINGER, K., KONRADI, C., RIEDERER, P., SVOMA, E. & THIBAULT, J. 1988. Topographic immunocytochemical mapping of monoamine oxidase-A, monoamine oxidase-B and tyrosine hydroxylase in human post mortem brain stem. Neuroscience, 26:791–802.

DRUCHARCH, B. & MUISWINKEL, F.L. 2000. Drug treatment of Parkinson's disease. Biochemical pharmacology, 59:1023–1031.

EDMONDSON, D.E., BINDA, C. & MATTEVI, A. 2004. The FAD binding sites of human monoamine oxidase A and B. Neurotoxicology, 25:63–72.

FEIGIN, A. 2003. Nondopaminergic symptomatic therapies for Parkinson's disease: a case-control study in southeastern Sweden. Moving disorders, 14:28–37.

FINK, J.S., WEAVER, D.R., RIVKEES, S.A., PETERFREUND, R.A., POLLACK, A.E. & ADLER, E.M. 1992. Molecular cloning of the rat A_2 adenosine receptor: selective co-

expression with D_2 dopamine receptors in rat striatum. Molecular brain research, 14:186–195.

FOWLER, C.J. & TIPTON, K.F. 1984. The kinetics of monoamine oxidase inhibitors in relation to their clinical behaviour. (In: Tipton, K.F., Dostert, P. & Benedetti, M.S., ed., Monoamine oxidase and disease. Prospects for the therapy with reversible inhibitors. London.: Academic Press. p.27–40.)

FOWLER, J.S., LOGAN, J., MACGREGOR, R., PAPPAS, N., SHEA, C., VOLKOW, N.D. & WANG, G.J. 1997. Age-related inceases in brain monoamine oxidase B in living healthy human subjects. Neurobiology of aging, 18:431–435.

FOYLE, P., GERLACH, M., RIEDERE, P. & YOUDIM, M.B.H. 2000. MAO-B inhibitors: multiple roles in the therapy of neurodegenerative disorders? Parkinsonism & related disorders, 6:25–47.

FREDHOLM, B.B., BATTIG, K., HOLMEN, J., NEHLIG, A. & ZVARTAU, E.E. 1999. Actions of caffeine in the brain with special reference to factors that contribute to its widespread use. Pharmacological review, 51:83–133.

FREDHOLM, B.B., AP, I.J., JACOBSON, K.A., KLOTZ, K.N. & LINDEN, J. 2001. International union of pharmacology: XXV. Nomenclature and classification of adenosine receptors. Pharmacological review, 53:527–552.

FUJITA, T., IWASA, J. & HANSCH, C. 1964. A new substituent constant, π, derived from partition coefficients. Journal of the American chemical society, 86: 5175–5180.

FULLER, R.W., MARSH, M.M. & MILLS, J. 1968. Inhibition of monoamine oxidase by N-(phenoxyethyl)cyclopropylamines. Correlation of inhibition with Hammett constants and partition coefficients. Journal of medicinal chemistry, 11:387–398.

GEHA, R.M., CHEN, K., WOUTERS, J., OOMS, F. & SHIH, J.C. 2002. Analysis of Conserved Active Site Residues in Monoamine Oxidase A and B and Their Three-dimensional Molecular Modeling. Journal of biological chemistry, 277:17209–17216.

GERFEN, C.R., ENGBER, T.M., MAHAN, L.C., SUSEL, Z., CHASE, T.N., MONSMA, F.J. JR. 1990. D_1 and D_2 dopamine receptor-regulated gene expression of stratonigral and stratopallidal neurons. Science, 250:1429–1432.

GERLACH, M., RIEDERE, P. & YOUDIM, M.B.H. 1996. Molecular mechanisms for neurodegeneration: synergism between reactive oxygen species, calcium and excitotoxic amino acids. Advances in neurology, 69:177–194.

GNERRE, C., CATTO, M., LEONETTI, F., WEBER, P., CARRUPT, P.-A., ALTOMARE, C., CAROTTI, A. & TESTA, B. 2000. Inhibition of monoamine oxidases by functionalized coumarin derivatives: biological activities, QSARs, and 3D-QSARs. Journal of medicinal chemistry, 43:4747–4758.

GREEN, A.R., MITCHELL, B., TORDOFF, A. & YOUDIM, M.B.H. 1977. Evidence that dopamine deamination by both type A and type B monoamine oxidase in rat brain *in vivo* and for the degree of enzyme inhibition necessary to increase functional activity of dopamine and 5-hydroxytryptamine. British journal of pharmacology, 60:343–349.

GRIMSBY, J., LAN, N.C., NEVE, R., CHEN, K. & SHIH, J.C. 1990. Tissue distribution of human monoamine oxidase A and B mRNA. Journal of neurochemistry, 55:1166–1169.

GRONDIN, R., BEDARD, P.J., TAHAR, A.H., GREGOIRE, L., MORI, A. & KASE, H. 1999. Antiparkinsonian effect of a new selective adenosine A_{2A} receptor antagonist in MPTP-treated monkeys. Neurology, 52:1673–7.

HANSCH, C. & LEO, A. 1995. Exploring QSAR. Fundamentals and applications in chemistry and biology. American Chemical Society, p557.

HANSCH, C. & LEO, A. 1979. Substituent constants for correlation analysis in chemistry and biology. John Wiley and Sons. New York, pp 352–352.

HANSCH, C., LEO, A. & HOEKMAN, D. 1995. Exploring QSAR. Hydrophobic, electronic and steric constants, American Chemical Society, Washington, DC.

HAPPE, S., LUDEMANN, P. & BERGER, K. 2002. The association between disease severity and sleep-related problems in patients with Parkinson's disease. Neuropsychobiology, 46:90–96.

HARTMANN, C. & MCINTYRE, W.S. 1997. Flavins and Derivatives Methods in enzymology, 280:98–150.

HEIKKILA, R.E., MANZINO, L., CABBAT, F.S. & DUVOISON, R.C. 1984. Protection against the dopaminergic neurotoxicity of 1-methyl-4-phenyl-1,2,5,6-tetrahydropyridine by monoamine oxidase inhibitors. Nature, 311:467–469.

HETTINGER, B.D., LEE, A., LINDEN, J. & ROSIN, D.L. 2001. Ultrastructural localization of adenosine A_{2A} receptors suggests multiple cellular sites for modulation of GABAergic neurons in rat striatum. Journal of computational neurology, 431:331–346.

HUBALEK, F., BINDA, C., KHALIL, A., LI, M., MATTEVI, A., CASTAGNOLI, N. & EDMONDSON, D.E. 2005. Demonstration of isoleucine 199 as a structural determinant for the selective inhibition of human monoamine oxidase B by specific reversible inhibitors. Journal of biological chemistry, 280:15761–15766.

HUBER, E.W., OHLWEILER, D.F. & THOMAS, C.E. 1997. Hydroxyl and peroxyl radical trapping by the monoamine oxidase-B inhibitors deprenyl and MDL 72,974A: implications for protection of biological substrates. Free radicals in biology and medicine, 22:733–737.

HUTTENLOCHER, P.R. 1979. Synaptic density in human frontal cortex – developmental changes and effects of aging. Brain research, 163:195–205.

IKEDA, K., KUROKAWA, M., AOYAMA, S. & KUWANA, Y. 2002. Neuroprotection by adenosine A_{2A} receptor blockade in experimental models of Parkinson's disease. Jounal of neurochemistry, 80:262–270.

INOUE, H., CASTAGNOLI, K., VAN DER SCHYFF, C., MABIC, S., IGARASHI, K. & CASTAGNOLI, N. JR. 1999. Species-Dependent Differences in Monoamine Oxidase A and B-Catalyzed Oxidation of Various C4 Substituted 1-Methyl-4-phenyl-1,2,3,6-

tetrahydropyridinyl Derivatives Journal of pharmacology and experimental therapeutics, 291:856–864.

JACOBSON, K.A., GALLO-RODRIGUEZ, C., MELMAN, N., FISCHER, B., MAILLARD, M., VAN BERGEN, A., VAN GALEN, P.J.M. & KARTON, Y. 1993. Structure-activity relationships of 8-styrylxanthines as A2-selective adenosine antagonists Journal of medicinal chemistry, 36:1333–1342.

JARVIS, M.F. & WILLAIMS, M. 1989. Direct autoradiographic localization of adenosine A_2 receptors in the rat brain using the A_2-selective agonsit, [3H]CGS 21680. European journal of pharmacology, 168:243–246.

JENNER, P. 2003. A_{2A} antagonists as novel non-dopaminergic therapy for motor dysfunction in PD. Neurology, 61:S32–S38.

JOHNSTON, J.P. 1968. Some observations upon a new inhibitor of monoamine oxidase in brain tissue. Biochemical pharmacology, 17:1285–1297.

JOHNSON, M.S., MORETTI, L., PENTIKAINEN, O.T. & SETTIMO, L. 2004. Model structures of N-methyl-D-aspartate receptor subunit NR1 explain the molecular recognition of agonist and antagonist ligands. Journal of structural biology, 145:205–215.

KAKKAR, T., BOXENBAUM, H. & MAYERSOHN, M. 1999. Estimation of Ki in a competitive enzyme-inhibition model: comparisons among three methods of data analysis. Drug metabolism and disposition, 27:756–762.

KEARNEY, E.B., SALACH, J.I., WALKER, W.H., SENG, R.L., KENEY, W. & ZESZOTEK, E. 1971. The covalently bound flavin of hepatic monoamine oxidase. 1. Isolation and sequence of a flavin peptide and evidence for binding at the 8α-position. European journal of biochemistry, 24:321–327.

KIRKSEY, T.J., KWAN, S.-W. & ABELL, C.W. 1998. Argine-42 and threonine-45 are required for FAD incorporation and catalytic activity in human monoamine oxidase B. Biochemistry, 37:12360–12366.

KOLLER, W.C. 1984. Sensory symptoms in Parkinson's disease. Neurology, 34:957–959.

KRUEGER, M.J., MAZOUZ, F., RAMSAY, R., MILCENT, R. & SINGER, T.P. 1995. Dramatic species differences in the susceptibility of monoamine oxidase B to a group of powerful inhibitors. Biochemical and biophysical research communications, 206:556–562.

KULL, B., FERRE, S., ARSLAN, G., SVENNINGSSON, P., FUXE, K. & OWMAN, C. 1999. Reciprocal interactions between adenosine A_{2A} and dopamine D_2 receptors in Chinese hamster ovary cells co-transfected with the two receptors. Biochemistry & pharmacology, 58:1035–1045.

KULL, B., SVENNINGSSON, P. & FREDHOLM, B.B. 2000. Adenosine A(2A) receptors are colocalized with and and activate g(olf) in rat striatum. Molecular pharmacology, 58:771–777.

KUTTER, E. & HANSCH, C. 1969. Steric parameters in drug design. Monoamine oxidase inhibitors and antihistamines. Journal of medicinal chemistry, 12:647–652.

LEDENT, C., VAUGEOIS, J.M., SCHIFFMANN, S.N., PEDRAZZINI, T., EL YACOUBI, M. & VANDERHAEGEN, J.J. 1997. Aggressiveness, hypoalgesia and high blood pressure in mice lacking the adenosine A_{2A} receptor. Nature, 388:674–678.

LEWITT, P.A. & THE 6002-US-005/US-006 CLINICAL INVESTIGATOR GROUP, 2004. "Off" time reduction from adjunctive use of istradefylline (KW-6002) in levodopa-treated patients with advanced Parkinson's disease. Movement disorders, 19:S222-P624.

LIVINGSTONE, D.J. & SALT, D.W. 2005. Judging the significance of multiple linear regression models. Journal of medicinal chemistry, 48:661–663.

MACCOLLIN, M., PETERFREUND, R., MACDONALD, M., FINK, J.S. & GUSELLA, J. 1994. Mapping of a human A_{2A} adenosine receptor (ADORA2) to chromosome 22. Genomics, 20:332–333.

MASSEY, V. 2000. The Chemical and Biological Versatility of Riboflavin Biochemical society transactions, 28:283–296.

MILLER, J.R. & EDMONDSON, D.E. 1999. Structure-activity relationships in the oxidation of para-substituted benzylamine analogues by recombinant human liver monoamine oxidase A. Biochemistry, 38:13670–13683.

MORELLI, M., FENU, S., PINNA, A. & DI CHIARA, G. 1994. Adenosine A_2 receptors interact negatively with dopamine D_1 and D_2 receptors in unilaterally 6-hydroxydopamine-lesioned rats. European journal of pharmacology, 251:21–25.

MÜLLER, C.E., GEIS, U., HIPP, J., SCHOBERT, U., FROBENIUS, W., PAWLOWSKI, M., SUZUKI, F. & SANDOVAL-RAMINEZ, J. 1997. Synthesis and Structure-Activity Relationships of 3,7-Dimethyl-1-propargylxanthine Derivatives, A_{2A}-Selective Adenosine Receptor Antagonists. Journal of medicinal chemistry, 40:4396–4405.

NASH, J.E. & BROTCHIE, J.M. 2000. A common signalling pathway for stratial NMDA and adenosine A_{2A} receptors: implications for the treatment of Parkinson's disease. Journal of neuroscience, 20:7782–7789.

NICOTERA, A., PARVEZ, H. PIERUCCI, F. & SENATORI, O. 2004. Monoamine oxidase expression during development and aging. Neurotoxicology, 25:155–165.

NIMKAR, S.K., ANDERSON, A., RIMOLDI, J.M., STANTON, J.M., CASTAGNOLI, K.P., MABIC, S., WANG, Y.-X. & CASTAGNOLI, N. Jr. 1996. Synthesis and monoamine oxidase B catalyzed oxidation of C-4 heteroaromatic substituted 1,2,3,6-tetrahydropyridine derivatives. Chemical research in toxicology, 9:1013–1022.

OOMS, F., FREDERICK, R., DURANT, F., PETZER, J.P., CASTAGNOLI, N. JR., VAN DER SCHYF, C.J. & WOUTERS, J. 2003. Rational approaches towards the reversible inhibition of type B monoamine oxidase. Design and evaluation of a novel 5H-indeno[1,2-*c*]pyridazin-5-one derivative. Bioorganic & medicinal chemistry letters, 13:69–73.

OTTOBONI, S., CALDERA, P., TREVOR, A., CASTAGNOLI, N., Jr. 1989. Deuterium isotope effect measurements on the interactions of the neurotoxin 1-methyl-4-phenyl-

1,2,3,6-tetrahydropyridine with monoamine oxidase B. Journal of biological chemistry, 264:13684–13688.

PARKINSON, J. 1817. An essay on the shaking palsy. London: Sherwood, Neely and Jones.

PETZER, J.P., STEYN, S., CASTAGNOLI, K.P., CHEN, J-.F., SCHWARZSCHILD, M.A., VAN DER SCHYF, C.J. & CASTAGNOLI, N. 2003. Inhibition of monoamine oxidase B by selective adenosine A_{2A} receptor antagonists. Bioorganic & medicinal chemistry, 11:1299–1310.

POIRIER, J., QUIRION, R. & THIFFAULT, C. 1997. The effect of L-deprenyl, D-deprenyl and MDL 72974 on mitochondrial respiration: a possible mechanism leading to an adaptive increase in superoxide dismutase activity. Molecular brain research, 49:127–136.

PORKKA-HEISKANEN, T., STRECKER, R.E., THAKKER, M., BJORKUM, A.A., GREENE, R.W. & MCCARLEY, R.W. 1997. Adenosine: a mediator of the sleep-inducing effects of prolonged wakefulness. Science, 273:1265–1268.

RABEY, J.M., SAGI, L., HUBERMAN, M. MELAMED, E. KOREZYN, A., GILADI, M., INZELBERG, R., DJADETTI, R., KLEIN, C. & BERECZ, G. 2000. Rasagiline mesylate, a new MAO-B inhibitor for the treatment of Parkinson's disease: a double-blind study as adjunctive therapy to levodopa. Clinical neuropharmacology, 23:324–330.

RIEDERER, P., REICHMANN, H., JANETZKY, B., SIAN, J., LESCH, K-.P., LANGE, K.W., DOUBLE, K.L., NAGATSU, T. & GERLACH, M. 2001. Neural degeneration in Parkinson's disease. Advanced Neurology, 86:125–136.

RODWELL, V.W. 1993. Enzymes: kinetics. (*In*: R.K. MURRAY, D.K. GRANNER, P.A. MAYES & V.W. RODWELL, *ed.* Harpers' Biochemistry, 23rd ed. Connecticut: Appleton & Lange. 71 p.

ROSIN, D.L., ROBEVA, A., WOODARD, R.L., GUYENET, P.G. & LINDEN, J. 1998. Immunohistochemical localization of adenosine A_{2A} receptors in the rat central nervous system. Journal of computational neurology, 401:163–186.

SALACH, J. & WEYLER, J. 1987. Preparation of the flavin-containing aromatic amine oxidases of human placenta and beef liver. Methods in enzymology, 142:627–637.

SAURA, S., LUQUE, J.M., CESURA, A.M. DA PRADA, M., CHAN-PALAY, V., HUBER, G., LOFFLER, J. & RICHARDS, J.G. 1994. Increased monoamine oxidase B activity in plaque-associated astrocytes of Alzheimer brain revealed by quantitative enzyme autoradiography. Neuroscience, 62:15–30.

SEGEL, I.H. 1993. Enzyme kinetics, Wiley, New York. pp. 100–125.

SHIMADA, J., KOIKE, N., NONAKA, H., SHIOZAKI, S., YANAGAWA, K., KANADA, T., KOBAYASHI, H. & FUMIO, S. 1997. Adenosine A_{2A} antagonists with potent anti-cataleptic activity. Bioorganic & medicinal chemistry letters, 7:2349–2352.

SILVERMAN, R.B. 1995. Radical thoughts about the life of MAO. Progress in brain research, 106:23–31.

SQUIRES, R.F. 1972. Multiple forms of monoamine oxidase in intact mitochondria as characterized by selective inhibitors and thermal stability: a comparison of eight mammalian species. Advances in biochemical psychopharmacology, 5:355–370.

STANDAERT, D.G. & YOUNG, A.B. 2000. Treatment of central nervous system degenerative disorders. (In Gardman, J.G., Limbird, L.E., *ed.* Goodman & Gillman's The Pharmacological basis of therapeutics. Tenth Edition. New York : McGraw-Hill. P549-568.)

SVENNINGSSON, P., LE MOINE, C., KULL, B., SUNAHARA, R., BLOCH, B. & FREDHOLM, B.B. 1997. Cellular expression of adenosine A_{2A} receptor messenger RNA in the rat central nervous system with special reference to dopamine innervated areas. Neuroscience, 80:1171–1185.

SVENNINGSON, P., LE MOINE, C., AUBERT, I., BURBAUD, P., FREDHOLM, B.B. & BLOCH, B. 1998. Cellular distribution of adenosine A_{2A} receptor mRNA in the primate striatum. Journal of computational neurology, 399:229–240.

SVENNINGSSON, P., LE MOINE, C., FISONE, G. & FREDHOLM, B.B. 1999. Distribution, biochemistry and function of striatal adenosine A_{2A} receptors. Progress in neurobiology, 59:355–396.

SUZUKI, F., SHIMADA, J., SHIOZAKI, S., ICHIKAWA, S., ISHII, A., NAKAMURA, J., NONAKA, H., KOBAYASHI, H. & FUSE, E. 1993. Adenosine A_1 antagonists. 3. Structure-activity relationships on amelioration against scopolamine- or N^6-((R)-phenylisopropyl)adenosine-induced cognitive disturbance. Journal of medicinal chemistry, 36:2508–2518.

SUZUKI, F., SHIMADA, J., KOIKE, N., NAKAMURA, J., SHIOAZAKI, S., ICHIKAWA, S., ISHII, A. & NONAKA, H. 1996, Jan 16. United states patent, PN/5,484,920.

SWAIN, C.G. & LUPTON, E.C., Jr. 1968. Field and resonance components of substituent effects. Journal of the American chemical society, 90: 4328–4337.

TATTON, W.G. 1993. Selegiline can mediate neuronal rescue rather than neuronal protection. Movement disorders, 8:20–30.

TATTON, W.G. & GREENWOOD, C.E. 1991. Rescue of dying neurons a new action for deprenyl in MPTP parkinsonism. Journal of neuroscience research, 30:666–667.

URADE, Y., EGUCHI, N., QU, W.M., SKAKTA, M., HUANG, Z.L. & CHEN, J.F. 2003. Sleep regulation in adenosine A_{2A} receptor-deficient mice. Neurology, 61:S94–S96.

VOLZ, H.P. & GLEITER, C.H. 1998. Monoamine oxidase inhibitors : a perspective on their use in the elderly. Drugs in the aging, 13:341–355.

VON LUBITZ, D.K., LIN, R.C., POPIK, P., CARTER, M.F. & JACOBSON, K.A. 1994. Adenosine A_3 receptor stimulation and cerebral ischemia. European journal of pharmacology, 263:59–67.

WALKER, M.C. & EDMONDSON, D.E. 1994. Structure-activity relationships in the oxidation of benzylamine analogues by bovine liver mitochondrial monoamone oxidase B. Biochemistry, 33:7088–7098.

WALKINSHAW, G. & WATERS, C.M. 1995. Induction of apoptosis in catecholaminergic PC12 cells by L-dopa. Implications for the treatment of Parkinson's disease. Journal of clinical investigation, 95:2458–2464.

WANG, X. & SILVERMAN, R.B. 2000. Monoamine oxidase-catalysed oxidation of endo,endo-2-amino-6[(Z)-2'-phenyl]ehtylbicyclo[2.2.1]heptane, a potential probe for a radical cation intermediate. Bioorganic and medicinal chemistry, 8:1645–1651.

WEYLER, W., HSU, Y.P. & BREAKEFIELD, X.O. 1990. Biochemistry and genetics of monoamine oxidase. Pharmacology & Therapy, 47:391–417.

WOUTERS, J. 1998. Structural aspects of monoamine oxidase and its reversible inhibition. Current Medical Chemistry, 5:137–162.

WU, R.M., CHIEUH, C.C., PERT, A. & MURPHY, D.L. 1993. Apparent antioxidant effect of L-deprenyl on hydroxyl radical formation and nigral injury elicited by MPP^+ *in vivo*. European journal of pharmacology, 243:241–247.

XU, K., BASTIA, E. & SCHWARZSCHILD. M.A. 2005. Therapeutic potential of adenosine A_{2A} receptor antagonists in Parkinson's disease. Pharmacology & therapeutics, 105:267–310.

YOUDIM, M.B., FRIDKIN, M., ZHENG, H. 1995. Bifunctional drug derivatives of MAO-B inhibitor rasagiline and iron chelator VK-28 as a more effective approach to treatment of brain ageing and ageing neurodegenerative diseases. Mechanisms of ageing and development, 126:317–326.

YOUDIM, M.B. & RIEDERER, P.F. 2004. A review of the mechanisms and role of monoamine oxidase inhibitors in Parkinson's disease. Neurology, 63:S32–35.

YU, P.H. 1994. Pharmacological and clinical implications of MAO-B inhibitors. General pharmacology: The vascular system, 25:1527–1539.

ZHOU, B.P. WU, B., KWAN, S.W. & ABELL, C.W. 1998. Characterization of a highly conserved FAD-binding site in human monoamine oxidase B. Journal of biological chemistry, 273:14862–14868.

APPENDIX A

MS, ^{1}H-NMR, ^{13}C-NMR Spectra.

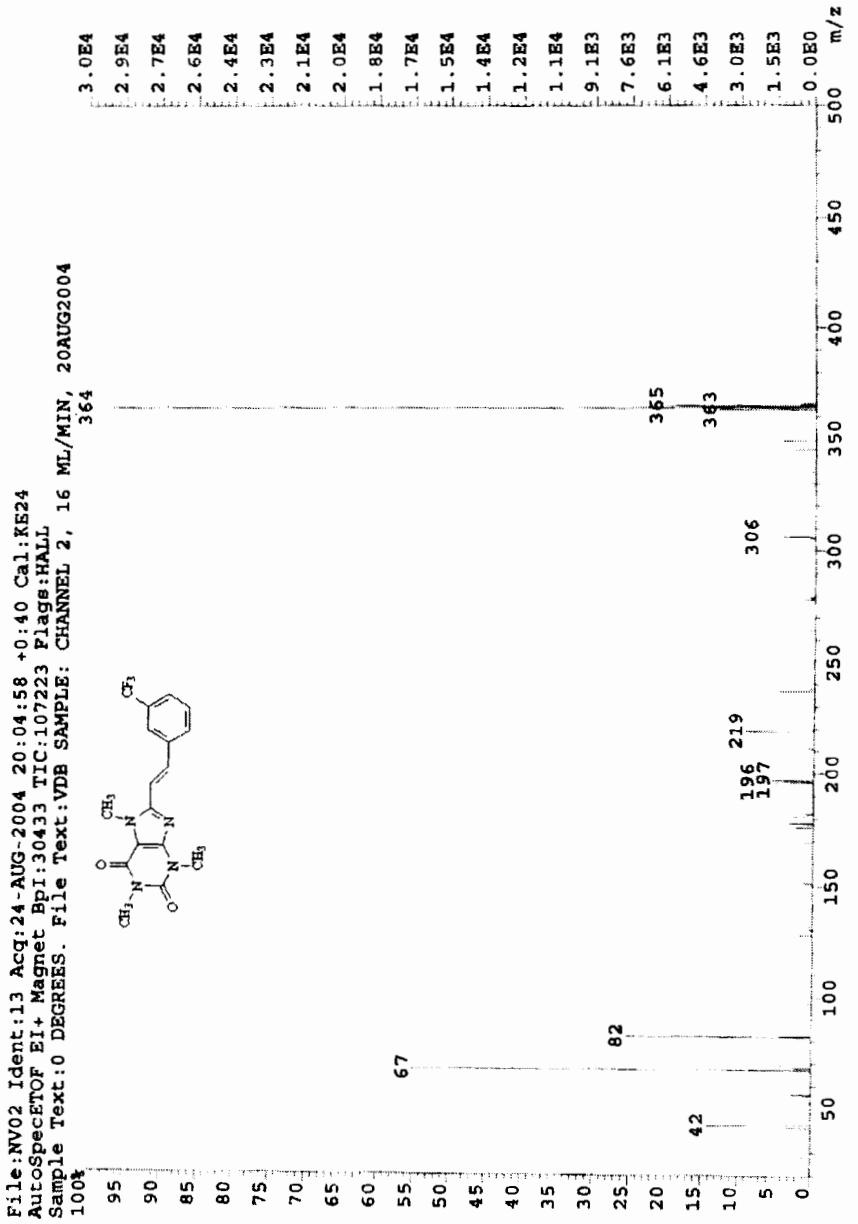

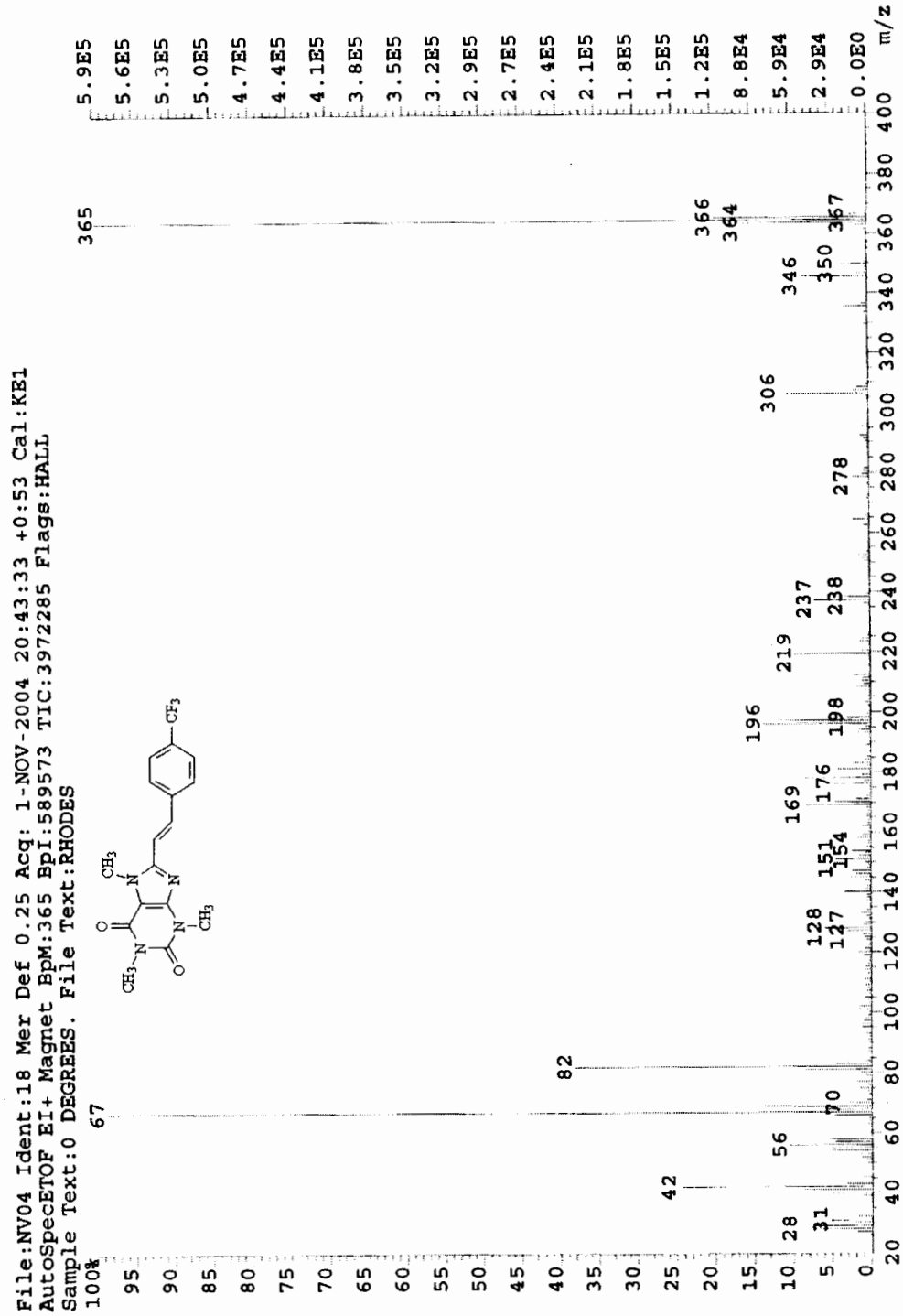
File:NV04 Ident:18 Mer Def 0.25 Acq: 1-NOV-2004 20:43:33 +0:53 Cal:KE1
AutoSpecETOF EI+ Magnet BpM:365 BpI:589573 TIC:3972285 Flags:HALL
Sample Text:0 DEGREES. File Text:RHODES
100%
m/z
5.9E5
5.6E5
5.3E5
5.0E5
4.7E5
4.4E5
4.1E5
3.8E5
3.5E5
3.2E5
2.9E5
2.7E5
2.4E5
2.1E5
1.8E5
1.5E5
1.2E5
8.8E4
5.9E4
2.9E4
0.0E0
365
366
364
367
346
350
306
278
237
238
219
196
198
169
176
151
154
128
147
82
67
70
56
42
31
28

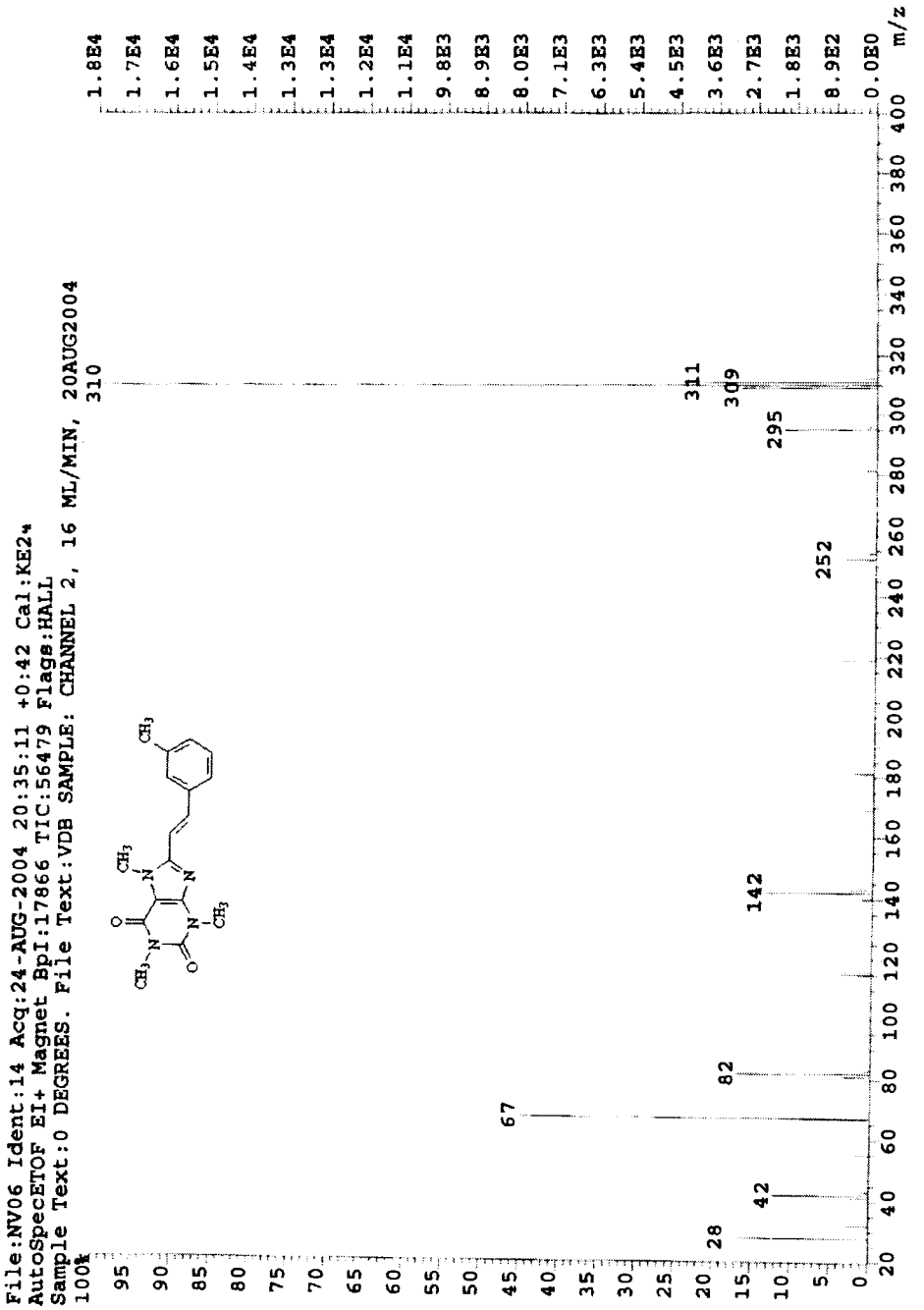
File:NV06 Ident:14 Acq:24-AUG-2004 20:35:11 +0:42 Cal:KE24
AutoSpecETOF EI+ Magnet BpI:17866 TIC:56479 Flags:HALL
Sample Text:0 DEGREES. File Text:VDB SAMPLE: CHANNEL 2, 16 ML/MIN, 20AUG2004
100%
310
311
309
295
252
142
82
67
42
28
m/z

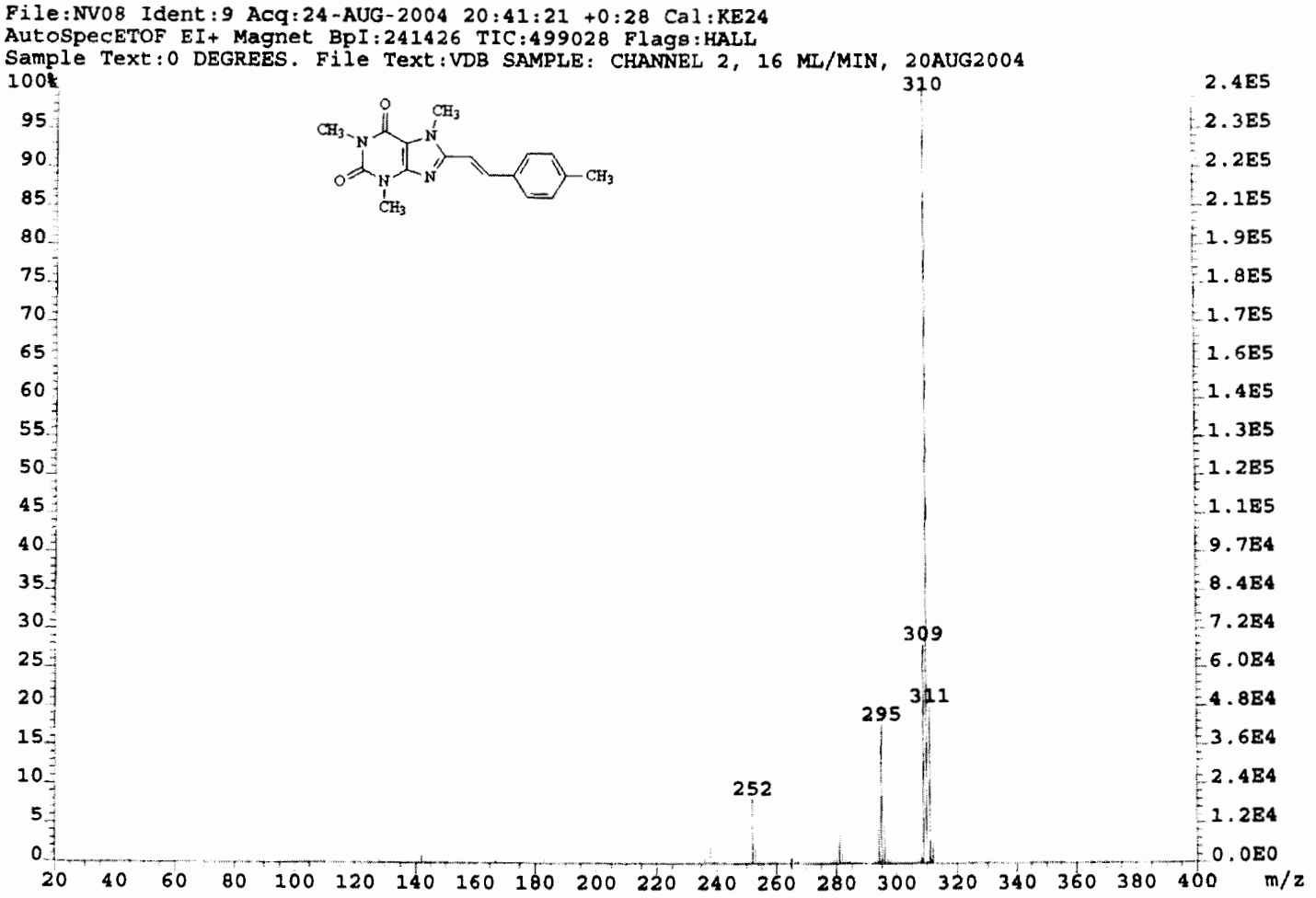
File:NV08 Ident:9 Acq:24-AUG-2004 20:41:21 +0:28 Cal:KE24
AutoSpecETOF EI+ Magnet BpI:241426 TIC:499028 Flags:HALL
Sample Text:0 DEGREES. File Text:VDB SAMPLE: CHANNEL 2, 16 ML/MIN, 20AUG2004
100%
95
90
85
80
75
70
65
60
55
50
45
40
35
30
25
20
15
10
5
0
2.4E5
2.3E5
2.2E5
2.1E5
1.9E5
1.8E5
1.7E5
1.6E5
1.4E5
1.3E5
1.2E5
1.1E5
9.7E4
8.4E4
7.2E4
6.0E4
4.8E4
3.6E4
2.4E4
1.2E4
0.0E0
310
309
311
295
252
20 40 60 80 100 120 140 160 180 200 220 240 260 280 300 320 340 360 380 400 m/z

File:NV10 Ident:19 Mer Def 0.25 Acq: 1-NOV-2004 20:41:05 +0:56 Cal:KE1
AutoSpecETOF EI+ Magnet BpM:330 BpI:14294976 TIC:136077024 Flags:HALL
Sample Text:0 DEGREES. File Text:RHODES

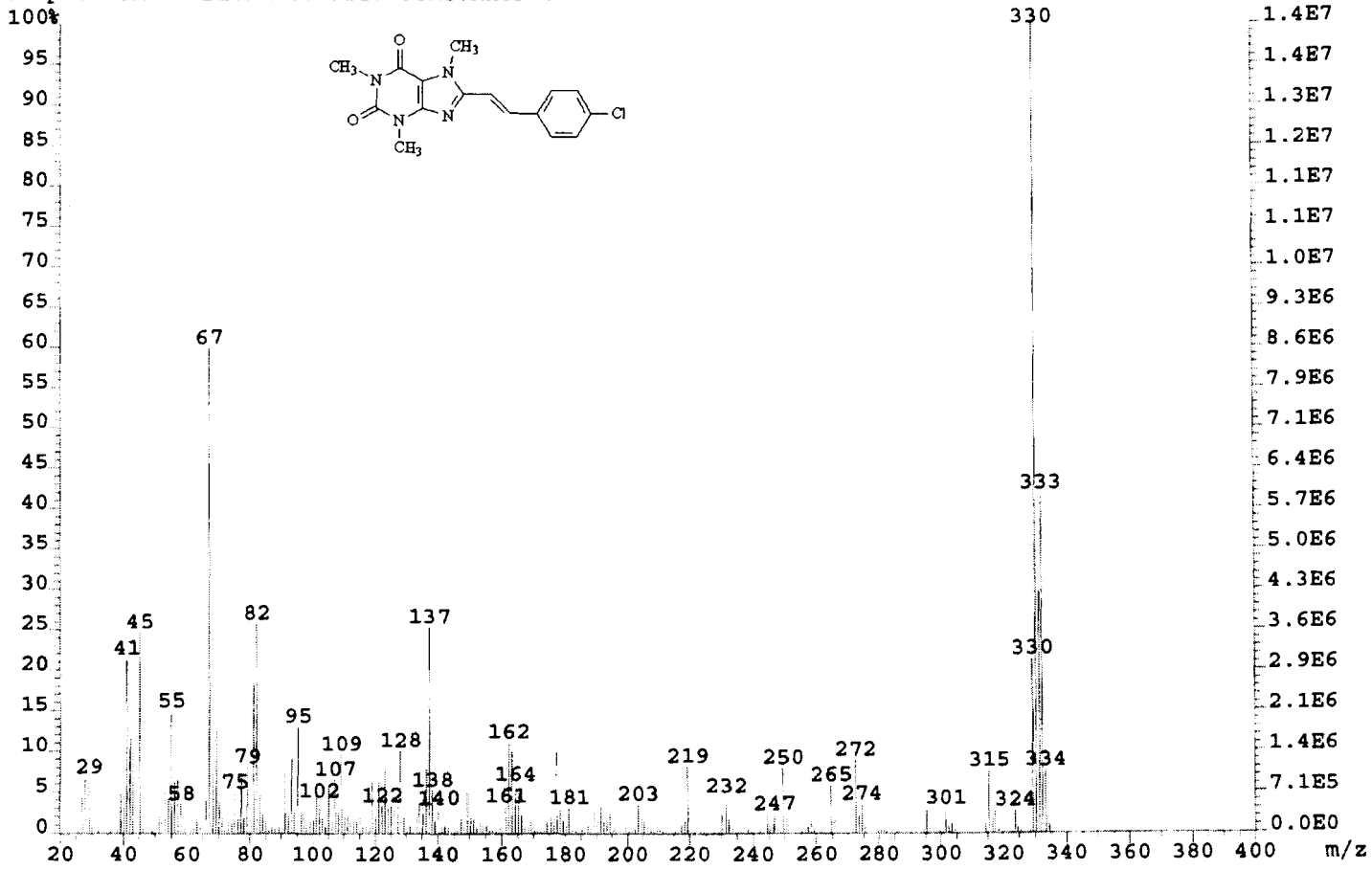

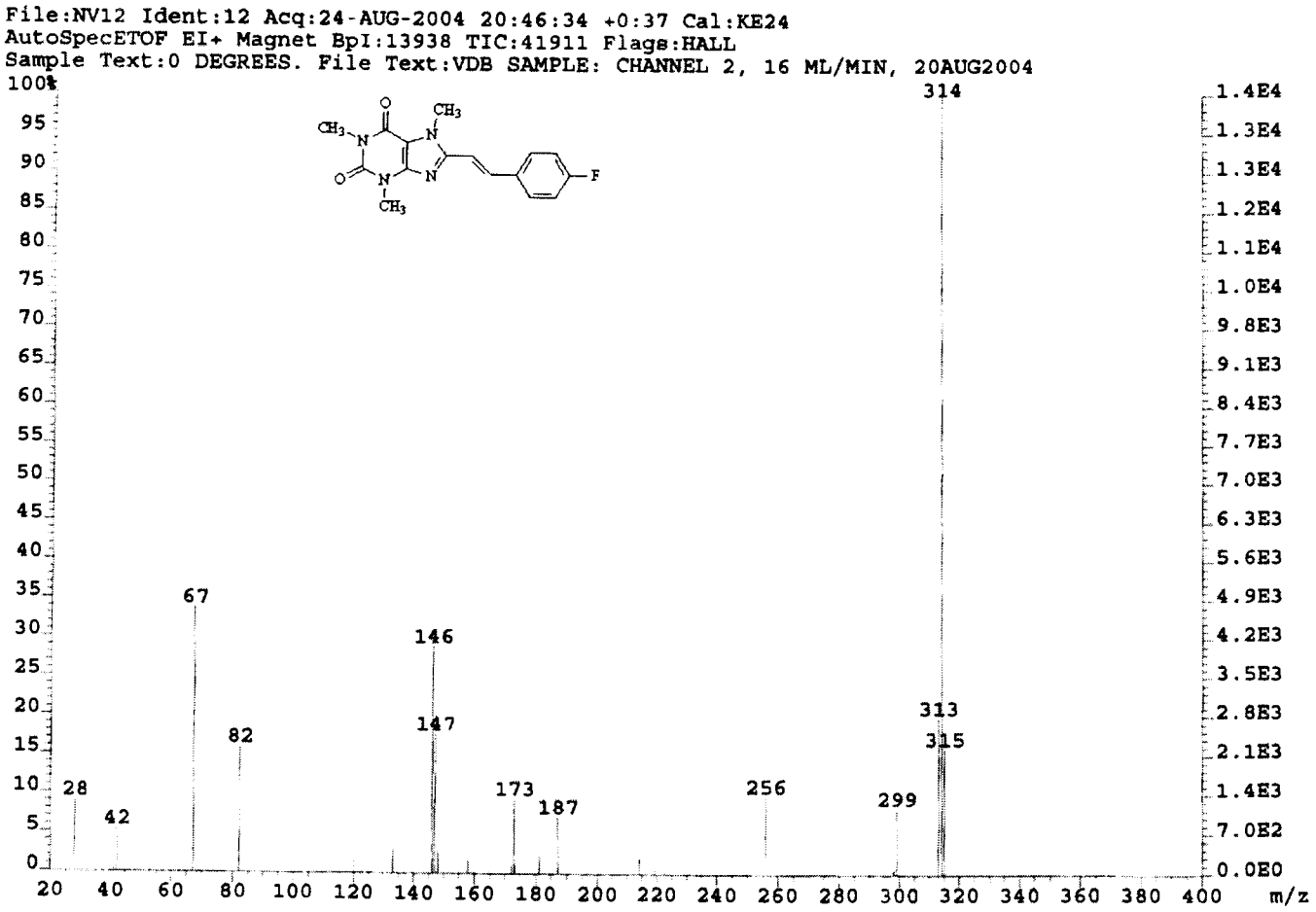
File:NV12 Ident:12 Acq:24-AUG-2004 20:46:34 +0:37 Cal:KE24
AutoSpecETOF EI+ Magnet BpI:13938 TIC:41911 Flags:HALL
Sample Text:0 DEGREES. File Text:VDB SAMPLE: CHANNEL 2, 16 ML/MIN, 20AUG2004
100%
95
90
85
80
75
70
65
60
55
50
45
40
35
30
25
20
15
10
5
0
1.4E4
1.3E4
1.3E4
1.2E4
1.1E4
1.0E4
9.8E3
9.1E3
8.4E3
7.7E3
7.0E3
6.3E3
5.6E3
4.9E3
4.2E3
3.5E3
2.8E3
2.1E3
1.4E3
7.0E2
0.0E0
20 40 60 80 100 120 140 160 180 200 220 240 260 280 300 320 340 360 380 400 m/z
314
67
146
147
82
313
315
28
42
173
187
256
299
CH3
N
O
F

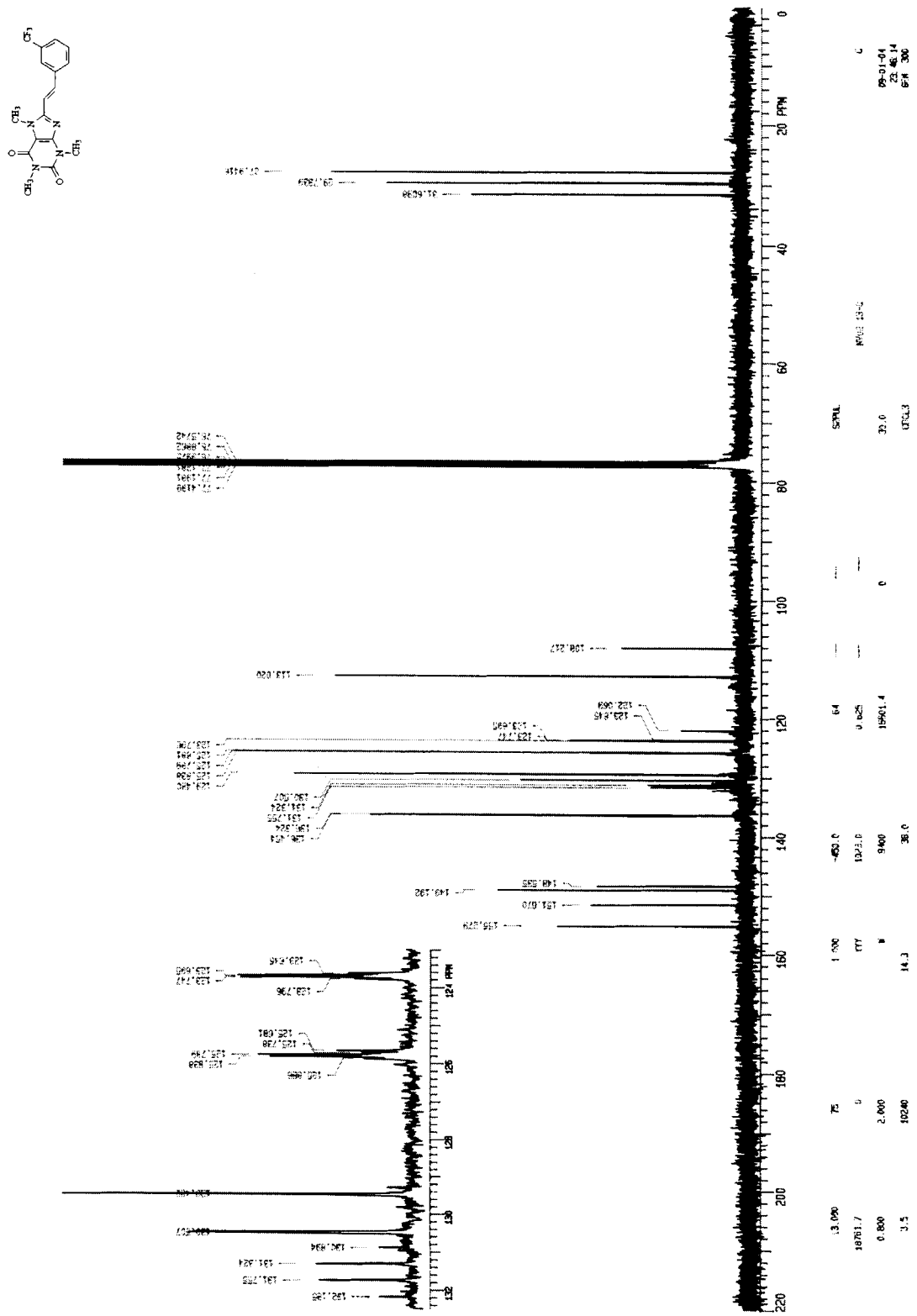

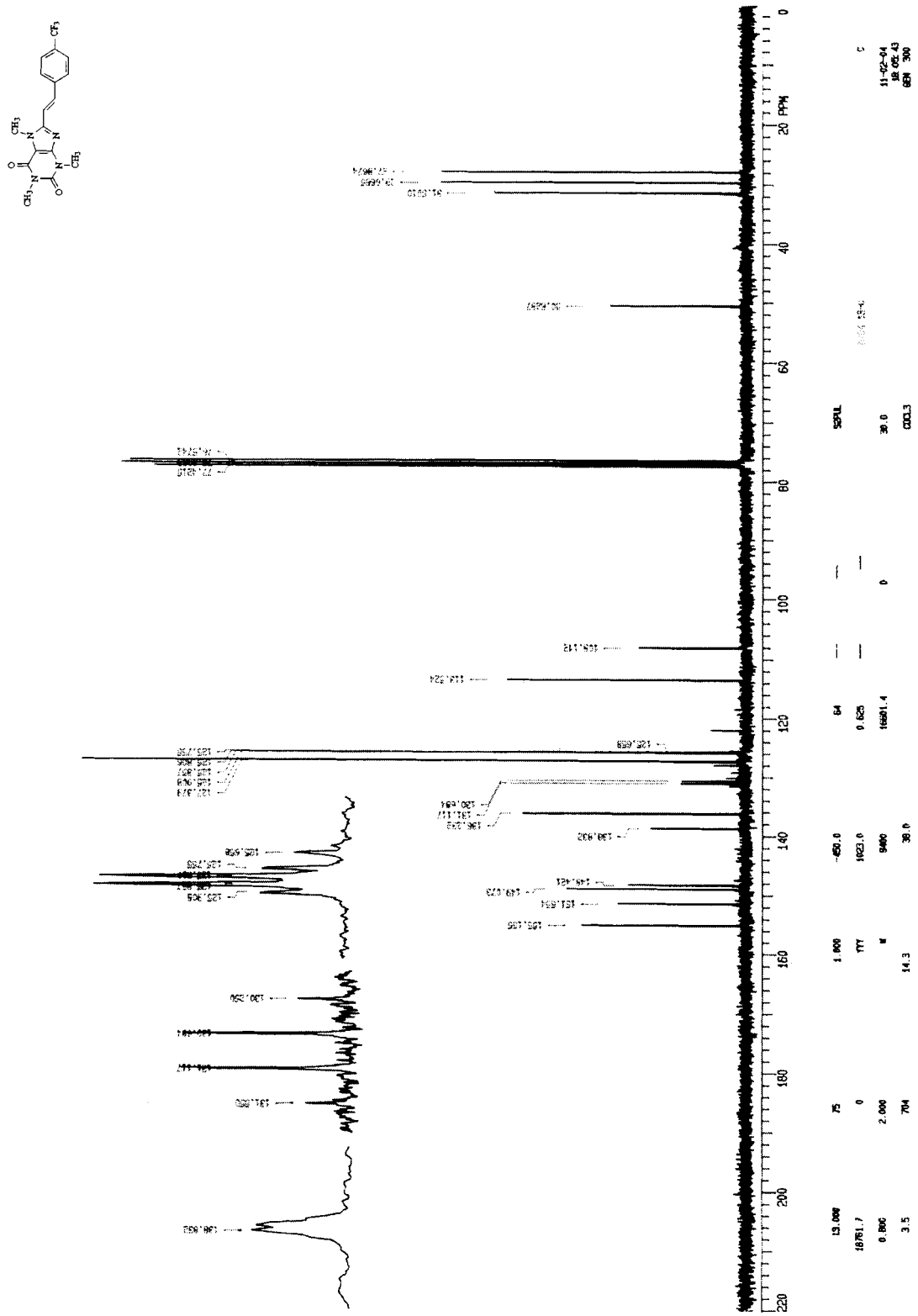

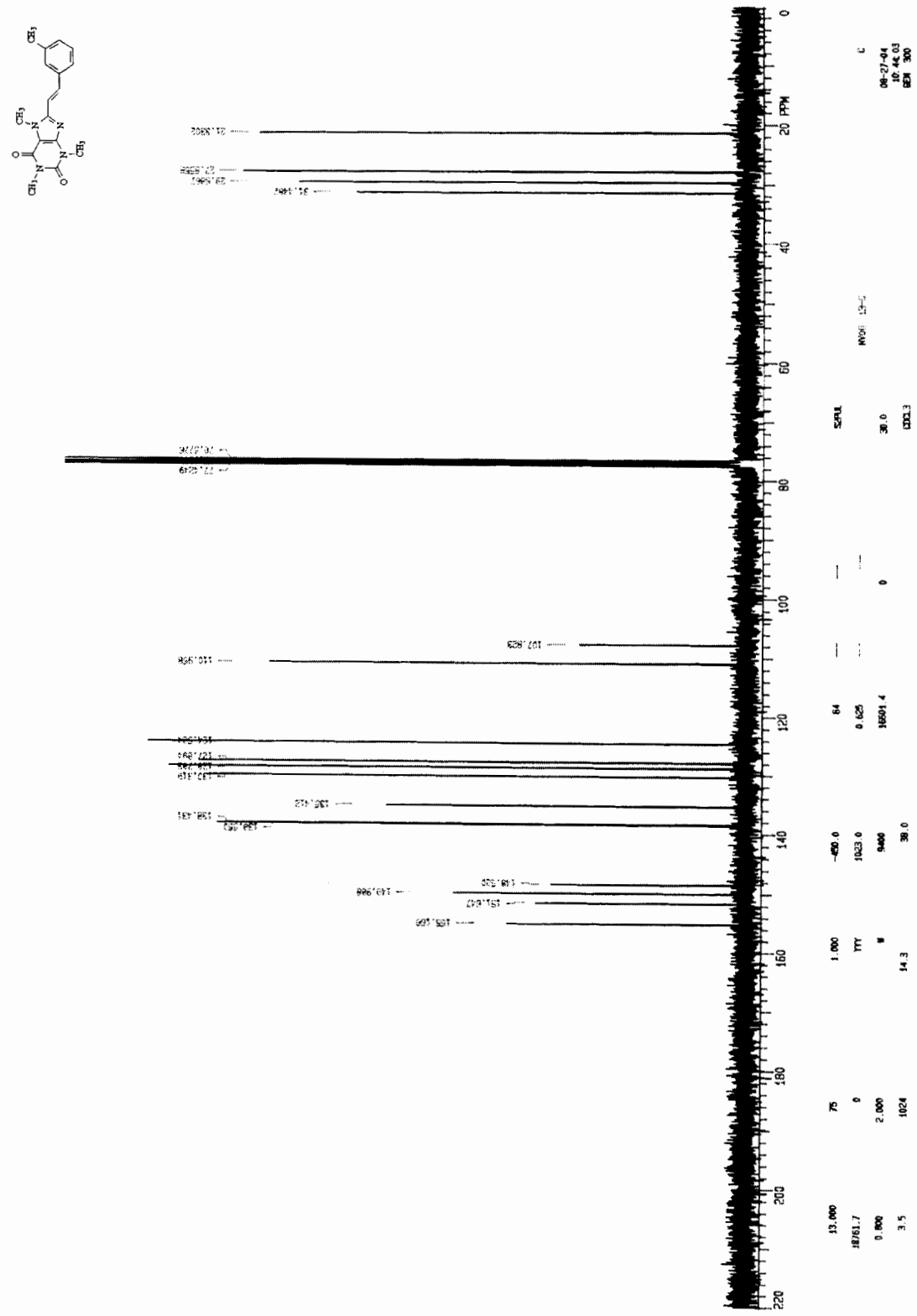

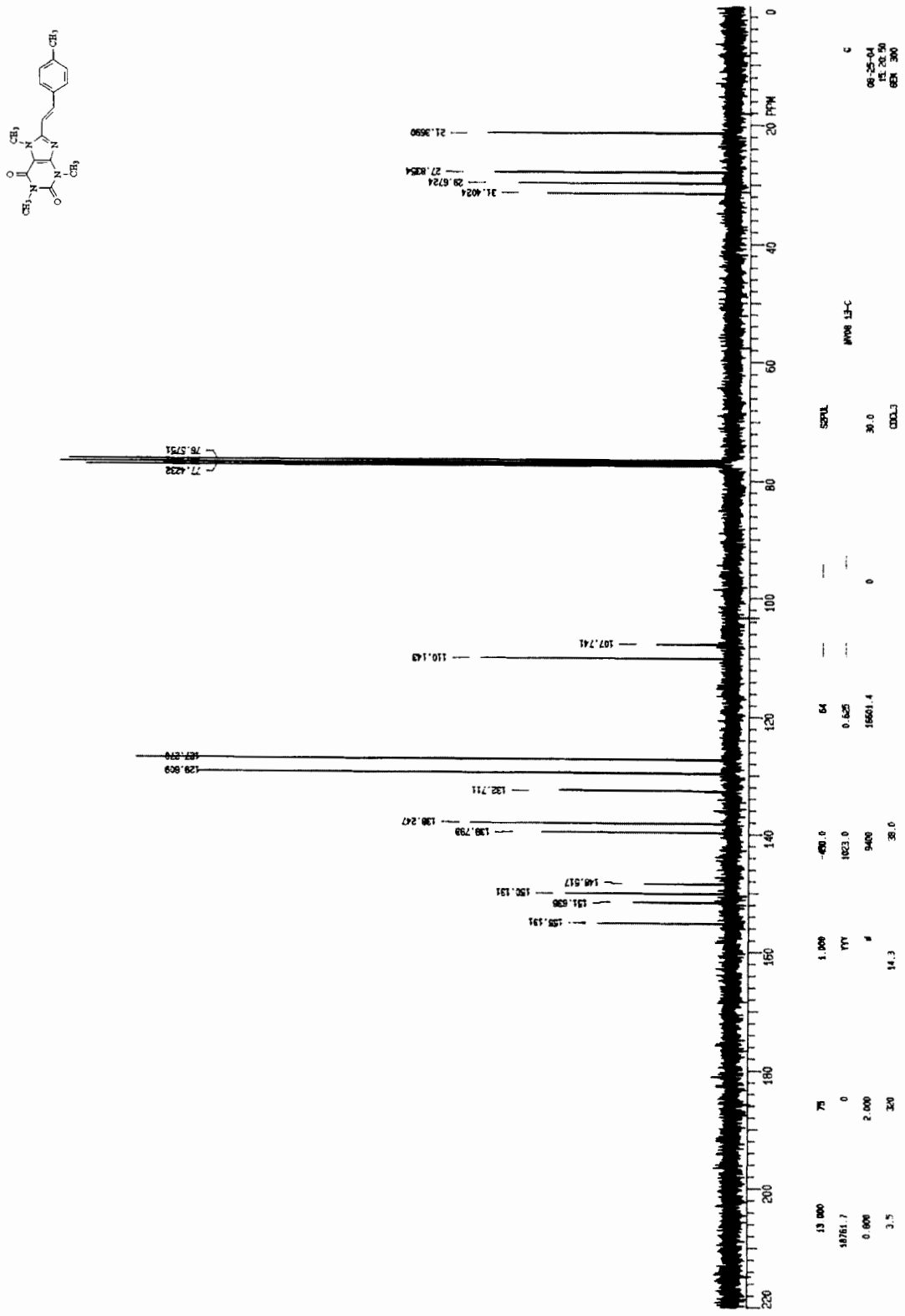
21.3690
27.8264
29.6724
31.4024
76.5751
77.4232
107.741
110.143
128.809
132.711
138.247
138.798
146.517
150.191
151.636
158.191
PPM
0
20
40
60
80
100
120
140
160
180
200
220

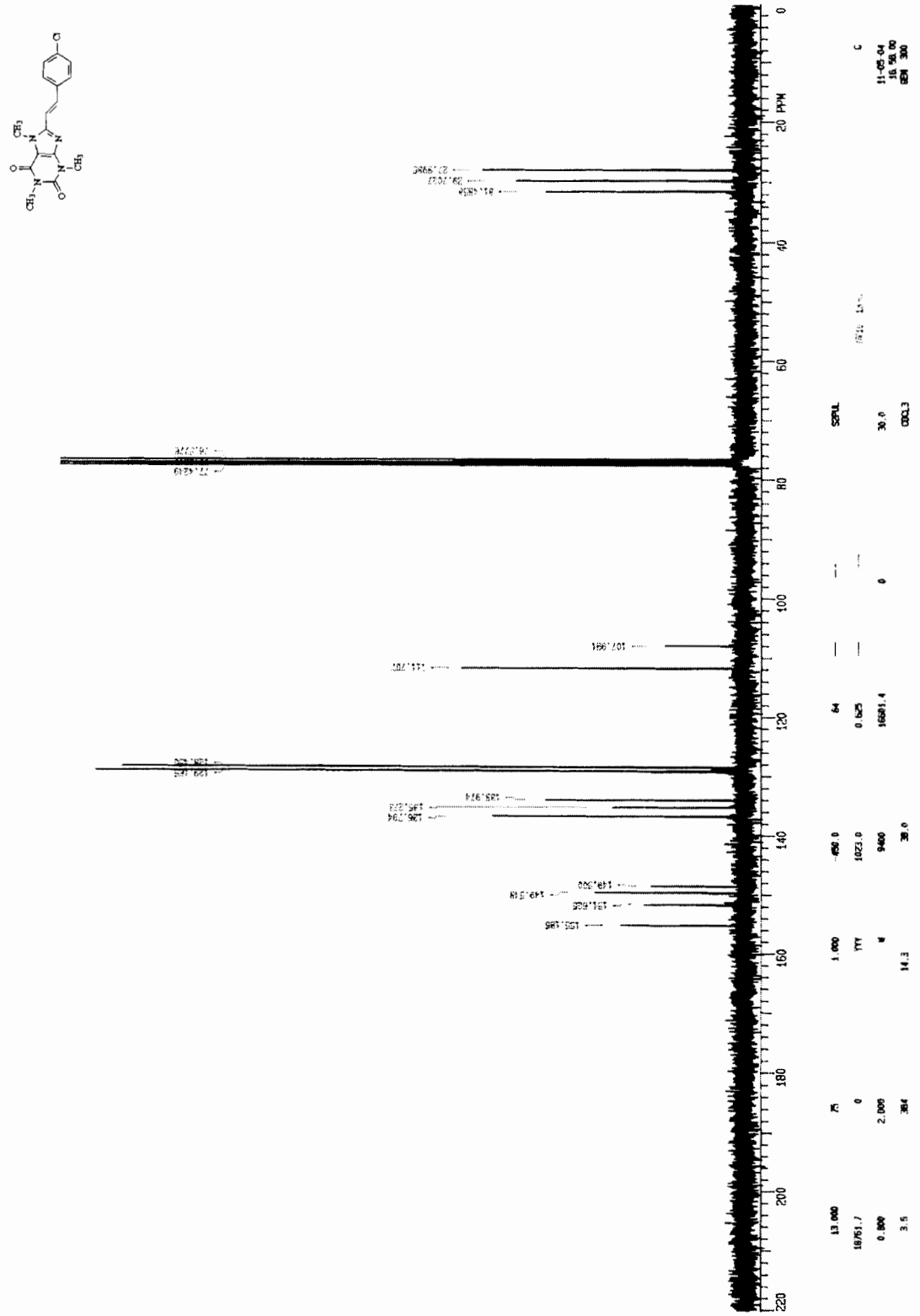

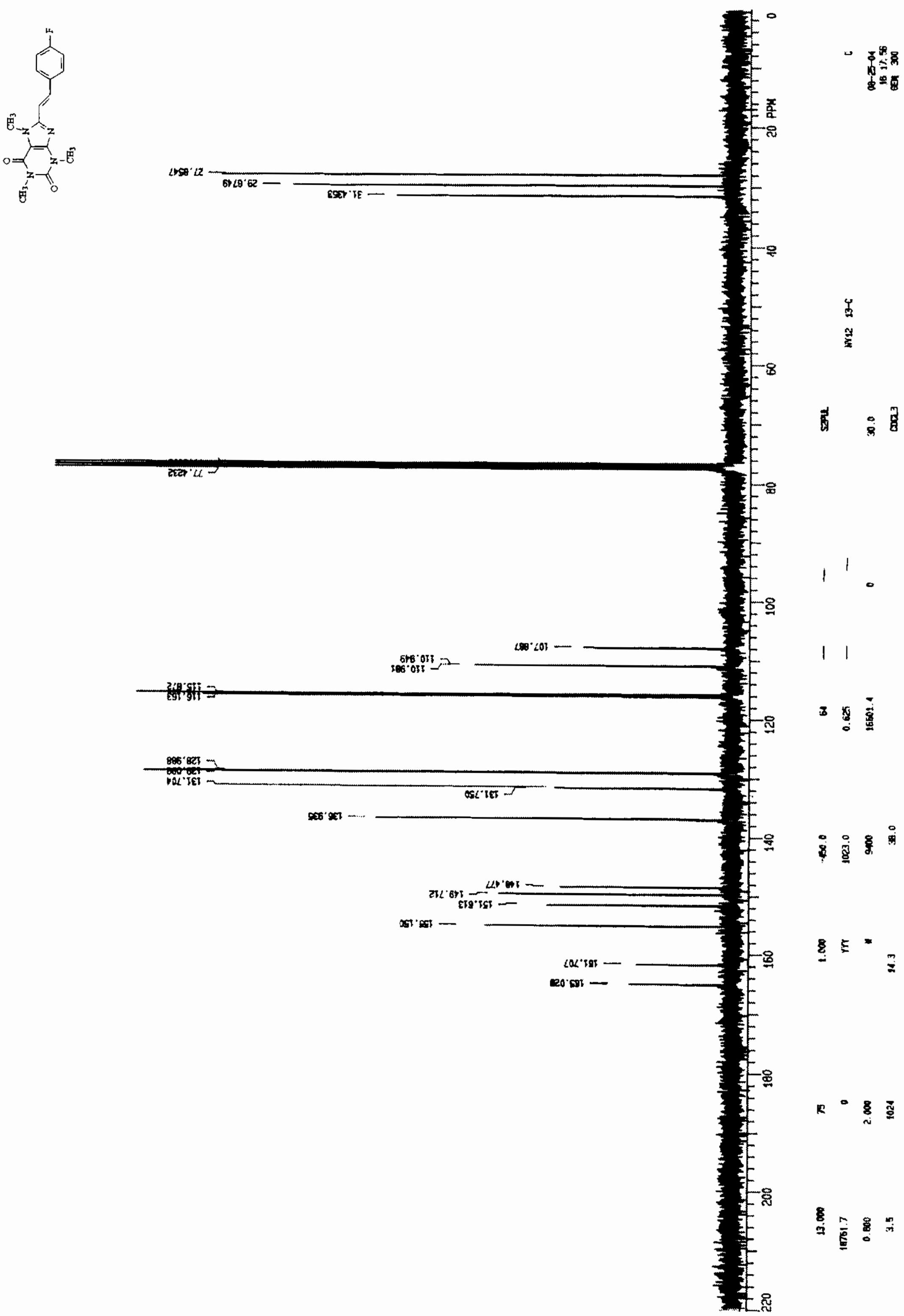

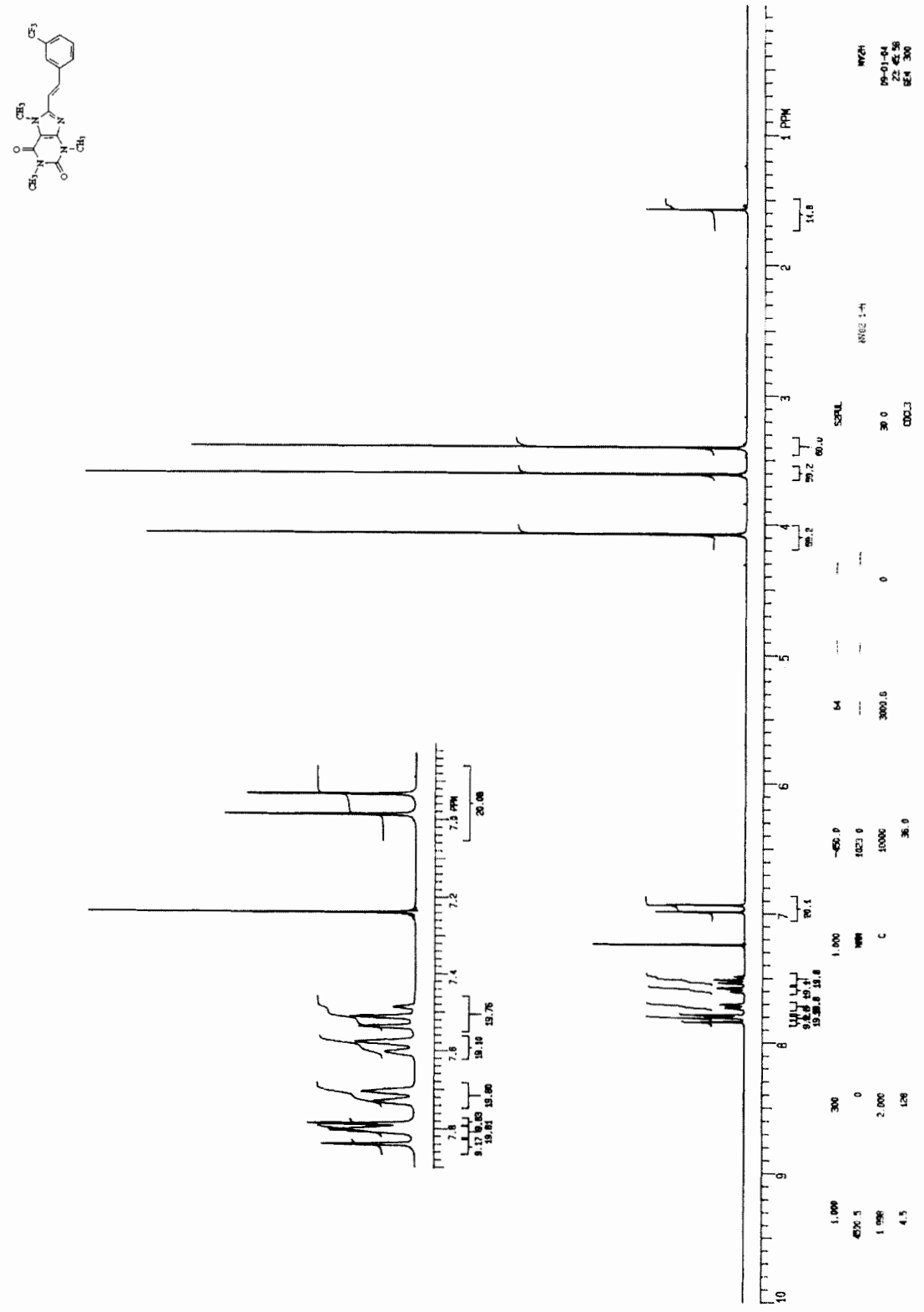

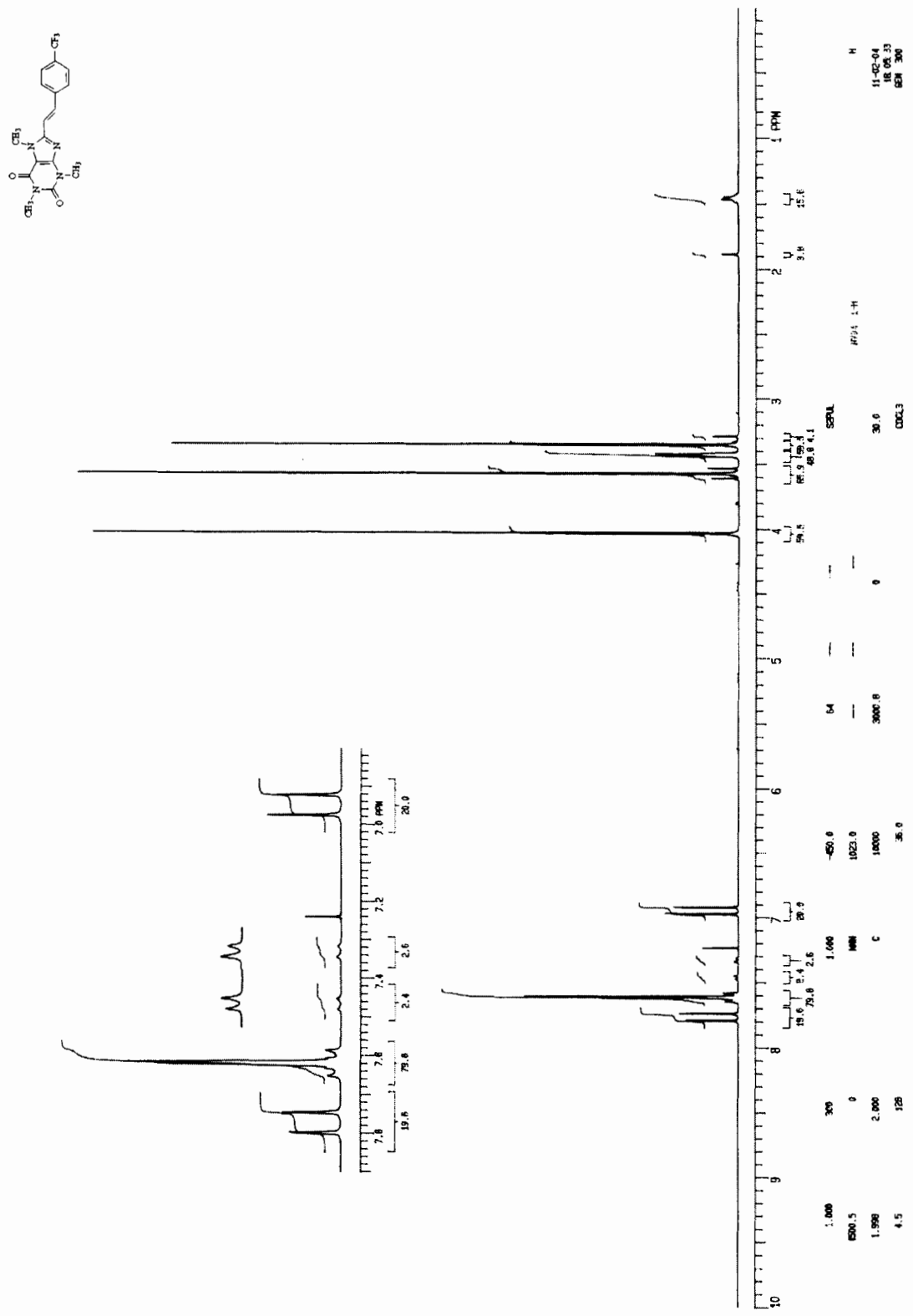

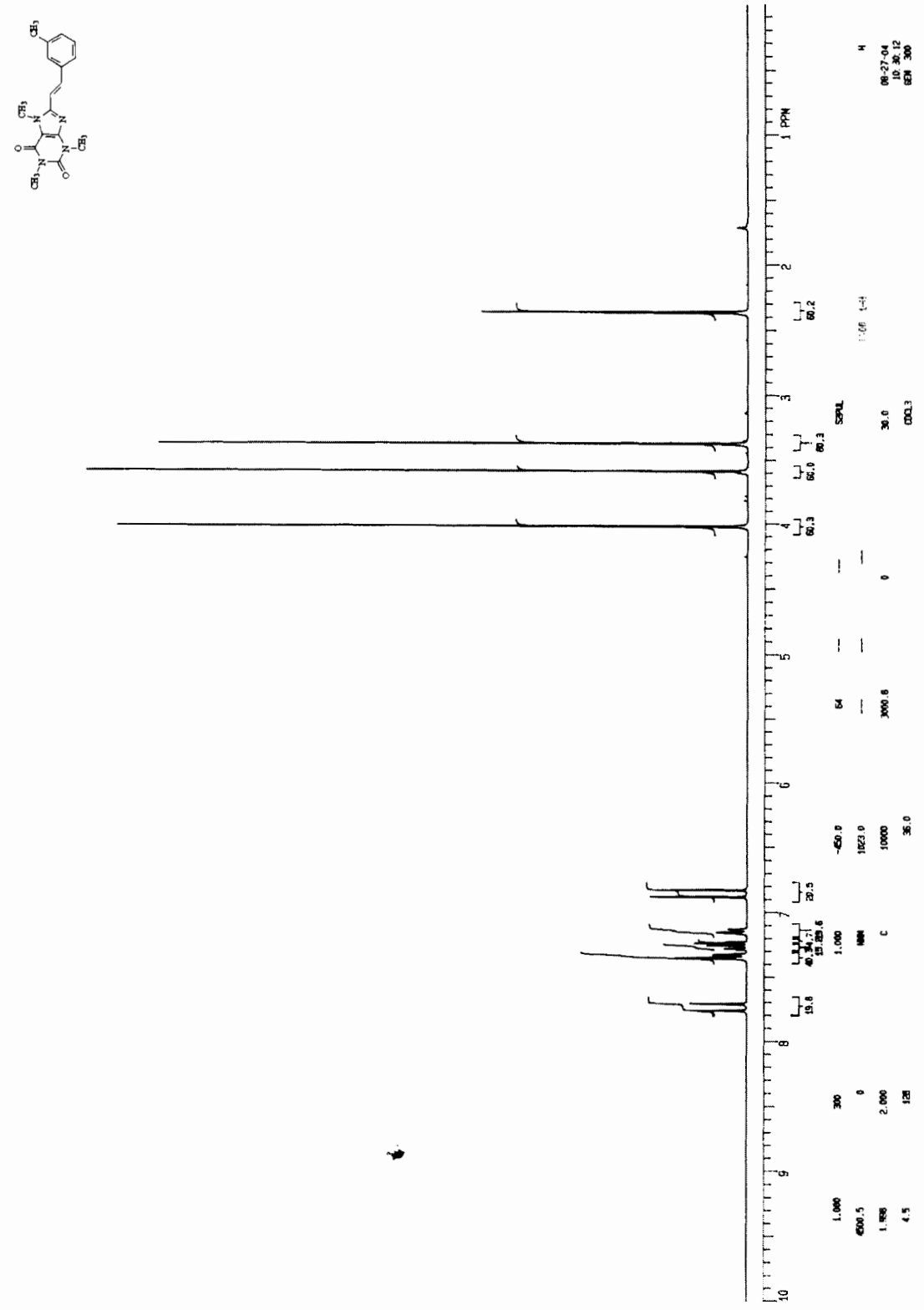

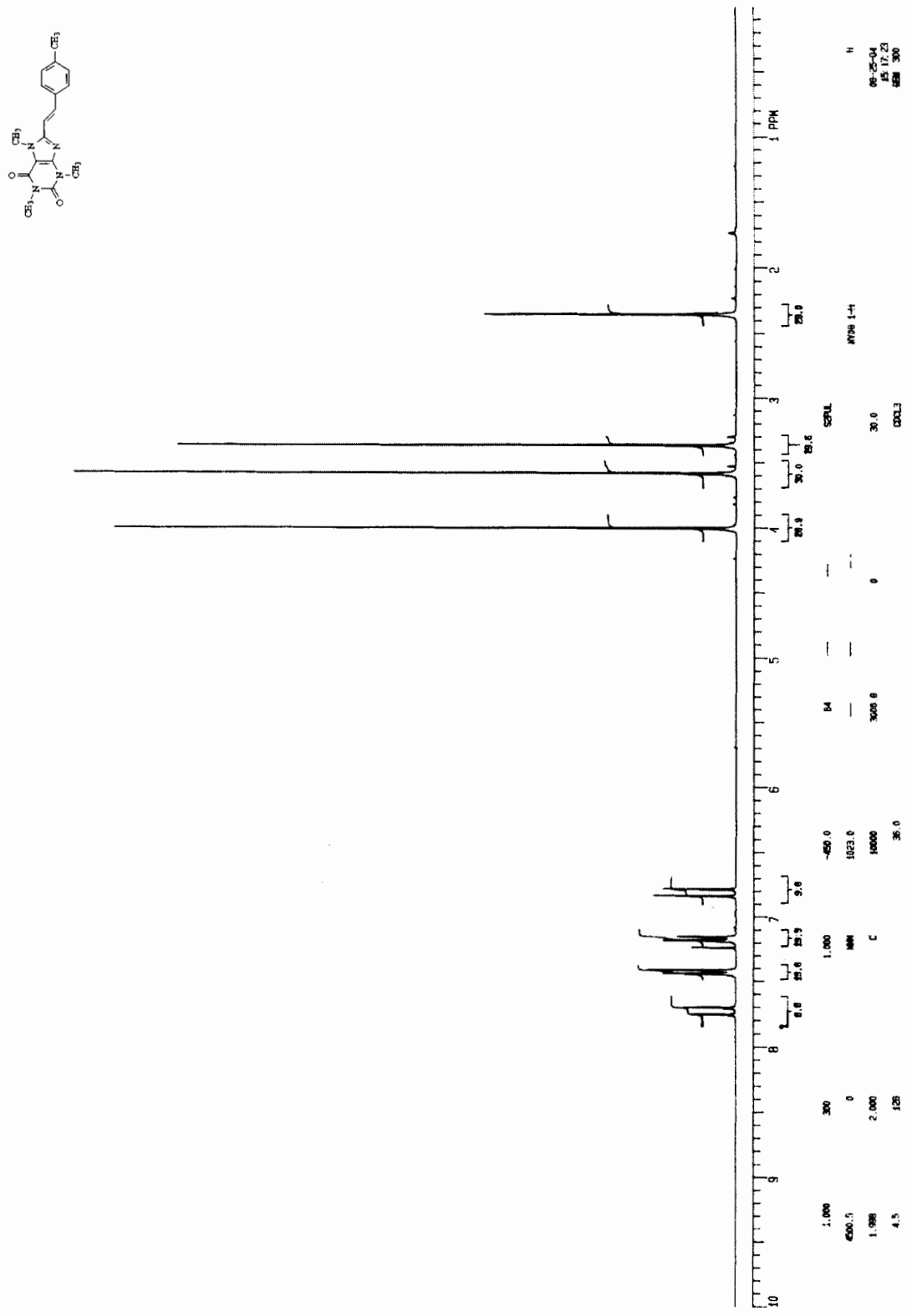

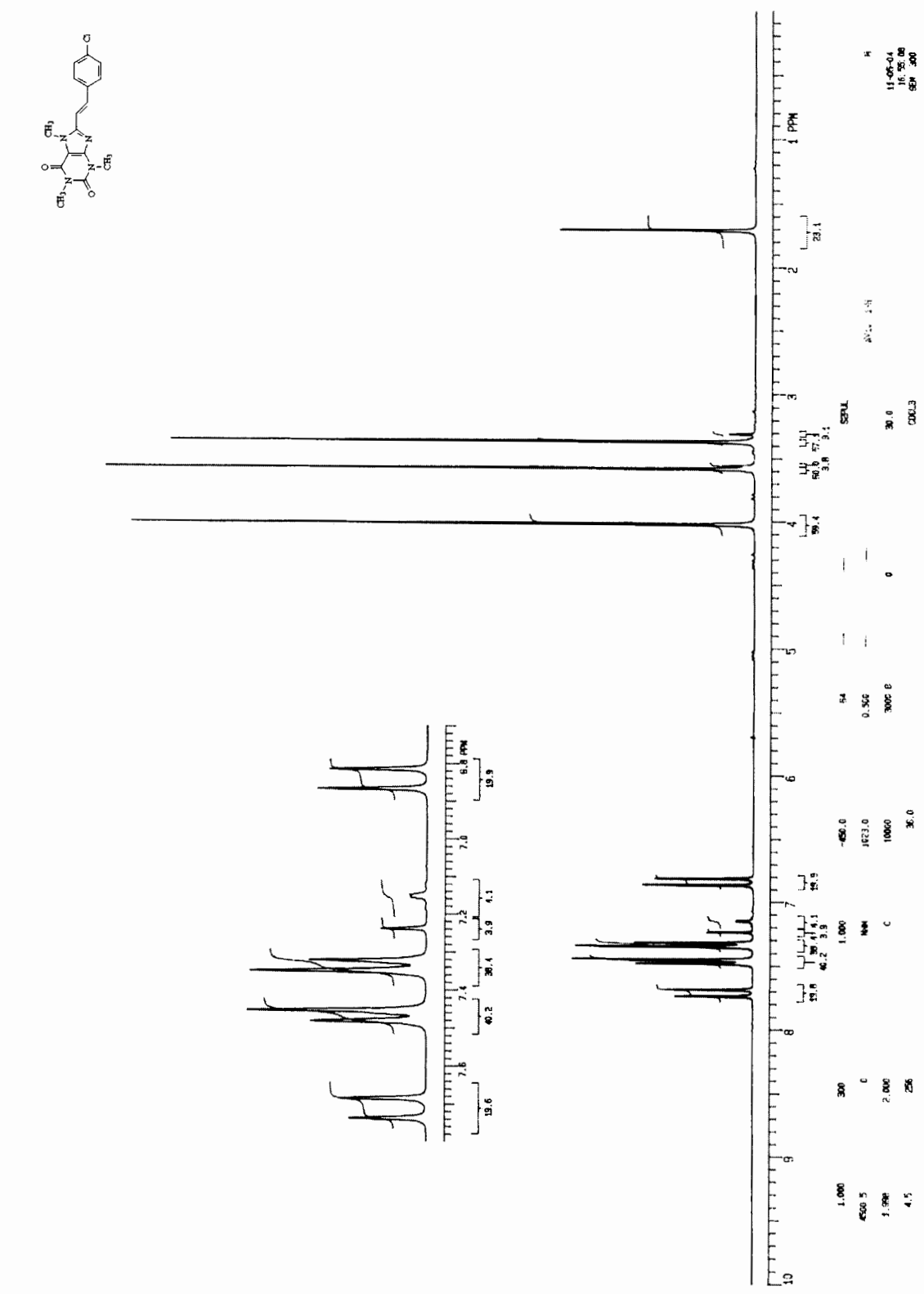

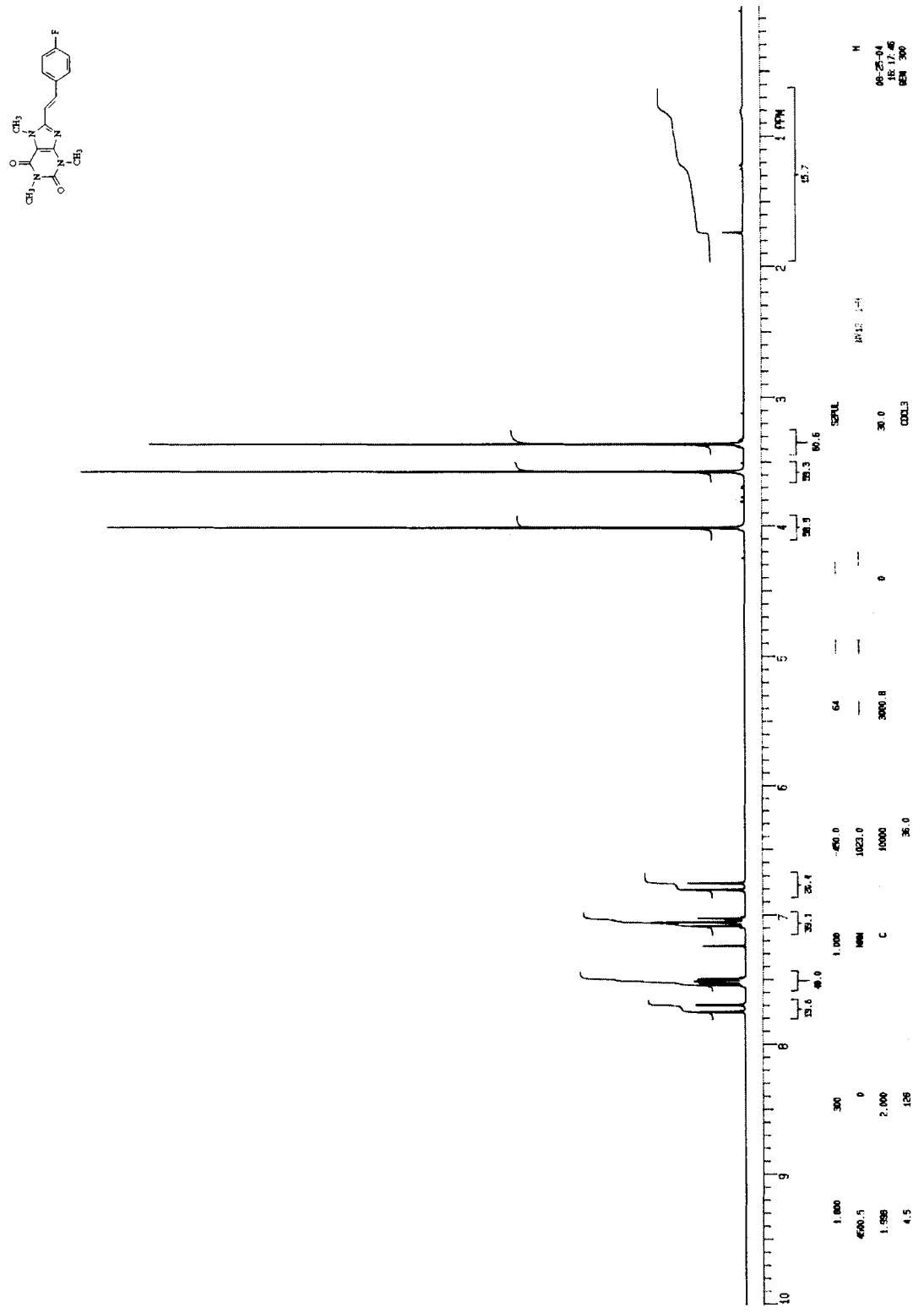

APPENDIX B

Concept article

Inhibition of Monoamine Oxidase B by Analogues of the Adenosine A_{2A} Receptor Antagonist (*E*)-8-(3-chlorostyryl)caffeine (CSC)

Nevil Vlok,[a] Sarel F. Malan,[a] Neal Castagnoli, Jr.,[b] Jacobus J. Bergh,[a] and Jacobus P. Petzer [a,*]

[a]*Pharmaceutical Chemistry, School of Pharmacy, North-West University, Potchefstroom, 2520, South Africa*

[b]*Department of Chemistry, Virginia Tech, Blacksburg, VA 24061, USA*

Abstract: The adenosine A_{2A} receptor has emerged as a possible target for the treatment of Parkinson's disease (PD). Evidence suggests that antagonism of the A_{2A} receptor not only improves the symptoms of the disease but may also protect against the underlying neuronal degeneration. We have recently reported that several known adenosine A_{2A} receptor antagonists (A_{2A} antagonists) also are moderate to very potent inhibitors of monoamine oxidase B (MAO-B). The most potent among these was found to be (*E*)-8-(3-chlorostyryl)caffeine (CSC), a compound frequently used when examining the *in vivo* pharmacological effects of A_{2A} antagonists. Since MAO-B inhibitors are also frequently used as antiparkinsonian agents, dual targeting drugs that block both MAO-B and A_{2A} receptors may have enhanced therapeutic potential in the treatment of PD. In this study we prepared selected analogues of CSC in an attempt to examine specific structural features that may be important for potent MAO-B inhibition. The results of a limited SAR study established that the potency of MAO-B inhibition by (*E*)-8-styrylcaffeinyl analogues depends upon the van der Waals volume (V_w), lipophylicity (π) as well as the Swain–Lupton electronic parameter (F) of the substituents attached to C-3 of the styryl ring. Potency also varies with substituents attached to C-4 but in this case bulkiness (such as V_w) and lipophylicity (π) are the principal substituent descriptors.

Keywords: adenosine, A_{2A} receptor, monoamine oxidase B, structure-activity relationship, SAR, MAO-B

Introduction

Due to their role in the metabolism of monoamine transmitters, monoamine oxidase A and B (MAO-A and -B) are of considerable pharmacological interest. Inhibitors of MAO provide a therapeutically useful approach for the treatment of neurological and psychiatric diseases. In particular reversible MAO-A inhibitors are used as antidepressant and antianxiety drugs (Volz & Gleiter, 1998), while selective inhibitors of MAO-B are in use and under investigation for the treatment of the symptoms or the underlying

neurodegeneration of Parkinson's disease (PD) (Youdim & Riederer, 2004; Riederer *et al.*, 2004) and Alzheimers disease (Saura, 1994). The mechanism-based inactivator of MAO-B, (*R*)-deprenyl (**1**), is frequently used in combination with L-DOPA as dopamine replacement therapy in PD (Rabey *et al.*, 2000). The beneficial effects of (*R*)-deprenyl may be dependent on the inhibition of the MAO-B catalyzed oxidation of dopamine in the CNS, consequently conserving the depleted supply of dopamine and delaying the need for levodopa therapy in patients diagnosed with early PD (Rabey *et al.*, 2000). Inhibition of dopamine oxidation also results in the stoichiometric reduction of the production of hydrogen peroxide, which is thought to play a role in the etiology of neurodegenerative diseases such as PD (Youdim *et al.*, 1995; Cohen, 1983). (*R*)-deprenyl is also reported to exert a neuroprotective effect by blocking apoptotic cell death (Tatton & Greenwood, 1991; Tatton, 1993) and may be clinically useful in postponing the emergence of symptoms that require the initiation of levodopa therapy in PD patients (LeWitt, 2004). In contrast with reversible inhibitors, return of enzyme activity following treatment with inactivators such as (*R*)-deprenyl requires *de novo* synthesis of the MAO-B protein. Aside from the safety considerations associated with irreversible inhibitors, (*R*)-deprenyl is also metabolized to (*R*)-methamphetamine, a compound with vasopressor properties (Riederer *et al.*, 2004). For these reasons, several studies are currently underway to develop safer inhibitors of MAO-B as an alternative to (*R*)-deprenyl (Gnerre *et al.*, 2000; Mazouz *et al.*, 1993). In contrast to (*R*)-deprenyl, these inhibitors are designed to be reversible while retaining selectivity towards MAO-B.

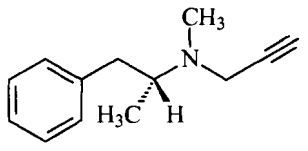

(R)-Deprenyl (1)

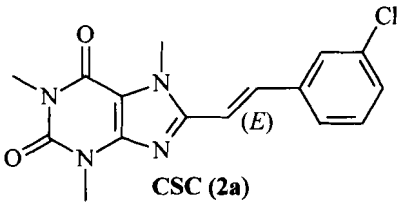

CSC (2a)

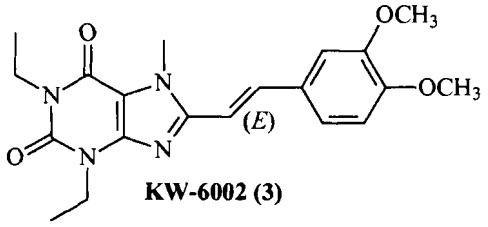

KW-6002 (3)

Figure 1. The structures of the MAO-B inactivator (*R*)-deprenyl (**1**) and the A_{2A} antagonists, CSC (**2a**) and KW-6002 (**3**).

(*E*)-8-(3-Chlorostyryl)caffeine (CSC) (**2a**) had been identified and employed as a selective inhibitor of the A_{2A} subtype of adenosine receptor (Jacobson *et al*, 2003b; Suzuki *et al.*, 1993; Müller *et al.*, 1997). However, it was recently found to inhibit MAO-B with a K_i value of 70 nM independent of its actions on the A_{2A} receptor (Chen *et al.*, 2002). Several analogues of CSC were also prepared as part of an effort to define the structural requirements of this class of compounds to act as inhibitors of MAO-B (Petzer *et al.*, 2003; Castagnoli *et al.*, 2003).

The adenosine A_{2A} receptor antagonist (A_{2A} antagonist) properties of (*E*)-8-styrylcaffeinyl analogues (Suzuki *et al.*, 1993; Müller *et al.*, 1997) have been of special interest because A_{2A} antagonists are currently being investigated as possible therapeutic agents for the symptomatic treatment of motor deficits in PD (Xu *et al.*, 2005). One such compound, KW-6002 (**3**), is currently undergoing clinical trials for this purpose (Bara-Jiminez *et al.*, 2003; Shimada *et al.*, 1997). Results from recent studies in animal models of PD suggest that antagonism of the A_{2A} receptor may not only relieve the symptoms of the disease but may also protect against underlying neuronal degeneration processes (Ikeda *et al.*, 2002; Chen *et al.*, 2001; Schwarzschild *et al.*, 2003). Since MAO-B inhibitors are frequently used as antiparkinsonian agents, the possibility of designing drugs that act both as A_{2A} antagonists and inhibitors of MAO-B may be of value. We have therefore chosen to examine additional analogues (**2b–i,** Figure. 2) of CSC in an attempt to identify specific structural features of CSC that may be responsible for its potency as an MAO-B inhibitor. Earlier studies suggested that structural features important for MAO-B inhibition are the *trans* configuration of the styryl moiety and 1,3,7-trimethyl substitution of the xanthinyl ring system (Petzer *et al.*, 2003). As part of a limited SAR analysis, the compounds investigated in this study retained these features and only differed in the substituents on C-3 and C-4 of the styryl ring. The principal aim was to determine whether substitution of C-3 of the styryl ring with an electron withdrawing group is essential for potent MAO-B inhibition as suggested by the structure of CSC and an earlier study (Petzer *et al.*, 2003).

Results

Chemistry

The procedures by which (*E*)-8-styrylcaffeinyl analogues (**2a–c** and **2e–i**) may be prepared are documented in the literature (Figure 2) (Jacobson *et al.*, 1993; Suzuki *et al.*, 1993; Müller *et al.*, 1997). Compound **2d** was not prepared in this study and the K_i value for the inhibition of MAO-B was obtained from the literature (Petzer *et al.*, 2002). Because of the ease of synthesis and relatively good yields we followed the procedure according to Suzuki *et al.* (1993) (Figure 2). Acylation of 1,3-dimethyl-5,6-diaminouracil (**4**) with commercially available *trans*-cinnamic acid (**5e**) and 3-chloro- (**5a**), 3-trifluoromethyl- (**5b**), 3-methyl- (**5c**), 4-chloro- (**5f**), 4-trifluoromethyl- (**5g**), 4-methyl (**5h**) or 4-fluoro- (**5i**), *trans*-cinnamic acids in the presence of a carbodiimide reagent (1-ethyl-2-[3-(dimethylamino)propyl]-carbodiimide, EDAC) followed by treatment with sodium hydroxide resulted in the corresponding 1,3-dimethyl-(*E*)-8-styryl-7*H*-xanthinyl analogues (**6**). Without further purification, the precipitate obtained from this reaction was selectively *7N*-methylated in the presence of an excess of iodomethane and potassium carbonate to yield the target compounds **2a–c** and **2e–i**. Following recrystalization from a suitable solvent the structures and purity of the compounds were verified by mass spectrometry, ^{1}H-NMR and ^{13}C-NMR. For compound **2a** and **2e** the physical data was compared to the corresponding literature values as cited in the Experimental Section. The *trans* geometry of the styryl alkene was confirmed by proton-proton coupling constants in the range of 15.7–15.8 Hz for the olefinic proton signals.

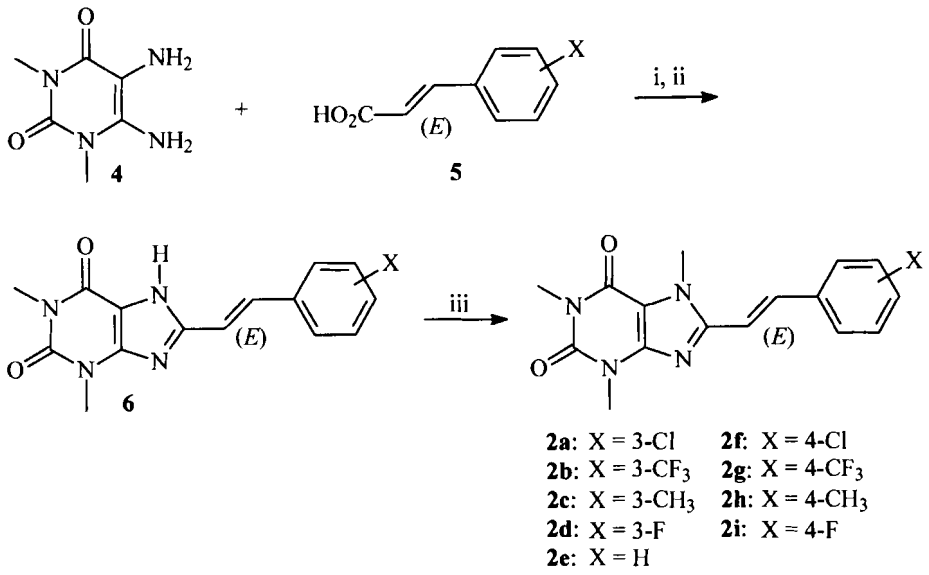

Figure 2. Synthetic pathway to *(E)*-8-styrylcaffeinyl analogues **2**. Key: (i) EDAC, dioxane/H_2O; (ii) NaOH (aq), reflux; (iii) CH_3I, K_2CO_3, DMF.

Enzymology

The *Ki* values for the competitive inhibition of MAO-B by compounds **2a–c** and **2e–i** were estimated by two different assays. In the first instance the extent by which various concentrations of the test inhibitor slowed the rate of the oxidation of 1-methyl-4-(1-methylpyrrol-2-yl)-1,2,3,6-tetrahydropyridine (MMTP) (**7**) to the corresponding dihydropyridinium metabolite ($MMDP^+$) (**8**) was measured spectrophotometrically (Inoue *et al.*, 1999; Nimkar *et al.*, 1996). $MMDP^+$ production was measured at 420 nm, a wavelength at which neither the substrate nor the test inhibitors absorb light. Because of the favorable chromophoric characteristics and *in vitro* chemical stability of $MMDP^+$ this assay is frequently used to estimate *Ki* values for the inhibition of both MAO-A and –B (Hubálek *et al.*, 2005; Castagnoli *et al.*, 1997). In order to prevent any contribution towards the oxidation of MMTP by MAO-A, the source of the MAO-B enzyme must either be devoid of any MAO-A activity or the oxidation of MMTP by MAO-A must be prevented by inactivating the enzyme with the selective mechanism-based inactivator clorgyline. Since we used the mitochondrial fraction isolated from baboon liver mitochondria, a source which is reported (Inoue *et al.*, 1999) to be devoid of MAO-A activity, our assays were carried out in the absence of clorgyline pre-inactivation. The absence of MAO-A activity in the baboon liver mitochondrial fraction was confirmed, since pre-incubation of the enzyme with clorgyline (3×10^{-8} M) failed to decrease the rate at which MMTP is oxidized, while (*R*)-deprenyl (3×10^{-7} M) almost completely prevented oxidation (data not shown).

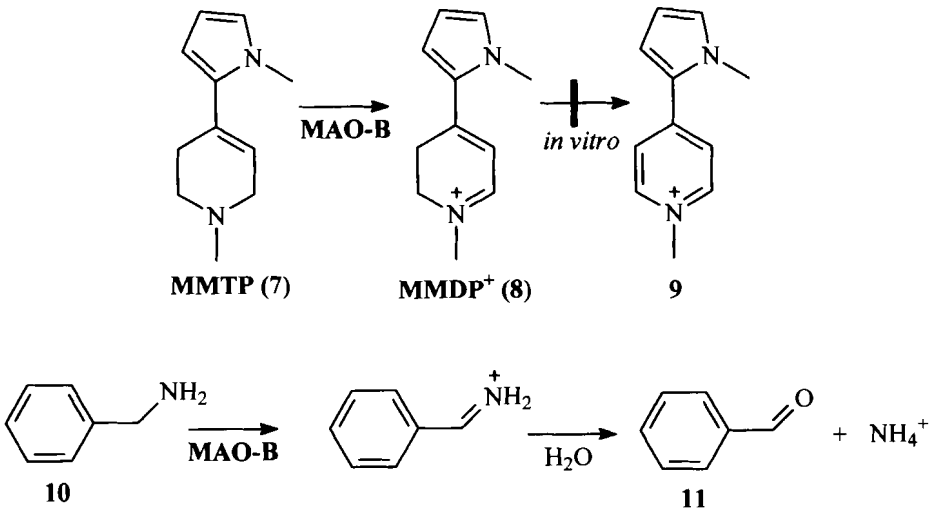

Figure 3. The MAO-B catalyzed oxidation of MMTP (7) and benzylamine (**10**) to the corresponding dihydropyridinium product **8** and benzaldehyde (**11**), respectively. The *in vitro* oxidation of **8** to the pyridinium species (**9**) is not observed.

In the second approach we utilized the selective MAO-B substrate benzylamine (**10**) to measure *Ki* values. Benzylamine is arguably the most thoroughly characterized substrate of MAO-B and is frequently used in inhibition (Krueger *et al.*, 1995) and mechanistic (Walker & Edmondson, 1994; Silverman & Hawe, 1995) studies involving this enzyme. When using purified MAO-B as enzyme source, which is relatively free from background interference, the concentration of the of the α-carbon oxidation product, benzaldehyde (λ_{max} = 250 nm), may be measured spectrophotometrically (Walker & Edmondson, 1994; Newton-Vinson *et al.*, 2000). In contrast, background absorption in the near-UV wavelength range when using mitochondrial fraction as enzyme source is too high to measure benzaldehyde concentrations by spectrophotometry. Even protein precipitation and subsequent centrifugation (the last two steps during a discontinuous assay) of the incubations do not solve this problem. For this reason we chose to measure the extent of benzylamine oxidation by HPLC-UV analysis following a discontinuous assay. Figure 4 presents an example of the chromatogram tracings routinely observed during this study. The incubation time of the enzyme catalyzed reaction was chosen to be 8 minutes since the benzylamine oxidation appeared to be linear (Figure 5) for at least 10 minutes at all substrate concentrations used (125–750 μM). Also in order to select appropriate substrate concentrations for the inhibition assays, the K_m for benzylamine oxidation by baboon liver MAO-B was estimated. Considering the similarity of the steady-state kinetic parameters (K_m and V_{max}) between baboon and human MAO-B for tetrahydropyridinyl substrates (Inoue *et al.*, 1999), it may be expected that the K_m values for benzylamine oxidation by the two enzymes should also be similar. In accordance with this argument, the K_m value for benzylamine oxidation by baboon liver MAO-B was estimated to be 616 ± 23 μM (Figure 6) while the reported value with human MAO-B is 500 ± 0.1 μM (Newton-Vinson *et al.*, 2000).

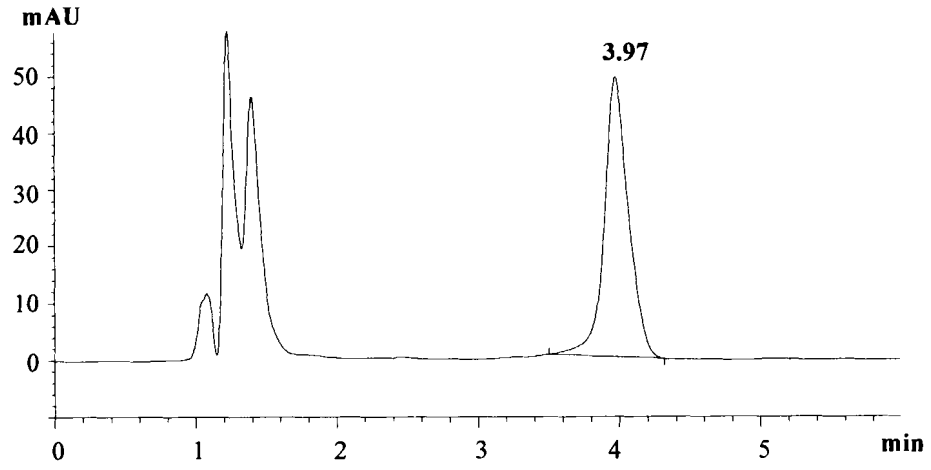

Figure 4. An HPLC-UV tracing showing the presence of benzaldehyde (retention time of 3.97 minutes) in an incubation of benzylamine (750 μM) with baboon liver MAO-B (0.15 mg protein/mL of the mitochondrial preparation). Following an 8 minute incubation at 37 °C, the reaction was terminated by precipitating the mitochondrial protein with perchloric acid. After centrifugation, 50 μL of the supernatant was injected into the HPLC and the effluent was monitored at a wavelength of 250 nm.

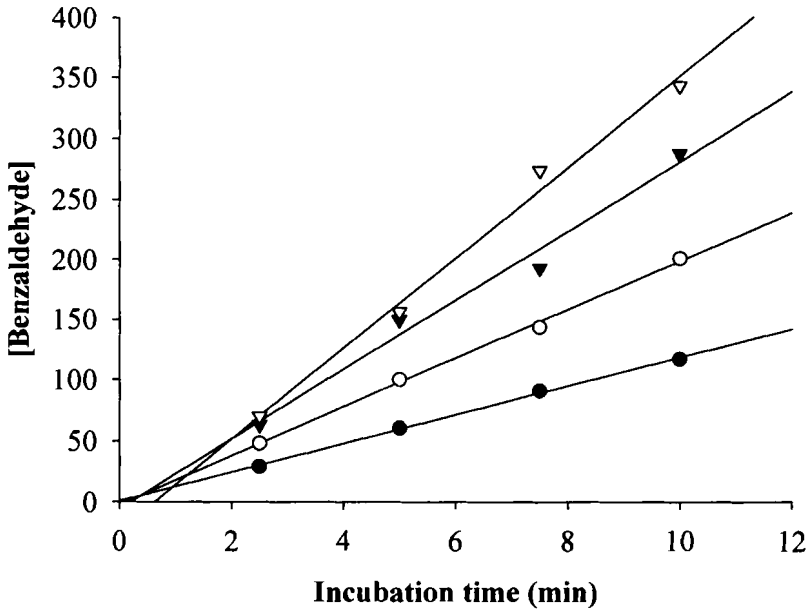

Figure 5. Linearity in the oxidation of benzylamine by baboon liver MAO-B (0.15 mg/mL of the mitochondrial preparation). The concentration of benzaldehyde produced was measured by HPLC analysis following termination of the enzyme catalyzed reaction at time points of 2.5, 5, 7.5 or 10 minutes. The concentration of benzaldehyde produced is expressed as nmoles/mg mitochondrial protein. The

concentrations of benzylamine used in this study were 125 μM (filled circles), 250 μM (open circles), 500 μM (filled triangles) and 750 μM (open triangles).

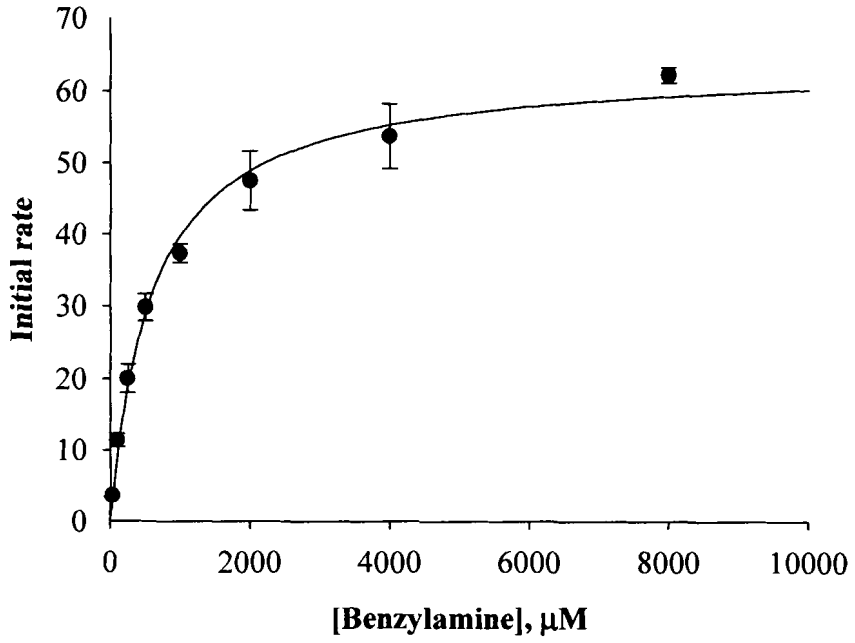

Figure 6. Determination of the K_m value of benzylamine oxidation by baboon liver MAO-B. The concentration of benzaldehyde produced was measured by HPLC analysis following an 8 minute incubation with 0.15 mg/mL baboon liver mitochondria at 37 °C. A K_m value of 616 ± 23 μM was estimated by fitting the data to the Michaelis–Menten equation using a nonlinear least-squares fitting routine. All measurements were conducted in triplicate and the benzylamine concentration in the incubations ranged from 25 to 8000 μM. The initial rates are expressed as nmoles.mg protein^{-1}.min^{-1} of benzaldehyde formed.

Inhibition studies

All of the (*E*)-8-styrylcaffeinyl analogues (**2a–c** and **2e–i**) tested were found to be inhibitors of MAO-B. As demonstrated by example with (*E*)-8-(4-methylstyryl)caffeine (**2h**) (Figure 7), the lines of the Lineweaver–Burke plots intersected, indicating that the mode of inhibition was competitive (Segel, 1993). The K_i values for the inhibition of MAO-B are presented in Table 1. The lead compound for this study, CSC (**2a**), was confirmed (Chen *et al.*, 2002) to be a very potent inhibitor with a K_i value of 148 nM for the inhibition of benzylamine oxidation by MAO-B. The similarity in range of this value with that obtained with MMTP as substrate (128 nM) is an indication of the reliability of the K_i estimations and also suggests that specific alterations in experimental conditions (such as change of substrate or analytical technique) do not affect the estimated values to a large extent. In accordance with this view, for the other analogues (**2b–c** and **2e–i**)

tested, the differences between the K_i values estimated by the two different techniques are within the range expected for experimental error (Table 1).

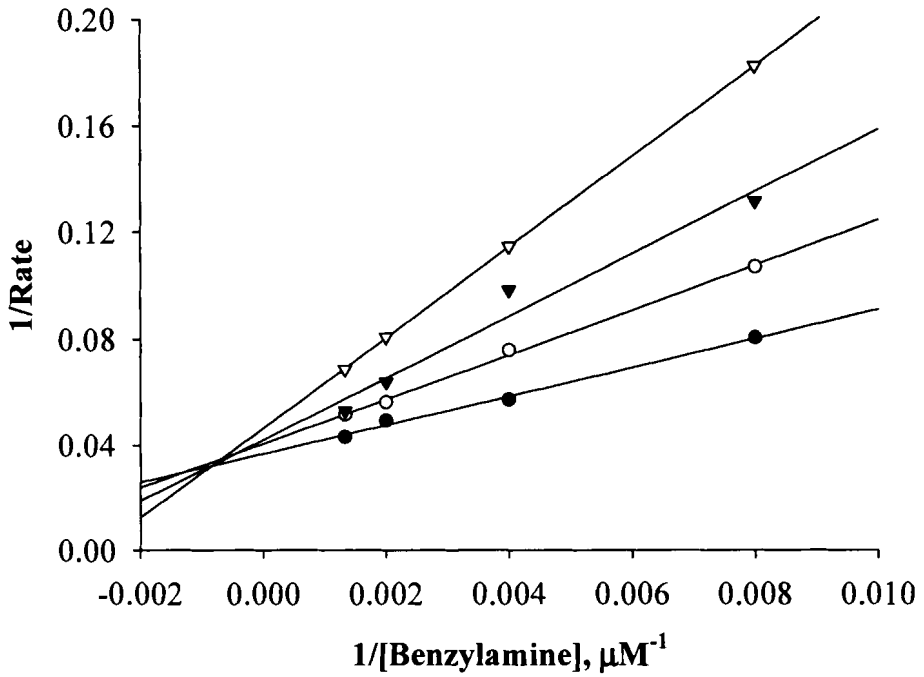

Figure 7. Lineweaver–Burke plots of the oxidation of benzylamine by baboon liver MAO-B in the absence (filled circles) and presence of various concentrations of **2b** (open circles, 0.1 μM; filled triangles, 0.2 μM; open triangles, 0.4 μM. The concentration of the baboon liver mitochondrial preparation was 0.15 mg/mL and the rates are expressed as nmoles.mg protein^{-1}.min^{-1} of benzaldehyde formed.

Table 1. The K_i values for the inhibition of MAO-B by (*E*)-8-styrylcaffeinyl analogues. The values of the selected physiochemical parameters used in the SAR study are also listed (Hansch & Leo, 1995; Hansch & Leo, 1979).

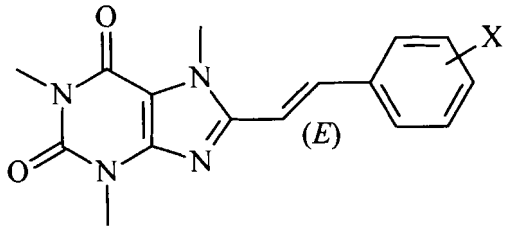

		K_i value (nM) [a]				
Compd	X	**7** as substrate [b]	**10** as substrate [c]	V_w [d]	π [e]	F [e]
2a	3-Cl	70 [f], 128	148	1.07	0.71	0.42
2b	3-CF_3	133	188	1.11	0.88	0.38
2c	3-CH_3	1431	1526	1.01	0.56	0.01
2d	3-F	400 [g]	–	0.36	0.14	0.45
2e	H	2704 [g], 2864	2316	0.08	0.00	0.00
2f	4-Cl	260	187	1.07	0.71	0.42
2g	4-CF_3	245	238	1.11	0.88	0.38
2h	4-CH_3	367	373	1.01	0.56	0.01
2i	4-F	1559	1374	0.36	0.14	0.45

[a] The enzyme source used was MAO-B from baboon liver mitochondria. [b] MMTP served as enzyme substrate. [c] Benzylamine served as enzyme substrate. [d] Values obtained from reference (Hansch & Leo, 1979). [e] Values obtained from reference (Hansch & Leo, 1995). [f] K_i value obtained from reference (Chen *et al.*, 2002). [g] K_i value obtained from reference (Petzer *et al.*, 2003).

Qualitative inspection of the results in Table 1 suggests that the potency of MAO-B inhibition by (*E*)-8-styrylcaffeinyl analogues bearing substituents on C-3 of the styryl ring (**2a–d**) depends upon the electronic characteristics of the substituent since those analogues with electron withdrawing groups (**2a–b** and **2d**) are significantly more potent as inhibitors than the unsubstituted analogue (**2e**) and the analogue bearing an electron releasing methyl group (**2c**). In contrast, potency of inhibition by analogues bearing substituents on C-4 of the styryl ring (**2f–i**) appears to be dependent upon the size of the substituent since inhibition by those analogues with relatively bulky substituents (**2f–h**) are more potent than the unsubstituted analogue (**2e**) and the analogue bearing a C-4 fluorine substituent (**2i**). In order to quantify these apparent relationships between MAO-B inhibitory activity and the physiochemical properties of the substituents, a Hansch-type SAR study (Hansch & Leo, 1995; Kutter & Hansch, 1969; Fuller *et al.*, 1968) study was carried out by stepwise multiple linear regression analysis. Five parameters were used to describe each substituent. The van der Waals volume (V_w) (Bondi, 1964) and Taft steric parameter (E_s) (Hansch *et al.*, 1995) were used as descriptors of bulkiness while the lipophylicities of the substituents were described by

the Hansch constant (π) (Fujita *et al.*, 1964). The classical Hammett (σ_m or σ_p) and Swain–Lupton (F) constants (Swain & Lupton, 1968) served as electronic parameters. All physiochemical values of the substituents were obtained from standard compilations (Hansch & Leo, 1995; Hansch *et al.*, 1995; Hansch & Leo, 1979). The analogues were divided into two groups – those bearing substituents on C-3 of the styryl ring (**2a–d**) and those with substituents on C-4 of the styryl ring (**2f–i**). The unsubstituted (*E*)-8-styrylcaffeinyl analogue (**2e**) was considered a member of each group. Results of the statistical analysis for the two groups are shown in Table 2 and 3, respectively. These tabulated results were generated using only the K_i values obtained with MMTP (7) as substrate.

For analogues substituted at C-3 of the styryl ring (Table 2) the only single substituent parameter that show a meaningful correlation with the logarithm of the K_i values (expressed in μM) are the Hammett electronic parameter (σ_m) and the Swain–Lupton F constant. Regression analysis of logK_i with σ_m and F exhibits moderate correlations with R^2 values of 0.86 and 0.80, respectively. The statistical F test values were found to be 18.9 and 12.3 for the two correlations (a higher F value indicates a better fit) (Livingstone & Salt, 2005) with confidence levels of 97.8% and 96.1%, respectively. All other single-parameter correlations with the logK_i values exhibited poorer statistical correlations. Correlation may be improved by addition of an additional substituent parameter to the regression analysis. Two-parameter fits with V_w and σ_m or with π and σ_m yield correlation coefficients of 0.99 and 0.98, respectively. For these correlations, the probabilities that V_w and π are zero are 3.3% and 9%, respectively. Therefore, the best mathematical description of binding affinity (logK_i) of C-3 substituted (*E*)-8-styrylcaffeinyl analogues to MAO-B is:

$$\text{Log}K_i = -2.10(\pm 0.19)\sigma_m - 0.49(\pm 0.09)V_w + 0.49(\pm 0.07)$$
$$(F = 109.8 \text{ and } R^2 = 0.99)$$

The negative signs of both the σ_m (–2.10 ± 0.19) and the V_w (–0.49 ± 0.09) parameter coefficients indicate that the potency (logK_i) by which (*E*)-8-styrylcaffeinyl analogues inhibit MAO-B may be enhanced by substitution with larger C-3 functional groups with electron withdrawing characteristics. Since the Hansch constant (π) is also negatively correlated (–0.61 ± 0.20; Table 2) with logK_i, C-3 lipophylic substituents also appear to enhance MAO-B inhibition potency.

For analogues substituted at C-4 of the styryl ring (Table 3) the single-parameter fit that shows the best correlations with the logK_i values is the van der Waals volume V_w and the Hansch constant (π) of the substituents. The regression analysis exhibits R^2 values of 0.99 and 0.96 with a confidence level of >99.6% for the two correlations. The mathematical description of the binding affinity (logK_i) of C-4 substituted (*E*)-8-styrylcaffeinyl analogues to MAO-B may therefore be presented as:

$$\text{Log}K_i = -1.03(\pm 0.04)V_w + 0.55(\pm 0.04)$$

(F = 608.6 and R^2 = 0.99)

or

$$\text{Log}K_i = -1.28(\pm 0.15)\pi + 0.39(\pm 0.08)$$

(F = 75.2 and R^2 = 0.96)

As observed with the analogues substituted at the C-3 position, the negative sign of the V_w parameter coefficient (–1.03 ± 0.04) suggests that the potency (logK_i) of MAO-B inhibition may be enhanced by substitution with bulky C-4 functional groups. On the other hand, the electronic contribution of the C-4 substituents to logK_i appears to be negligible since in a two-parameter fit with V_w and σ_p, the probability of the term containing σ_p being zero is 21%. The same argument applies to the other electronic parameter (F) considered in this study (data not shown). There is also a meaningful correlation (R^2 = 0.96; F = 75.2) between the Hansch constants (π) of the C-4 substituents and the logK_i values. Hydrophobic C-4 functional groups appear to favour inhibition potency since the sign of the π parameter coefficient (–1.28 ± 0.15) is negative. Again there does not seem to be an electronic contribution of the C-4 substituents to logK_i since in a two parameter fit of logK_i with π and σ_p or of logK_i with π and F the probability of the terms containing σ_p and F being zero are 13.9% and 86.8%, respectively (data not shown).

Table 2. Correlatons of the MAO-B inhibition constants (logK_i) of (*E*)-8-styrylcaffeinyl analogues bearing substituents on C-3 of the styryl ring (**2a–e**) with steric, electronic and hydrophobic substituent parameters [a].

Parameter	Correlation (slope)	y-intercept	Coefficient of determination	F [b]	Significance [c]
σ_m	-2.44 ± 0.56	0.21 ± 0.17	0.86	18.9	0.022
F	-2.40 ± 0.68	0.29 ± 0.22	0.80	12.3	0.039
V_w	-0.83 ± 0.56	0.29 ± 0.47	0.42	2.2	0.23
E_s	0.42 ± 0.30	0.11 ± 0.39	0.39	1.9	0.26
π	-1.17 ± 0.64	0.23 ± 0.36	0.53	3.3	0.16
$V_w + \sigma_m$	-0.49 ± 0.09	0.49 ± 0.07	0.99	109.8	0.033
	-2.10 ± 0.19				0.0079
$\pi + \sigma_m$	-0.61 ± 0.20	0.39 ± 0.10	0.98	41.2	0.090
	-1.98 ± 0.32				0.025

[a] The logK_i values (expressed in μM) obtained with substrate 7 (MMTP) were used in the linear regression analysis; [b] The F test statistic relates the mean squares due to regression to the error variance. Higher F values indicate a better fit and a regression equation with an F value higher than the critical F value may be judged as significant. Critical F values may be calculated as described recently (Livingstone & Salt, 2005). [c] The significance is the fractional probability that the coefficient of the added variable is zero.

Table 3. Correlatons of the MAO-B inhibition constants ($\log K_i$) of (*E*)-8-styrylcaffeinyl analogues bearing substituents on C-4 of the styryl ring (**2e–i**) with steric, electronic and hydrophobic substituent parameters [a].

Parameter	Correlation (slope)	*y*-intercept	Coefficient of determination	F [b]	Significance [c]
σ_p	-0.86 ± 0.92	-0.08 ± 0.25	0.22	0.86	0.42
F	-0.72 ± 1.17	-0.02 ± 0.38	0.11	0.38	0.58
V_w	-1.03 ± 0.04	0.55 ± 0.04	0.99	608.6	0.00015
E_s	0.45 ± 0.17	0.26 ± 0.22	0.70	7.0	0.077
π	-1.28 ± 0.15	0.39 ± 0.08	0.96	75.2	0.0032
$V_w + \sigma_p$	-1.00 ± 0.03	0.55 ± 0.03	0.99	542.0	0.0012
	-0.11 ± 0.06				0.21

[a] The $\log K_i$ values (expressed in μM) obtained with substrate 7 (MMTP) were used in the linear regression analysis; [b] The F test statistic relates the mean squares due to regression to the error variance. Higher F values indicate a better fit and a regression equation with an F value higher than the critical F value may be judged as significant. Critical F values may be calculated as described recently (Livingstone & Salt, 2005). [c] The significance is the fractional probability that the coefficient of the added variable is zero.

Discussion

Recent descriptions of the crystal structures of human recombinant MAO-B co-crystallized with several propargylamine inactivators (Binda *et al.*, 2001; Binda *et al.*, 2004) have led to the proposal that the substrate must transverse an "entrance cavity" in order to gain access to the "substrate cavity". The "gate" separating the two cavities appears to be the side chain of Ile-199 which may exhibit different rotamer conformations which allows for the fusion of the two cavities in order to accommodate larger inhibitors such as the reversible inhibitor 1,4-diphenyl-2-butene (Binda *et al.*, 2003). For this inhibitor the first phenyl ring extends into the entrance cavity space where it is in contact with specific hydrophobic amino acid residues (Phe-103, Ile-199 and Ile 316) whereas the second phenyl ring is in contact with Tyr-398 and Tyr 435 in the substrate cavity space. The latter two amino acids together with the FAD co-factor, which exists in a bent and twisted conformation, form an aromatic cage for the substrate amine recognition. Since compounds **2a–i** and 1,4-diphenyl-2-butene are similar in size it may be expected the phenyl ring of **2a–i** projects into the entrance cavity in a similar manner as that observed for 1,4-diphenyl-2-butene while polar functional groups of the caffeine aromatic ring are in contact with the flavin within the substrate cavity. A similar binding mode is observed for the reversible MAO-B inhibitor, *trans,trans*-farnesol (Hubalek *et al.*, 2005), which also spans both the entrance and substrate cavities with the polar OH moiety in close contact with the flavin. Extension and binding of the styryl moiety into the entrance cavity may be responsible for the high potency of certain (*E*)-8-styrylcaffeinyl analogues as MAO-B inhibitors (Binda *et al.*, 2003). In accordance with this hypothesis caffeine was found to be a very weak competitive inhibitor of MAO-B (Chen *et al.*, 2002). In this study it was shown that C-3 and C-4 substitution of the phenyl ring has a

considerable effect on the potency by which (*E*)-8-styrylcaffeinyl analogues inhibit MAO-B. This may be in part due to specific interactions between the substituents and amino acid side chains in the entrance cavity. Since the entrance cavity is lined by the side chains of hydrophobic amino acids, these interactions are likely to be van der Waals forces. In accordance with this view, the SAR study indicates that increasing inhibition potency correlates with increasing hydrophobicity and size of the C-3 and C-4 substituents. Interestingly it appears that electron withdrawing substituents at C-3 enhances MAO-B inhibition of the analogues tested in this study. A possible explanation is that electron withdrawing functionalities at C-3, but not at C-4, causes positive charge localization in the phenyl ring which in turn leads to π-π interactions with peptide bonds located near the entrance cavity. With electron withdrawing functionalities at C-4 a similar charge localization may be diminished via delocalization via the styryl double bond to the xanthine ring.

Experimental Section

***Caution**: MMTP (7) is a structural analogue of the known nigrostriatal neurotoxin 1-methyl-4-phenyl-1,2,3,6-tetrahydropyridine (MPTP) and should be handled using disposable gloves and protective eyewear. Procedures for the safe handling of MPTP have been described previously (Pitts et al., 1986).*

Materials and instrumentation. All starting materials not described elsewhere were obtained from Sigma-Aldrich and were used without purification. The oxalate salt of MMTP (7) was prepared in the laboratory of Prof. Neal Castagnoli, Jr according to general procedures reported previously (Bissel *et al.*, 2002). 1,3-Dimethyl-5,6-diaminouracil (**4**) was prepared according to the reported procedure (Blicke & Godt, 1954). Because of chemical instability, this reagent was used within three hours of preparation. Melting points (mp) were determined on a Gallenkamp melting point apparatus or by differential scanning calorimetry (DSC) on a Shimadzu DSC-50 instrument. All melting points are uncorrected. Proton and carbon NMR spectra were recorded on a Varian Gemini 300 spectrometer. Proton (^{1}H) spectra were recorded at a frequency of 300 MHz and carbon (^{13}C) spectra at 75 MHz. Chemical shifts are reported in parts per million (δ) downfield from the signal of tetramethylsilane added to deuterated chloroform ($CDCl_3$). Spin multiplicities are given as s (singlet), d (doublet), t (triplet), q (quartet) or m (multiplet) and the coupling constants (*J*) are given in hertz (Hz). Direct insertion electron ionization mass spectra (EI-MS) was obtained on a VG 7070E mass spectrometer. HPLC analyses were performed with an Agilent 1100 HPLC system equipped with a variable wavelength detector and a Macherey-Nagel CC 125/4 Nucleosil C18 column (4.6 × 100 mm, 5 μm). UV-Vis spectra were recorded on a Milton-Roy Spectronic 1201 spectrophotometer.

General procedure for the preparation of (*E*)-8-styrylcaffeinyl analogues (2a–i). The preparations of **2a–c** and **2e–i** were accomplished using the procedure described by Suzuki *et al.* (1993). To a solution of

1,3-dimethyl-5,6-diaminouracil (**4**, 2.7 mmol) and 1-ethyl-2-[3-(dimethylamino)propyl]-carbodiimide hydrochloride (EDAC; 3.9 mmol) in 20 mL dioxane/H_2O (1:1) was added the appropriately substituted *trans*-cinnamic acid (**5**, 2.9 mmol). The pH of the suspension was adjusted to 5 with 2 N aqueous hydrochloric acid and stirring was continued for an additional 2 hours. Following neutralization with 1 N aqueous sodium hydroxide the reaction was cooled to 0 °C and the precipitate was collected by filtration. The crude product was dissolved in 30 mL aqueous sodium hydroxide (1 N)/dioxane (1:1) and refluxed for 45 minutes. After cooling to 0 °C the solution was acidified to a pH of 4 with 4 N aqueous hydrochloric acid and the resulting precipitate was collected by filtration. The resulting 1,3-methyl-(*E*)-8-styryl-7*H*-xanthinyl analogues (**6**) may be used in the subsequent reaction without further purification. To a stirred suspension of **6** (0.16 mmol) and potassium carbonate (0.25 mmol) in 5 mL DMF was added iodomethane (0.32 mmol). After the mixture was stirred at 50 °C for 60 minutes, the insoluble materials were removed by filtration and sufficient water was added to the filtrate to precipitate the product (**2**) which was collected by filtration. Following recrystallization from a mixture of methanol/ethyl acetate (9:1) analytically pure samples of **2** were obtained. For previously reported **2a** and **2e** we found the melting points to be 212 °C and 222 °C [from methanol/ethyl acetate (9:1)] while the reported melting points are 205 °C and 220-222 °C, respectively (Jacobson *et al.*, 1993). The characterizations of previously unreported compounds (**2b–c** and **2f–i**) are summarized below.

(*E*)-8-(3-trifluoromethylstyryl)caffeine (2b) was prepared from 1,3-dimethyl-5,6-diaminouracil (**4**) and *trans*-3-trifluoromethylcinnamic acid in a yield of 35%: mp 243.7 °C (238 °C by capillary method); ^{1}H-NMR ($CDCl_3$) δ 3.40 (s, 3H), 3.61 (s, 3H), 4.08 (s, 3H), 6.96 (d, 1H, J = 15.8 Hz), 7.51 (m, 1H), 7.59 (d, 1H, J = 7.8 Hz), 7.72 (d, 1H, J = 6.32 Hz), 7.80 (s, 1H), 7.81 (d, 1H, J = 15.8 Hz); ^{13}C-NMR ($CDCl_3$) δ 27.94 (CH_3), 29.73 (CH_3), 31.61 (CH_3), 108.22 (C), 113.02 (CH), 122.07 (C), 123.72 (CH), 125.81 (CH), 129.48 (CH), 130.51 (CH) , 131.32 (C), 131.76 (C), 136.45 (CH), 148.53 (C), 149.19 (C), 151.67 (C), 155.28 (C); EI-MS *m/z* 364 ($M^{\cdot+}$).

(*E*)-8-(3-methylstyryl)caffeine (2c) was prepared from 1,3-dimethyl-5,6-diaminouracil (**4**) and *trans*-3-methylcinnamic acid in a yield of 24%: mp 216.1 °C (219 °C by capillary method); ^{1}H-NMR ($CDCl_3$) δ 2.36 (s, 3H), 3.37 (s, 3H), 3.59 (s, 3H), 4.02 (s, 3H) 6.86 (d, 1H, J = 15.8 Hz), 7.15 (d, 1H, J = 7.0 Hz), 7.26 (m, 1H), 7.34 (d, 2H, J = 7.9 Hz), 7.74 (d, 1H, J = 15.8 Hz); ^{13}C-NMR ($CDCl_3$) δ 21.33 (CH_3), 27.86 (CH_3), 29.69 (CH_3), 31.45 (CH_3), 107.82 (C), 110.96 (CH), 124.58 (CH), 127.89 (CH), 128.78 (CH), 130.32 (CH), 135.41 (C), 138.43 (CH), 138.55 (C), 148.52 (C), 149.99 (C), 151.65 (C), 155.17 (C); EI-MS *m/z* 310 ($M^{\cdot+}$).

(*E*)-8-(4-chlorostyryl)caffeine (2f) was prepared from 1,3-dimethyl-5,6-diaminouracil (**4**) and *trans*-4-chlorocinnamic acid in a yield of 17%: mp 226.9 °C (232 °C by capillary method); ^{1}H-NMR ($CDCl_3$) δ 3.37 (s, 3H), 3.58 (s, 3H), 4.02 (s, 3H), 6.84 (d, 1H, J = 15.7 Hz), 7.34 (d, 2H, J = 8.5 Hz), 7.47 (d, 2H, J =

8.5 Hz), 7.71 (d, 1H, J = 15.8 Hz); ^{13}C-NMR ($CDCl_3$) δ 27.89 (CH_3), 29.70 (CH_3), 31.49 (CH_3), 107.99 (C), 111.71 (CH), 128.45 (CH), 129.17 (CH), 133.97 (C), 135.28 (C), 136.79 (CH), 148.50 (C), 149.55 (C), 151.63 (C), 155.19 (C); EI-MS *m/z* 330 ($M^{\cdot+}$).

(*E*)-8-(4-trifluoromethylstyryl)caffeine (2g) was prepared from 1,3-dimethyl-5,6-diaminouracil (**4**) and *trans*-4-trifluoromethylcinnamic acid in a yield of 64%: mp 230.2 °C (235 °C by capillary method); ^{1}H-NMR ($CDCl_3$) δ 3.35 (s, 3H), 3.57 (s, 3H), 4.04 (s, 3H), 6.95 (d, 1H, J = 15.8 Hz), 7.62 (m, 4H), 7.77 (d, 1H, J = 15.7 Hz); ^{13}C-NMR ($CDCl_3$) δ 27.87 (CH_3), 29.67 (CH_3), 31.50 (CH_3), 108.14 (C), 113.52 (CH), 125.76 (CH), 127.38 (CH), 130.68 (C), 131.12 (C), 136.28 (CH), 138.83 (C), 148.42 (C), 149.07 (C), 151.55 (C), 155.16 (C); EI-MS *m/z* 364 ($M^{\cdot+}$).

(*E*)-8-(4-methylstyryl)caffeine (2h) was prepared from 1,3-dimethyl-5,6-diaminouracil (**4**) and *trans*-4-methylcinnamic acid in a yield of 80%: mp 205.5 °C (208 °C by capillary method); ^{1}H-NMR ($CDCl_3$) δ 2.35 (s, 3H), 3.37 (s, 3H), 3.58 (s, 3H), 4.00 (s, 3H) 6.81 (d, 1H, J = 15.7 Hz), 7.17 (d, 2H, J = 8.0 Hz), 7.43 (d, 2H, J = 8.1 Hz), 7.73 (d, 1H, J = 15.8 Hz); ^{13}C-NMR ($CDCl_3$) δ 21.37 (CH_3), 27.83 (CH_3), 29.67 (CH_3), 31.40 (CH_3), 107.74 (C), 110.14 (CH), 127.27 (CH), 129.61 (CH), 132.71 (C), 138.25 (CH), 139.79 (C), 148.52 (C), 150.13 (C), 151.64 (C), 155.13 (C); EI-MS *m/z* 310 ($M^{\cdot+}$).

(*E*)-8-(4-fluorostyryl)caffeine (2i) was prepared from 1,3-dimethyl-5,6-diaminouracil (**4**) and *trans*-4-fluorocinnamic acid in a yield of 55% yield: mp 242.26 °C (245 °C by capillary method); ^{1}H-NMR ($CDCl_3$) δ 3.36 (s, 3H), 3.58 (s, 3H), 4.02 (s, 3H), 6.78 (d, 1H, J = 15.8 Hz), 7.13 (m, 2H), 7.52 (m, 2H), 7.72 (d, 1H, J = 15.8 Hz); ^{13}C-NMR ($CDCl_3$) δ 27.85 (CH_3), 29.67 (CH_3), 31.44 (CH_3), 107.87 (C), 110.95 (CH), 128.99 (CH), 129.10 (CH), 131.75 (C), 136.93 (CH), 148.48 (C), 149.71 (C), 151.61 (C), 155.15 (C), 161.71 (C); EI-MS *m/z* 314 ($M^{\cdot+}$).

MAO-B activity measurements and inhibition studies. Mitochondria were isolated from baboon liver tissue as described by Salach and Weyler (1987) and stored at –70 °C. The mitochondrial isolate was suspended in sodium phosphate buffer (100 mM, pH 7.4 containing 50% glycerol, w/v) and the protein concentration was determined by the method of Bradford (1976). For the inhibition studies on MAO-B we utilized the MAO-A and –B mixed substrate MMTP (K_m = 60.9 μM for baboon liver MAO-B) (Inoue *et al.*, 1999) and the MAO-B selective substrate benzylamine (K_m = 616 ± 23 μM for baboon liver MAO-B). Since baboon liver mitochondria are devoid of MAO-A activity, inactivation of this enzyme was unnecessary in the studies where MMTP was utilized as substrate (Inoue *et al.*, 1999). A typical incubation (500 μL final volume in 100 mM sodium phosphate buffer, pH 7.4) contained MMTP (30–120 μM) or benzylamine (125–750 μM), the mitochondrial isolate (0.15 mg protein/mL) and various concentrations of the test inhibitors. Stock solutions of the inhibitors were prepared in DMSO and were added to the incubation mixtures to yield a final DMSO concentration of 4% (v/v). DMSO concentrations higher than 4% are reported to negatively affect MAO-B activity (Gnerre *et al.*, 2000). The samples were incubated at

37 °C and the incubation times were 15 min for MMTP and 8 min for benzylamine. For these time periods the MAO-B catalyzed production of $MMDP^+$ (Inoue *et al.*, 1999) and benzaldehyde were linear with time. The reactions were terminated by the addition of 10 µL 70% perchloric acid and the samples were centrifuged at 16,000*g* for 10 minutes. The supernatant fractions were removed and the concentrations of the MAO-B generated products, $MMDP^+$ (where MMTP served as substrate) and benzaldehyde (where benzylamine served as substrate), were measured. $MMDP^+$ formation was monitored spectrophotometrically at a wavelength of 420 nm (ε = 25,000 M^{-1}) (Inoue *et al.*, 1999) while benzaldehyde concentrations were measured via HPLC analysis (see Materials and instrumentation). In the latter case, a reversed phase C18 column was used and the mobile phase consisted of 60% distilled water [containing 0.6% (v/v) glacial acetic acid and 1% (v/v) triethylamine], 30% methanol and 10% acetonitrile at a flow rate of 1 mL/min. A volume of 50 µL of the supernatant was injected into the HPLC system and the elution of benzaldehyde (3.97 min) was monitored at a wavelength of 250 nm. Quantitative estimations of benzaldehyde were made by means of a linear calibration curve ranging from 6.25 to 50 µM. Initial rates were expressed as nmoles of product ($MMDP^+$ or benzaldehyde) formed per mg mitochondrial protein per min. Competitive K_i values were determined by calculating the initial rates of substrate oxidation in the absence and presence of varying concentrations of the inhibitors and constructing Lineweaver-Burke plots with increasing concentrations of the inhibitor. The slopes of the Lineweaver-Burke plots were plotted as a function of the inhibitor concentration and the K_i value were determined from the abscissa intercept (intercept = $-K_i$) (Segel, 1993). Linear regression analysis was performed using the SigmaPlot software package (Systat Software Inc.).

Linearity of benzylamine oxidation with time. In order to select a suitable incubation time for benzylamine with baboon liver MAO-B, we determined the time interval for which the MAO-B catalyzed benzaldehyde formation remains linear under our assay conditions. Various concentrations of benzylamine (125–750 µM) were incubated with the mitochondrial isolate (0.15 mg protein/mL) at 37 °C for various periods of time (2.5–10 min). The same incubation conditions were followed as described above. For the purpose of this study no inhibitor was included in the reaction incubations. Following termination of the reactions by the addition of 10 µL perchloric acid, the concentrations of the MAO-B generated benzaldehyde were measured by HPLC analysis. Graphs of benzaldehyde concentration as a function of time were constructed.

K_m determination of benzylamine for baboon liver MAO-B. The steady state rate of benzylamine oxidation by baboon liver MAO-B was measured by HPLC analysis as outlined above. In order to estimate a K_m value for the oxidation of benzylamine, rates were measured at eight different substrate concentrations spanning at least two orders of a magnitude (25–8000 µM). The enzyme concentration utilized was 0.15 mg/mL of the baboon liver homogenate and all incubations were carried out at 37 °C for a time period of 8 min. Benzaldehyde concentrations were measured with the aid of a linear calibration curve prepared over a

range of 1.5 to 50 μM. The kinetic data (initial rates as a function of substrate concentration) were fitted to the Michaelis-Menten equation (Segel, 1993) using a nonlinear least-squares fitting routine incorporated into the SigmaPlot software package. This determination was carried out in triplicate and the K_m value was expressed as mean ± standard deviation.

SAR studies. Values for the substituent parameters σ_m, σ_p, F, π and E_s were obtained from Hansch & Leo (1995) and those for the der Waals volume (V_w) were obtained from Hansch & Leo (1979). Stepwise multiple linear regression analysis of the logK_i values as a function of the substituent parameters was carried out with Statistica software package (StatSoft Inc.). In order to estimate the significance of the regression equations the F statistic was employed. An F value higher than the critical F value was judged to be significant and critical F values were calculated as described recently (Livingstone & Salt, 1995). The critical F value (F_{max}) for 5% significance for models constructed from five logK_i values (Table 2 and 3) and which contains one parameter (out of a possible five: V_w, E_s, π, σ_m, F) was calculated to be 34.29 while a model containing two parameters has an F_{max} value of 170.59.

Acknowledgements: We thank Dr. Jan du Preez and the staff of the Analytical Technology Laboratory as well as Dr. Douw van der Nest and the staff of the Experimental Animal Facility, North-West University for their support. The NMR and MS spectra were recorded by Mr. André Joubert and Dr. Louis Fourie of the SASOL Centre for Chemistry, North-West University. Assistance with the statistical analysis was provided by Dr. Suria Ellis of the Statistical Consultation Service, North-West University. This work was supported by grants from the National Research Foundation and the Medical Research Council, South Africa.

References

1. Volz, H.P. & Gleiter, C.H. 1998. Monoamine oxidase inhibitors: a perspective on their use in the elderly. *Drugs in the aging*, 13:341–355.
2. Saura, J., Luque, J.M., Cesura, A.M., Da Prada, M., Chan-Palay, V., Huber, G., Loffler, J. & Richards, J.G. 1994. Increased monoamine oxidase B activity in plaque-associated astrocytes of Alzheimer brain revealed by quantitative enzyme autoradiography. *Neuroscience*, 62:15–30.
3. Rabey, J. M., Sagi, L., Huberman, M., Melamed, E., Korezyn, A., Giladi, M., Inzelberg, R., Djaldetti, R., Klein, C. & Berecz, G. 2000. Rasagiline mesylate, a new MAO-B inhibitor for the treatment of Parkinson's disease: a double-blind study as adjunctive therapy to levodopa. *Clinical neuropharmacology*, 23:324–330.
4. Riederer, P., Lachenmayer, L. & Laux, G. 2004. Clinical applications of MAO-inhibitors. *Current medicinal chemistry*, 11:2033–2043.
5. Youdim, M.B. & Riederer, P.F. 2004. A review of the mechanisms and role of monoamine oxidase inhibitors in Parkinson's disease. *Neurology*, 63(7 Suppl 2):S32–35.

6. Tatton, W,G. 1993. Selegiline can mediate neuronal rescue rather than neuronal protection. *Movement disorders*, 8(Suppl.):20–30.
7. Tatton, W.G. & Greenwood, C.E. 1991. Rescue of dying neurons a new action for deprenyl in MPTP parkinsonism. *Journal of neuroscience research*, 30:666–667.
8. LeWitt, P.A. 2004. Clinical trials of neuroprotection for Parkinson's disease. *Neurology*, 63(7 Suppl 2):S23–31.
9. Gnerre, C., Catto, M., Leonetti, F., Weber, P., Carrupt, P.-A., Altomare, C., Carotti, A. & Testa, B. 2000. Inhibition of monoamine oxidases by functionalized coumarin derivatives: biological activities, QSARs, and 3D-QSARs. *Journal of medicinal chemistry*, 43:4747–4758.
10. Mazouz, F., Gueddari, S., Burstein, C., Mansuy, D. & Milcent, R. 5-[4-(Benzyloxy)phenyl]-1,3,4-oxadiazol-2(3H)-one derivatives and related analogues: new reversible, highly potent, and selective monamine oxidase type B inhibitors. *Journal of medicinal chemistry*, 36:1157–1167.
11. Chen, J.F., Steyn, S., Staal, R., Petzer, J.P., Xu, K., Van Der Schyf, C.J., Castagnoli, K., Sonsalla, P.K., Castagnoli, N., Jr. & Schwarzschild, M.A. 2002. 8-(3-Chlorostyryl)caffeine may attenuate MPTP neurotoxicity through dual actions of monoamine oxidase inhibition and A_{2A} receptor antagonism. *Journal of biological chemistry*, 277(39):36040–36044.
12. Chen, J.F., Xu, K., Petzer, J.P., Staal, R., Xu, Y.H., Beilstein, M., Sonsalla, P.K., Castagnoli, K., Castagnoli, N., Jr. & Schwarzschild, M.A. 2001. Neuroprotection by caffeine and A_{2A} adenosine receptor inactivation in a model of Parkinson's disease. *Journal of neuroscience*, 21(10):RC143.
13. Petzer, J.P., Steyn, S., Castagnoli, K.P., Chen, J.F., Schwarzschild, M.A., Van der Schyf, C.J. & Castagnoli, N., Jr. 2003. Inhibition of monoamine oxidase B by selective adenosine A_{2A} receptor antagonists. *Bioorganic and medicinal chemistry*, 11(7):1299–1310.
14. Suzuki, F., Shimada, J., Shiozaki, S., Ichikawa, S., Ishii, A., Nakamura, J., Nonaka, H., Kobayashi, H. & Fuse, E. 1993. Adenosine A_1 antagonists. 3. Structure-activity relationships on amelioration against scopolamine- or N^6-((R)-phenylisopropyl)adenosine-induced cognitive disturbance. *Journal of medicinal chemistry*, 36:2508–2518.
15. Müller, C.E., Geis, U., Hipp, J., Schobert, U., Frobenius, W., Pawlowski, M., Suzuki, F. & Sandoval-Ramirez, J. 1997. Synthesis and structure-activity relationships of 3,7-dimethyl-1-propargylxanthine derivatives, A_{2A}-selective adenosine receptor antagonists. *Journal of medicinal chemistry*, 40:4396–4405.
16. Castagnoli, N., Jr., Petzer, J.P., Steyn, S., Castagnoli, K., Chen, J.F., Schwarzschild, M.A. & Van der Schyf, C.J. 2003. Monoamine oxidase B inhibition and neuroprotection: studies on selective adenosine A_{2A} receptor antagonists. *Neurology*, 61(11 Suppl 6):S62–68.
17. Xu, K., Bastia, E. & Schwarzschild, M. 2005. Therapeutic potential of adenosine A_{2A} receptor antagonists in Parkinson's disease. *Pharmacology & Therapeutics*, 105:267–310.

18. Shimada, J., Koike, N., Nonaka, H., Shiozaki, S.,Yanagawa, K., Kanada, T., Kobayashi, H. & Fumio, S. 1997. Adenosine A_{2A} antagonists with potent anti-cataleptic activity. *Bioorganic & medicinal chemistry letters*, 7:2349–2352.
19. Bara-Jimenez, W., Sherzai, A., Dimitrova, T., Favit, A., Bibbiani, F., Gillespie, M., Morris, M.J., Mouradian, M.M. & Chase, T.N. Adenosine A_{2A} receptor antagonist treatment of Parkinson's disease. *Neurology*, 61:293–296.
20. Ikeda, K., Kurokawa, M., Aoyama, S. & Kuwana, Y. 2002. Neuroprotection by adenosine A_{2A} receptor blockade in experimental models of Parkinson's disease. *Journal of neurochemistry*, 80:262–270.
21. Schwarzschild, M.A., Xu, K., Oztas, E., Petzer, J.P., Castagnoli, K., Castagnoli, N., Jr. & Chen, J.F. 2003. Neuroprotection by caffeine and more specific A_{2A} receptor antagonists in animal models of Parkinson's disease. *Neurology*, 61(11 Suppl 6):S55–61.
22. Jacobson, K.A., Gallo-Rodriguez, C., Melman, N., Fischer, B., Maillard, M., Van Bergen, A., Van Galen, P.J.M. & Karton, Y. 1993. Structure–activity relationships of 8-styrylxanthines as A_2-selective adenosine antagonists. *Journal of medicinal chemistry*, 36:1333–1342.
23. Philip, J. & Szulczewski, D.H. 1973. Photo-induced isomerization of 8-(3,4,5-trimethoxystyryl)caffeine as possible route of drug decomposition. *Journal of pharmacological sciences*, 62:1885–1887.
24. Nonaka, Y., Shimada, J., Nonaka, H., Koike, N., Aoki, N., Kobayashi, H., Kase, H., Yamaguchi, K. & Fumio, S. 1993. Photo-isomerization of a potent and selective adenosine A_2 antagonist (E)-1,3-dipropyl-8-(3,4-dimethoxystyryl)-7-methylxanthine. *Journal of medicinal chemistry*, 36:3731–3733.
25. Hockemeyer, J., Burbiel, J.C. & Muller, C.E. 2004. Multigram-scale syntheses, stability, and photoreactions of A_{2A} adenosine receptor antagonists with 8-styrylxanthine structure: potential drugs for Parkinson's disease. Journal of organic chemistry, 69:3308–3318.
26. Inoue, H., Castagnoli, K., Van der Schyff, C.J., Mabic, S., Igarashi, K. and Castagnoli, N., Jr. 1999. Species-dependent differences in monoamine oxidase A and B-catalyzed oxidation of various C4 substituted 1-methyl-4-phenyl-1,2,3,6-tetrahydropyridinyl derivatives. *The journal of pharmacology and experimental therapeutics*, 291(2):856–864.
27. Nimkar, S.K., Anderson, A., Rimoldi, J.M., Stanton, J.M., Castagnoli, K.P., Mabic, S., Wang, Y.–X. & Castagnoli, N., Jr. 1996. Synthesis and monoamine oxidase-B catalyzed oxidation of C-4 heteroaromatic substituted 1,2,3,6-tetrahydropyridine derivatives. *Chemical research in toxicology*, 9:1013–1022.
28. Castagnoli, K., Palmer, S., Anderson, A., Bueters, T. & Castagnoli, N., Jr. 1997. The neuronal nitric oxide synthase inhibitor 7-nitroindazole also inhibits the monoamine oxidase-B-catalyzed oxidation of 1-methyl-4-phenyl-1,2,3,6-tetrahydropyridine. *Chemical research in toxicology*. 10:364–368.
29. Walker, M.C. & Edmondson, D.E. 1994. Structure-activity relationships in the oxidation of benzylamine analogues by bovine liver mitochondrial monoamone oxidase B. *Biochemistry*, 33:7088–7098.

30. Newton-Vinson, P., Hubalek, F. & Edmondson, D.E. 2000. High-level expression of human liver monoamine oxidase B in Pichia pastoris. *Protein expression and purification*, 20:334–345.
31. Krueger, M.J., Mazouz, F., Ramsay, R., Milcent, R. & Singer, T.P. 1995. Dramatic species differences in the susceptibility of monoamine oxidase B to a group of powerful inhibitors. *Biochemical and biophysical research communications*, 206:556–562.
32. Segel, I. H. 1993. *Enzyme kinetics*, Wiley, New York. pp 100–125.
33. Hubálec, F., Binda, C., Khalil, A., Li, M., Mattevi, A., Castagnoli, N., Jr. & Edmondson, D.E. 2005. Demonstration of isoleucine 199 as a structural determinant for the selective inhibition of human monoamine oxidase B by specific reversible inhibitors. *Journal of biological chemistry*, 280:15761-15766.
34. Hansch, C. and Leo, A. 1995. Exploring QSAR. Fundamentals and applications in chemistry and biology. American Chemical Society, p557.
35. Hansch, C. & Leo, A. 1979. Substituent constants for correlation analysis in chemistry and biology. John Wiley and Sons. New York, pp352–352.
36. Livingstone, D.J. & Salt, D.W. 2005. Judging the significance of multiple linear regression models. *Journal of medicinal chemistry*, 48:661–663.
37. Kutter, E. & Hansch, C. 1969. Steric parameters in drug design. Monoamine oxidase inhibitors and antihistamines. *Journal of medicinal chemistry*, 12:647–652.
38. Fuller, R.W., Marsh, M.M. & Mills, J. 1968. Inhibition of monoamine oxidase by N-(phenoxyethyl)cyclopropylamines. Correlation of inhibition with Hammett constants and partition coefficients. *Journal of medicinal chemistry*, 11:387–398.
39. Hansch, C., Leo, A. & Hoekman, D. 1995. Exploring QSAR. Hydrophobic, electronic and steric constants, American Chemical Society, Washington, DC.
40. Bondi, A, 1964. Van der Waals Volumes and Radii. *Journal of physical chemistry*, 68:441–451.
41. Swain, C.G. & Lupton, E.C., Jr. 1968. Field and resonance components of substituent effects. *Journal of the American chemical society*, 90: 4328–4337.
42. Pitts, S.M., Markey, S.P., Murphy, D.L. & Weisz, A. 1986. Recommended practices for the safe handling of MPTP. In *MPTP: A neurotoxin producing a Parkinsonian syndrome* (Markey, S.P., Castagnoli, N., Jr., Trevor, A.J. and Kopin, I.J. Eds.) pp 703–716, Academic Press, New York.
43. Bissel, P., Bigley, M.C., Castagnoli, K. & Castagnoli, N., Jr. 2002. Synthesis and biological evaluation of MAO-A selective 1,4-disubstituted-1,2,3,6-tetrahydropyridinyl substrates. *Bioorganic and medicinal chemistry*, 10:3031–3041.
44. Blicke, F.F. & Godt, H.C., Jr. 1954. Reactions of 1,3-dimethyl-5,6-diaminouracil. *Journal of the American chemical society*, 76:2798–2800.
45. Salach, J. & Weyler, J. 1987. Preparation of the flavin-containing aromatic amine oxidases of human placenta and beef liver. *Methods in enzymology*, 142:627–637.

46. Bradford, M.M. 1976. A rapid and sensitive method for the quantitation of microgram quantities of protein utilizing the principle of protein-dye binding. *Analytical biochemistry*, 72:247–254.

47. Fujita, T., Iwasa, J. & Hansch, C. 1964. A new substituent constant, π, derived from partition coefficients. *Journal of the American chemical society*, 86: 5175–5180.

48. Silverman, R.B. & Hawe, W.P. 1995. SAR studies of fluorine-substituted benzylamines and substituted 2-phenylethylamines as substrates and inactivators of monoamine oxidase B. *Journal of enzyme inhibition*, 9:203–215.

49. Binda, C., Newton-Vinson, P., Hubalek, F., Edmondson, D.E., & Mattevi, A. 2001. Structure of human monoamine oxidase B, a drug target for the treatment of neurological disorders. *Nature structural biology*, 9:22–26.

50. Binda, C., Hubalek, F., Li, M., Herzig, Y., Sterling, J., Edmondson, D.E., & Mattevi, A. 2004. Crystal structures of monoamine oxidase B in complex with four inhibitors of the N-propargylamineindan class. *Journal of medicinal chemistry*, 47:1767–1774.

51. Binda, C., Hubalek, F., Restelli, N., Edmondson, D.E., & Mattevi, A. 2003. Insights into the mode of inhibition of monoamine oxidase B from high-resolution crystal structures. *PNAS*, 100:9750–9755.

52. Youdim, M.B., Fridkin, M., Zheng, H. 1995. Bifunctional drug derivatives of MAO-B inhibitor rasagiline and iron chelator VK-28 as a more effective approach to treatment of brain ageing and ageing neurodegenerative diseases. *Mechanisms of ageing and development*, 126:317–326.

53. Cohen, G. 1983 The pathobiology of Parkinson's disease: biochemical aspects of dopamine neuron senescence. *Journal of neural transmission*, 19(Suppl.):89-103.

54. Jacobson, K. A., Nikodijevic, O., Padgett, W. L., Gallo-Rodriguez, C., Maillard, M., & Daly, J. W. 1993. 8-(3-Chlorostyryl)caffeine (CSC) is a selective A2-adenosine antagonist in vitro and in vivo. *FEBS Letters*, 323:141–144.

Running title: Dual targeting of adenosine A_{2A} receptors and MAO-B.

APPENDIX C

Poster presented at the annual congress of the Academy of Pharmaceutical Sciences 2004.

Rational Approaches Towards the Design of Novel (*E*)-8-(3-chlorostyryl)caffeine Analogues as Reversible Inhibitors of Monoamine Oxidase B

N Vlok[1], JP Petzer[1], JJ Bergh[1], N Castagnoli, Jr.[2], SF Malan[1]

[1]Pharmaceutical Chemistry, School of Pharmacy
North-West University, POTCHEFSTROOM, 2520, South Africa

[2]Department of Chemistry, Virginia Polytechnic Institute and State University, Blacksburg, Virginia, USA

[fchnv@puknet.puk.ac.za, ☎ +27-(0)18-299-4264, 🖷 +27-(0)18-299-4243]

INTRODUCTION

Reversible and selective inhibitors of MAO-B are under investigation for the treatment and prevention of Parkinsonism (PD) and Alzheimer's disease (AD). The mechanism-based inactivator of MAO-B, (*R*)-deprenyl, is frequently used in combination with L-DOPA as dopamine replacement therapy in PD. In contrast with reversible inhibitors, following treatment with inactivators such as (*R*)-deprenyl, enzyme activity can only be regained via *de novo* synthesis of the MAO-B protein. For this reason several studies are underway to develop safer inhibitors of MAO-B. In a recent study done by Petzer *et al.*^, (*E*)-8-(3-chlorostyryl)caffeine showed exceptional competitive inhibitory activity towards MAO-B. These caffeine analogues are also known to be potent antagonists of the adenosine A_{2A}-receptor subtype. Such antagonists are currently being investigated as possible therapeutic agents for the symptomatic treatment of motor deficits such as those encountered in PD. Since MAO-B inhibitors are currently under investigation as preventative agents in PD, the possibility of designing antiparkinsonian drugs that can act as both A_{2A} antagonists and inhibitors of MAO-B may be of value. In PD such drugs could potentially enhance motility through antagonism of A_{2A} receptors and protect against further neurodegenerative processes, through inhibition of MAO-B.

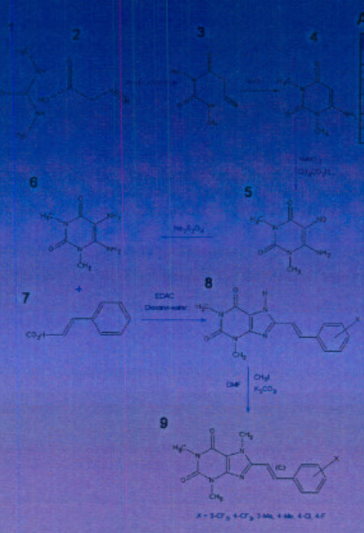

Fig.1 Reaction scheme of the synthesis pathway

MATERIALS AND METHODS

PREPARATION OF MAO-B: MAO-B is an integral protein of the outer wall of the mitochondria. As source of the enzyme we used crude mitochondrial fractions obtained from baboon and bovine liver tissue. These tissues are especially useful, since they are devoid of MAO-A activity.

SYNTHESIS: We prepared 6 (*E*)—8-(3-chlorostyryl)caffeine analogues as part of an ongoing investigation into the structural and electronic requirements of the compounds to act as competitive MAO-B inhibitors. The derivatives chosen for this study differed only in the substitution of the phenyl ring.

BIOLOGICAL TESTING: The synthetic targets were evaluated as competitive inhibitors of MAO-B using spectrophotometry. The potency by which the test compounds inhibit the MAO-B catalyzed oxidation of the substrate to a chromophoric product (λmax = 420nm) was expressed as Ki values. Ki values were determined from Lineweaver-Burke plots.

RESULTS

As indicated by the Lineweaver-Burke plots the Ki value for the inhibition of MAO-B by the 4-F substituted analogue was estimated to be 1.5 µM. This is approximately 3 times less potent than that of the 3-F analogue (Ki =0.4 µM), which is indicates that 3 substitutes may be essential for potent inhibition of MAO-B by this series of inhibitors.

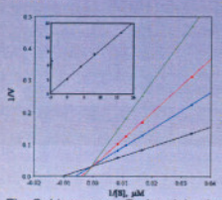

V = Velocity

[S] = substrate concentration

Fig. 2: Linewaever-Burke plots showing competitive inhibition by an (*E*)-8-(3-chlorostyryl)caffeine analogue. Inset is the replot of the slope vs. inhibitor concentration.

ANALYSIS

Compound	Melting point (°C)
1,3-dimethyl-8-(3-CF3-styryl)-7-methyl-xanthine	239
1,3-dimethyl-8-(4-CF3-styryl)-7-methyl-xanthine	219
1,3-dimethyl-8-(3-methylstyryl)-7-methyl-xanthine	215
1,3-dimethyl-8-(4-methylstyryl)-7-methyl-xanthine	255
1,3-dimethyl-8-(4-Cl-styryl)-7-methyl-xanthine	222
1,3-dimethyl-8-(4-F-styryl)-7-methyl-xanthine	245

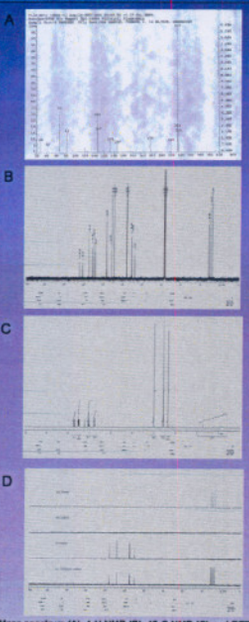

Fig. 2: Mass spectrum (A), 1-H NMR (B), 13-C NMR (C) and DEPT (D) of 1,3-dimethyl-8-(4-fluorostyryl)-7-methyl-xanthine.

DISCUSSION

The first two compounds evaluated as competitive inhibitors of MAO-B reveals interesting structure-activity relationship in that substitution in the 3-position on the phenyl ring is necessary for optimum inhibitory activity. Inhibition studies on further compounds in this series should give a clearer indication of SAR within this series. To gain further insight into the requirements for MAO-B inhibition we will also perform 3D-QSAR studies and docking of our inhibitor into the active site of MAO-B.

REFERENCES

Petzer, J.P., Steyn, S., Castagnoli, K.P., Chen, J-F., Schwarzschild, M.A., Van der Schyf, C.J., Castagnoli, N. 2003. *Inhibition of Monoamine Oxidase B by Selective Adenosine A_{2A} Receptor Antagonists.* Bioorganic & Medicinal Chemistry, 11:1299-1310.

YUNIBESITI YA BOKONE-BOPHIRIMA
NORTH-WEST UNIVERSITY
NOORDWES-UNIVERSITEIT

PUK
Potchefstroom Campus

Acknowledgements

- Firstly I want to praise the Almighty God for knowledge and opportunity. Thank you for granting me the ability and the opportunity. All praise to You.
- Prof. S.F. Malan. Thanks for your guidance and insight.
- Dr. J.P. Petzer. Thank you for all your time and effort. I greatly admire your passion for chemistry. If all people were as passionate, the world would be a perfect place.
- My boundless gratitude to my family for always loving and supporting me.
- My friends at Pharmaceutical Chemistry, how dull life would have been without you.
- JMS, thanks for your friendship. You make ordinary days extraordinary.
- Walter and Gerda Clark. May you be blessed for giving without wanting anything in return.
- Dedicated to the one who will one day own my heart…